TÉCNICO LISBOA

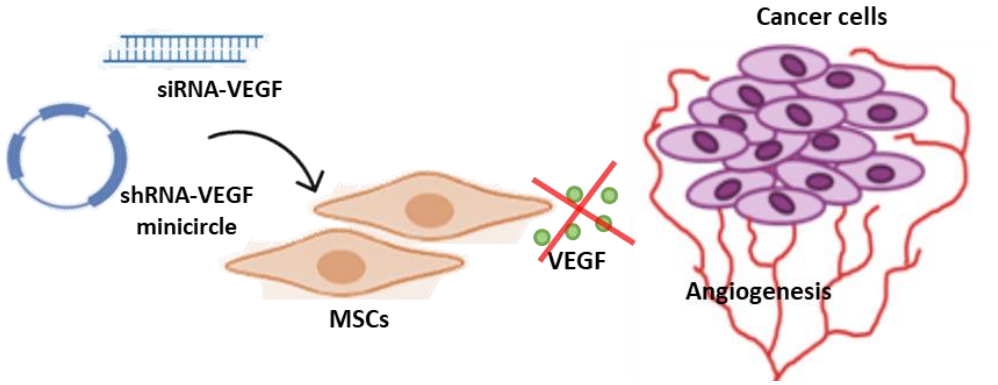

RNAi as a tool to inhibit the angiogenic potential of human Mesenchymal Stem/Stromal Cells in malignancy

Cristiana da Silva Ulpiano

Thesis to obtain the Master of Science Degree in

Biotechnology

Supervisors: Professor Gabriel António Amaro Monteiro

Professor Cláudia Alexandra Martins Lobato da Silva

Examination Committee

Chairperson: Professor Arsénio do Carmo Sales Mendes Fialho

Supervisor: Professor Gabriel António Amaro Monteiro

Members of the Committee: Doctor Nuno Filipe Santos Bernardes

October 2018

Acknowledgments

First of all, I would like to acknowledge Professor Joaquim Cabral for giving me the opportunity to work at SCERG, and of course, to my supervisors Professor Gabriel Monteiro and Professor Cláudia Lobato for all the guidance and support, and for trusting me such challenging and forefront field project.

I would like to thank to all my lab colleagues, at Alameda and Tagus Park, for always showing themselves available to help me. A special thanks to Cláudia Alves, Ana Rita Silva, Marília Silva and Joana Serra for their immense knowledge, support and patience. Also, a big thanks to Tiago Ligeiro, my lab twin, for the endless hours passed by my side.

I would like to thank to my Biotechnology Gang, who understand the most the accomplishment of this step, for the everyday moments that we spend together. Thank you for all the friendship, motivational talks and constant laughs, that always made me feel better specially on the days I felt down.

I would like to thank to my coach and swimming teammates, for a lifetime of companionship and for once more inspiring me to keep pushing on myself.

Finally, I am sincerely grateful to my family, boyfriend and friends, for always making me believe in myself and supporting me in everything in my life.

Thank you all!

Abstract

Mesenchymal Stem/Stromal Cells (MSCs) have an active role in supporting the maintenance of a homeostatic tissue microenvironment by secretion of a broad range of biologically active molecules. Upon interaction with cancer cells, MSCs became active participants in tumour development namely by promoting angiogenesis through the secretion of pro-angiogenic molecules, such as vascular endothelial growth factor (VEGF). Considering that tumour angiogenesis is one of the hallmarks of cancer progression, blocking VEGF production by the cells present in tumour microenvironment, might represent a potential approach to slow down tumour growth. In this context, RNA interference-mediated silencing appears a promising tool to suppress gene expression in mammalian cells.

In this regard, this project involves the transfection of human bone marrow MSCs and MCF-7, a human breast adenocarcinoma cell line, with small-interfering RNA (siRNA), synthetized outsource or expressed as a short-hairpin RNAs (shRNAs) from minicircle (MC) vectors, that target VEGF expression. Overall, RT-qPCR results revealed a VEGF-mRNA knockdown of 50% and 40% after synthetic siRNA transfection of MSCs and MCF-7, respectively. Similarly, ELISA results indicate a decrease in VEGF secretion. Regarding transfection results with MC vectors, similar results were expected, however, increased VEGF expression was consistently found at mRNA and protein levels after MSCs and MCF-7 cells transfection. Although further studies are required, these discrepancies appear to be related to the incorrect processing of the transcribed shRNA into a functional siRNA.

Overall, this study provides insights regarding the implementation of an siRNA-based system that targets VEGF expression, aiming at slowing down tumour angiogenesis.

Keywords

Tumour angiogenesis; Mesenchymal Stem/Stromal Cells; Vascular Endothelial Growth Factor; RNA interference

Resumo

Células Mesenquimais Estaminais/Estromais (MSC) desempenham um papel crucial na manutenção da homeostase nos tecidos secretando uma vasta gama de moléculas biologicamente ativas. Após a interação com cancro, as MSCs tornam-se participantes ativos no desenvolvimento tumoral, promovendo a angiogénese através da secreção de moléculas como fator de crescimento endotelial vascular (VEGF). Considerando que a angiogénese tumoral uma importante característica na progressão do cancro, o bloqueio da produção de VEGF no microambiente tumoral, poderá retardar o crescimento do tumor. Neste contexto, RNA de interferência (RNAi) é uma abordagem promissora correntemente utilizada na supressão a expressão génica em células de mamíferos.

Deste modo, este projeto envolve a transfeção de MSCs derivadas da medula óssea humana e MCF-7 (adenocarcinoma de mama humano), com *small interference RNAs* (siRNAs) sintéticos ou expressos como um *short-hairpin RNAs* a partir de um vetor minicírculo, que visam silenciar a expressão de VEGF. Em suma, um silenciamento de 50% e 40% a nível do mRNA de VEGF, após a transfeção de MSCs e MCF-7 com o siRNA, foi observado. Da mesma forma, uma diminuição na secreção de VEGF foi observada. Relativamente aos vetores minicírculo, contrariamente ao esperado, a expressão de VEGF aumentou a nível do mRNA e proteína, após transfeção das duas linhas celulares. Embora sejas requerido mais estudos, estas discrepâncias parentam estar relacionadas com o incorreto processamento do shRNA num siRNA funcional.

No geral, este estudo fornece conhecimentos em relação à implementação de um sistema baseado em RNAi que silencia a expressão de VEGF, visando retardar a angiogénese tumoral.

Palavras-chave

Angiogénese tumoral; Células Mesenquimais Estaminais; Fator de crescimento endotelial vascular; RNA interferência

Table of contents

List of Figures

List of Tables

List of Abbreviations

AAVs- Adeno-Associated Viruses

AGO- Argonaute protein

AT- Adipose Tissue

BM- Bone Marrow

BGH- Bovine Growth Hormone

CAF- Cancer Associated Fibroblasts

CHO- Chinese Hamster Ovary

CR – Cell Recovery

CM- Conditioned Medium

CMV- Cytomegalovirus

DGCR8- DiGeorge Syndrome Critical Region 8

DMEM- Dulbecco's Modified Eagle's Medium

dsRNA- double-stranded RNA

EBM-2- Endothelial Growth Basal Medium -2

EC - endothelial cells

ECM - Extracellular Matrix

EGF- Epidermal Growth Factor

ELISA- Enzyme-Linked Immunosorbent Assay

ERK- Extracellular Signal-regulated Kinase

FBS- Fetal Bovine Serum

FDA- Food and Drug Administration

FGF - Fibroblast Growth Factors

GAPDH- Glyceraldehyde 3-Phosphate Dehydrogenase

HGF- Hepatocyte Growth Factor

HIF-1- Hypoxia Inducible Factor-1

HUVEC- Human Umbilical Vein Endothelial Cells

IGF- Insulin-like Growth Factor

IL- Interleukin

IFN- Interferon

ISCT- International Society for Cellular Therapy

LF- Lipofectamine

MAPK- Mitogen Activated Protein Kinase

MC- Minicircle

MSC- Mesenchymal Stem/Stromal Cells

MHC- Major Histocompatibility Complex

miRNA- microRNA

MMP- Matrix Metalloprotease

MP- Miniplasmid

MRS- Multimer Resolution Sites

PBS- Phosphate Buffered Saline

PDGF- Platelet-Derived Growth Factor

pDNA- Plasmid DNA

PHD- Prolyl Hydroxylase

PKB/Akt -Protein Kinase B

PGF- Placental Growth Factor

Pol- RNA Polymerase

PP- Parental Plasmid

pri-miRNA- primary microRNA

RBDs- RNA-binding domains

RISC- RNA-Induced Silencing Complex

RNAi- RNA interference

RNase- Ribonuclease

RTK- Receptor Tyrosine Kinase

RT-qPCR- Real-time quantitative PCR

SDF1-α- Stromal Cell-Derived Factor 1 Alpha

shRNA- short-hairpin RNA

siRNA- small/short interfering RNA

STAT3- Activators of Transcription 3

TGF- Transforming Growth Factor

TNF- Tumour Necrosis Factor

UC- Umbilical Cord

UTR- Untranslated Region

VEGF- Vascular Endothelial Growth Factor

VHL- Von Hippel–Lindau

%KD- Percentage of Knockdown

1. Introduction

1.1. Angiogenesis in Cancer

1.1.1. The concept of angiogenesis

The generation of blood vessels occurs by different mechanisms. Vasculogenesis consists in the *de novo* formation of blood vessels from mesoderm-derived endothelial precursors. During embryologic development, these precursors (angioblasts) differentiate into endothelial cells (ECs), leading to the formation of lumens and establishment of primitive blood vessels, giving rise to the first vascular system of human body (*Figure 1.1A*). The remodelling and expansion of this network is achieved by a process called angiogenesis (*Figure 1.1B*), that is generally defined as the growth or formation of new blood vessels from the pre-existing vasculature.[1,2]

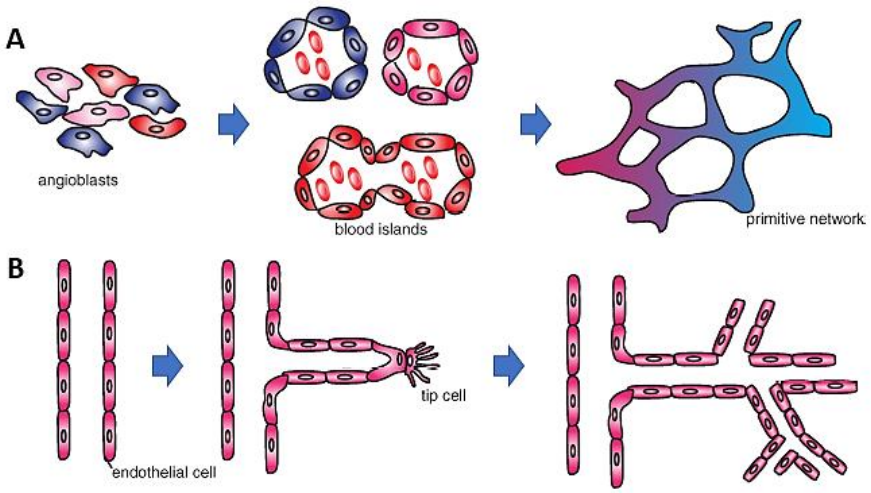

Figure 1.1- Different types of blood vessel growth: **(A)** Vasculogenesis is defined as the growth of a primitive vascular network out of precursory cells, the angioblasts; **(B)** Angiogenesis is the growth of new blood capillaries by sprouting from pre-existing blood vessels. Adapted from Bronckaers *et al* (2014)[3]

In healthy tissue, a regularly patterned and functioning vasculature is formed, in which the small blood capillaries are hollow tubes composed by a monolayer of ECs supported by mural cells, such as pericytes, and surrounded by a basement membrane and extracellular matrix (ECM).[4] The majority of blood vessels and ECs remain quiescent throughout adult life, however, they maintain the capacity to rapidly proliferate and sprout in response to angiogenic stimuli, such as hypoxia hypoxia (i.e. low oxygen tension compared to atmospheric air) and inflammation.[5,6] The process begins with the enzymatic degradation of capillary basement membrane and ECM, resulting in the dissociation of the mural cells and liberation of the ECs. The ECs proliferate and migrate towards the angiogenic stimulus through the guidance of the specialized endothelial “tip cell” that sprout through the ECM, aided by filopodia. This cell is followed by stalk cells which are responsible for the elongation of the sprout and formation of the

lumen of the primitive vessel. Then, the tip cells from adjacent sprouts fuse leading to the formation a continuous lumen through which blood can perfuse. Finally, stabilization of vessels by recruitment of pericytes is established and the ECs resume their quiescent state.[2,5]

Angiogenesis involves a complex and dynamic interaction between ECs and the corresponding extracellular environment, in which the balance between angiogenic activators and angiogenic inhibitors tightly controls the rate of blood vessel formation (*Figure 1.2*).[7] These factors include several cytokines and soluble growth factors that act as angiogenic stimulators, such as acidic and basic fibroblast growth factors (FGF) and vascular endothelial growth factor (VEGF), which are associated with EC growth and differentiation, or transforming growth factor (TGF) - β and angiogenin that enhance the differentiation of ECs. On the other hand, there are also factors that act as angiogenesis inhibitors, among them several ECM-bound cytokines such as angiostatin, thrombospondin, and endostatin. Sources of these factors include ECs, fibroblasts, smooth muscle cells, platelets, inflammatory cells, and cancer cells.[7,9]

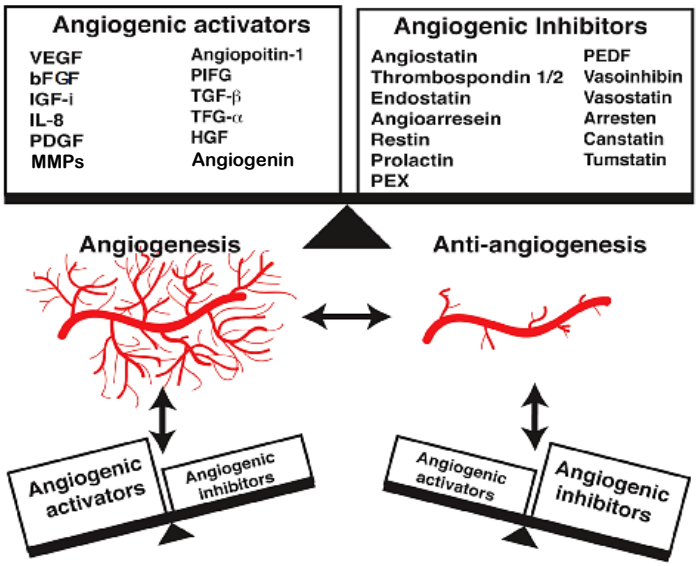

Figure 1.2 - The angiogenic balance between angiogenic activators and angiogenic inhibitors regulate vascular homeostasis. Adapted from Gunda *et al* (2012).[10]

The angiogenic process begins *in utero* and prolongs throughout life, occurring both in health and disease. In fact, this phenomenon is essential in various physiological processes within the human body, occurring not only during fetal development or in organ growth after birth, but also during adulthood. It has major role in reproduction, as it occurs naturally in the placenta and uterus during pregnancy and in the ovary during follicle development, ovulation and corpus luteum formation. Another instance in which it occurs later in life is in regeneration of damaged tissues during the wound healing in healthy adults. [2,6]

Nevertheless, several diseases include excessive or deficient angiogenesis as part of the pathology, as the balance between stimulant and inhibitory angiogenic factors is often disturbed. In conditions such as ischemic heart disease, peripheral arterial disease, preeclampsia, chronic wounds,

stroke or myocardial infarction the balance between angiogenic inhibitors and activators tilts towards inhibition of angiogenesis, which can lead to EC dysfunction, vessel malformation or regression and prevention of revascularization. Thus, stimulation of angiogenesis can be therapeutic in such diseases. On the other hand, in various disorders the angiogenic stimulus becomes excessive, resulting in an "angiogenic switch". The best-known conditions in which angiogenesis is switched on are malignant, ocular diseases, such as macular degeneration, and chronic inflammatory diseases, such as rheumatoid arthritis. In these disorders, therapeutic inhibition of angiogenesis can be an option of improvement.[2,6]

1.1.2. Vascular Endothelial Growth Factor A (VEGF-A)

VEGF is considered one of the most important pro-angiogenic factor during growth and development, as well as in diseases such as cancer, diabetes, and macular degeneration. VEGF stimulate the EC functions needed for new blood vessel formation, generally by inducing EC proliferation, survival, migration, and differentiation. VEGF also potentiates vascular permeability, which can both precede and accompany angiogenesis.[11,12]

In humans, the VEGF family currently comprises five members: VEGF-A, VEGF-B, VEGF-C, VEGF-D and placental growth factor (PGF). VEGF-A is the key regulator of blood vessel growth and VEGF-C and VEGF-D regulate lymphatic angiogenesis. The human VEGFA gene is organized in eight exons separated by seven introns, that by alternative exon splicing generates at least seven different molecular variants (*Figure 1.3*). $VEGF_{165}$ is the predominant isoform *in vivo*, lacking the residues present in exon 6.

VEGF-A exerts its biologic effect through interaction with cell-surface receptors, binding to two related transmembrane receptor tyrosine kinases (RTK): VEGFR-1 and VEGFR-2, selectively expressed on ECs.[11–13]

Interestingly, although VEGFR-1 has a high affinity for VEGF-A, its tyrosine kinase activity is approximately 10-fold weaker than that of VEGFR-2.[13] VEGFR-2 is considered the primary signalling receptor for VEGF, integrating VEGF ligand-mediated extracellular signals to activation of numerous transduction cascades, including mitogen activated protein kinase (MAPK), phosphatidyl inositol 3-kinase, protein kinase C, protein kinase B (Akt), and phospholipase C pathways, that can lead to ECs proliferation and migration, matrix metalloproteases (MMPs) expression, survival, and cell permeability.[11–13]

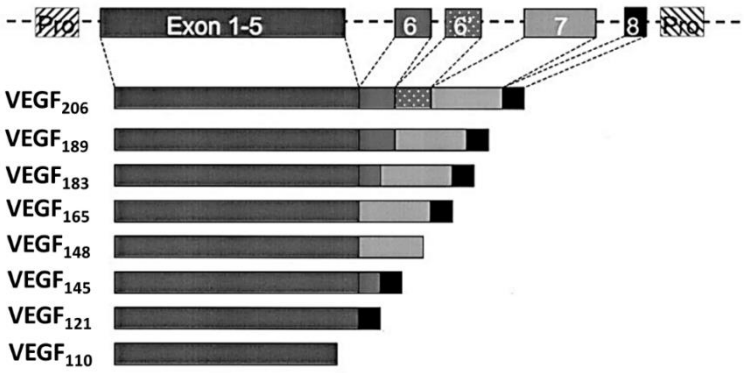

Figure 1.3- Gene structure of VEGF-A, comprising eight exons that give rise to at least seven isoforms of 121, 145, 148, 165, 183, 189, and 206 amino acids through alternative splicing. An additional isoform of 110 amino acids results from proteolytic cleavage. Adapted from Hoeben *et al* (2004)[12]

One of the most described regulation mechanisms of VEGF expression is oxygen tension, through the helix-loop-helix transcriptional regulator hypoxia inducible factor-1 (HIF-1) pathway. Briefly, under normoxic (atmospheric) conditions, α-ketoglutarate-dependent prolyl hydroxylases (PHDs) catalyse the hydroxylation of proline residues of HIF-1α allowing its association with the Von Hippel–Lindau (VHL) -E3 ubiquitin ligase complex that targets HIF-1α for ubiquitin-mediated proteosomal degradation. On the other hand, under hypoxic conditions, PHD and factor-inhibiting HIF activity is inhibited and unhydroxylated HIF-1α and HIF-2α translocate to the nucleus, forming a heterodimer complex with HIF-1β and p300. Finally, the transcriptional complex binds to hypoxia response elements in the promoter region of the VEGF gene to enhance VEGF transcriptional expression.[14]

Additionally, several major growth factors namely epidermal growth factor (EGF), TGF-α and β, insulin-like growth factor (IGF), FGF and platelet-derived growth factor (PDGF) and inflammatory cytokines such as Interleukin (IL) - 1α and IL-6 induce VEGF expression in several cell types, including epithelial, mesenchymal, and tumour cells, activating VEGFRs on the nearby endothelium, thus stimulating angiogenesis in the source tissue.[11]

1.1.3. Tumour angiogenesis

In growing cancers, tumour-infiltrating cells of hematopoietic origin are recruited from the bone marrow (BM) to the tumour via the systemic circulation including diverse leukocyte types and subtypes, such as monocytes and macrophages, neutrophils and lymphocytes. Non-haematopoietic, BM-derived endothelial or mesenchymal progenitors are also found to contribute to tumour angiogenesis. Additionally, tissue-resident cells are also recruited, including ECs, pericytes, fibroblasts and adipocytes.[15] Together, the broad range of signals secreted by tumour-associated cells, such as IL-1β, IL-6, FGF-2, tumour necrosis factor (TNF)-α and VEGF, and the ECM in which they are embedded sustain angiogenesis throughout the subsequent phases of tumour progression.[15]

Additionally, vessel growth is not only stimulated but can lead to the formation of abnormal vessels in terms of structure and function, including unusual leakiness, potential for rapid growth and remodelling, high tortuosity and sinusoidal appearance, poor coverage by vascular supportive cells and incorporation of tumour cells into the endothelial wall.[16] Abnormal tumour vessels can also contribute to the resistance of tumour cells to common therapies since they obstruct the function of immune cells in tumours, as well as the transport and distribution of chemotherapeutics.[2,4] Besides that, these phenotypes mediate the dissemination of tumour cells in the bloodstream and sustain the pathological characteristics of the tumour microenvironment.[16]

Moreover, tumour hypoxia arises due to a combination of excessive oxygen consumption by cancer cells and disorganized tumour-associated vasculature, leading to both acute fluxes in oxygen tension and diffusion-limited regions of low oxygen levels within the tumour.[14]

One essential pathway activated under hypoxia is the HIF signalling pathway that induce transcription of target genes important for various processes such as metabolism, cell growth and also angiogenesis, such as erythropoietin, VEGF and PDGF.[16] In some cancers, mutations of the machinery regulating HIF stability can result in constitutive activation of HIF signalling, and as a result these tumours are notoriously highly vascularized. For example, owing to its crucial role in HIF-α degradation, loss-of-function mutations in the VHL gene are characteristic in clear cell renal-cell carcinoma.[17]

Thus, given the fact that angiogenesis is a key step in the development and spread of cancer, blocking angiogenesis seems promising strategy to slow down tumour growth. In fact, several anti-angiogenic drugs were approved by Food and Drug Administration (FDA) and are currently used, in combination with conventional chemotherapeutics, for the treatment of several malignant diseases ranging from breast, lung, gastric, colorectal, hepatocellular, glioblastoma, and neuroendocrine tumours (*Table 1.1*).[18]

For example, Bevacizumab is a humanized monoclonal antibody that blocks tumour cell-derived VEGF-A, preventing its binding to VEGFR1 and VEGFR2 in ECs, impairing the development of new vessels and leading to tumour starvation and, consequently, growth inhibition. This drug is administered in combination with antineoplastic agents to treat several types of cancer, such as metastatic colorectal cancer.[19]

Another example is Temsirolimus, inhibitor of the mammalian target of rapamycin kinase, a component of intracellular signalling pathways involved in the growth and proliferation of cells and their response to hypoxic stress.[20] The inhibition of angiogenesis in advanced renal-cell carcinoma by Temsirolimus is clinically relevant because unregulated angiogenesis is prominent feature that particular cancer.

Furthermore, several drugs act as RTK inhibitors, such as Sorafenib, a multikinase inhibitor of the VEGF and PDGF receptor, used to treat in advanced hepatocellular carcinoma.[21]

Overall, the anti-angiogenic agents can improve the delivery of cytotoxic agents to the tumour site, may alter hypoxia in the tumour and sensitize it to chemotherapy or may impede the ability of the tumour to recover from cytotoxic effects of chemotherapeutic agents [16]

Table 1.1 - FDA-approved anti-angiogenic drugs, used for the treatment of several types of cancer. These strategies are being used in combination with conventional chemotherapeutics. Adapted from Rajabi *et al* (2017).[18]

Generic Name	FDA-Approved Indication
Bevacizumab	Colorectal, non-small-cell lung, and glioblastoma multiforme
Thalidomide	Myeloma
Lenalidomide	Myeloma (myelodysplastic syndrome (MDS))
Sorafenib	Renal cell and hepatocellular carcinoma
Sunitinib	Renal cell and gastrointestinal carcinoma
Temsirolimus	Renal cell carcinoma
Axitinib	Renal cell carcinoma
Pazopanib	Renal cell carcinoma, kidney cancer, and advanced soft tissue sarcoma
Cabozantinib	Thyroid cancer
Everolimus	Kidney cancer, advanced breast cancer, pancreatic neuroendocrine tumours (PNETs), and subependymal giant cell astrocytoma
Ramucirumab	Stomach cancer and gastroesophageal junction adenocarcinoma
Regorafenib	Colorectal cancer and gastrointestinal stromal tumour
Vandetanib	Thyroid cancer
Ziv-aflibercept	Colorectal cancer

1.2. Mesenchymal Stem/Stromal Cells (MSCs) angiogenic properties in Cancer

1.2.1. MSCs and their therapeutic properties

Mesenchymal Stem/Stromal Cells (MSCs) are a diverse subset of adult, fibroblast-like, multipotent precursors capable of differentiate into tissues of mesodermal origin, such as osteoblasts, chondrocytes and adipocytes.[22] MSCs are present in perivascular locations, on both arterial and venous vessels, from nearly all tissues in the adult body, providing stromal support to the maintenance of a dynamic and homeostatic tissue microenvironment.[23]

The usage of the term “Mesenchymal Stem Cells” has raised many questions so, in order to clarify confusing nomenclature, the International Society for Cellular Therapy (ISCT) suggested that the use of the term Mesenchymal Stromal Cells (also abbreviated to MSCs) should be applied for the *in vitro* cultured cells, restricting the term Stem Cell to designate the proposed *in vivo* precursors/stem cells.[24,25]

Although the identification of MSCs in mixed populations of cells is still challenging, there is a minimum criteria to define these cells proposed by the ISCT[26]: 1) Adherence to plastic in standard culture conditions; 2) Expression of the cell surface molecules CD105 (endoglin), CD73 (ecto 5′ nucleotidase) and CD90 (Thy-1) and the absence of the hematopoietic markers CD34, CD45, CD14 (or CD11b), CD79α (or CD19) and major histocompatibility complex (MHC) II class cellular receptor HLA-

DR; 3) *In vitro* differentiation into osteoblasts, adipocytes and chondrocytes, demonstrated by staining of cell culture.

In the last few years, the isolation of adult MSCs from various sources has been reported, however, Bone Marrow (BM)-derived stem cells first described by Friedenstein *et* al (1976),[27] are still considered the gold standard, being the most widely studied cell type. These sources include various adult tissues, such as adipose tissue (AT), peripheral blood, synovial fluid, lung, heart or dental tissues. Besides that, MSCs can also be isolated from several birth-associated tissues including placenta, amniotic fluid, amniotic membrane, umbilical cord (UC), cord blood, and Wharton's jelly.[28,29]

In terms of therapeutic applications, expanded MSCs are being extensively studied for their therapeutic properties including their differentiation potential, homing capacity, immunosuppressive activity, trophic/paracrine effects and transfer of vesicular components (*Figure 1.4*).

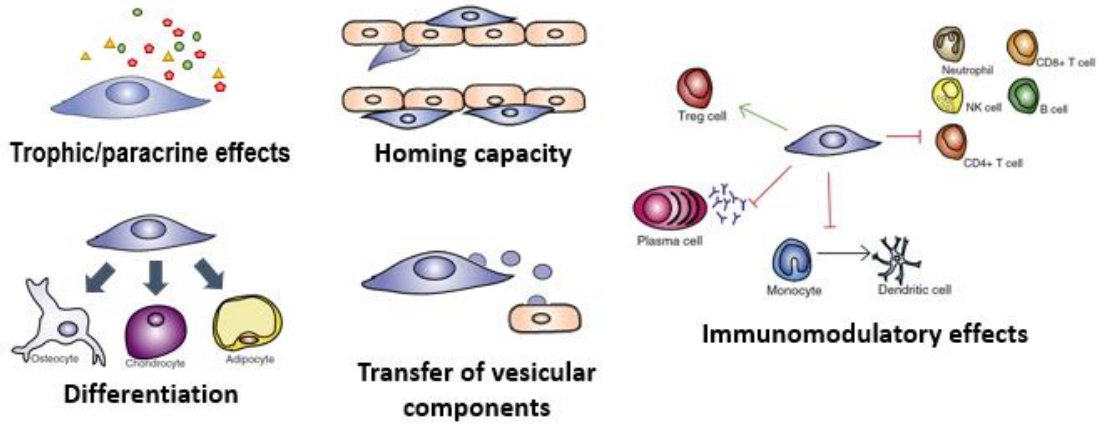

Figure 1.4 - Summary of the therapeutic properties of MSCs including their differentiation potential, homing capacity, immunosuppressive activity, trophic/paracrine effects and transfer of vesicular components. Adapted from Bronckaers *et al* (2014)[30]

Regarding their application in regenerative medicine, as MSCs display a broad differentiation capacity *in vitro*, it was originally hypothesized that MSC transplantation would be beneficial in the repair of serious connective tissue trauma and disease, as they would migrate to sites of injury, engraft, and differentiate into functional cells replacing the damaged host tissue. However, numerous studies revealed that these cells have a low engraftment efficacy as they engraft in low numbers and for short-term, not being sufficient to explain the beneficial effects of MSCs administration.[31]

Nevertheless, there is accumulating evidence that the positive results in terms of tissue replacement can be attributed to MSC's ability to locally modulate the host microenvironment by secretion of biologically active molecules that induce tissue repair, including a wide spectrum of growth factors, chemokines and cytokines. These molecules are generally defined as the MSC secretome and can have several trophic effects namely minimizing apoptosis, inducing angiogenesis, support of proliferation/differentiation of host's progenitors/stem cells and recruitment of endogenous cells.[31–33]

In addition, MSCs can preferentially migrate or dock at injured sites, process also referred as "homing", by chemoattraction and ligand/receptor interactions between MSCs and active ECs.[32] As

such, systemically delivered MSCs have the ability to migrate towards areas where their paracrine effects are most needed, adding to the regenerative properties of MSCs.

Furthermore, MSCs possess a broad range of immunomodulatory features that support their clinical use, as they can sense inflammation and adopt a pro-inflammatory or anti-inflammatory behaviour depending on the environment. MSCs affect both adaptive and innate immunity thought the secretion of soluble factors and cell contact-dependent mechanisms.[32] It is important to note that due to low expression of MHC I and lack of expression of MHC class II along with other co-stimulatory molecules, MSCs have reduced alloreactivity which is a major benefit in terms of host compatibility issues during MSCs transplantation.[34]

Another mechanism by which MSCs affect the host is through the transfer of vesicular components, namely exosomes carrying a variety of protein, lipids, and most importantly mRNAs and microRNAs (miRNAs).[31] Thus, MSC-derived vesicles are able to influence the recipient cells, both at genetic and biochemical levels, exerting a novel paracrine effect by modulation of several physiological processes.

1.2.2. MSCs and angiogenesis

As mentioned above, MSCs have the ability to induce angiogenesis. The process occurs mostly by the activation of host ECs by cell–cell contact or by secretion of a broad range of growth factors, cytokines and other proteins with pro-angiogenic properties, participating in various steps of the angiogenic process, such as EC proliferation, migration and tube formation, breakdown of the ECM and vessel stabilization. MSCs can also protect ECs from apoptosis (*Figure 1.5*).[3]

Currently, as reviewed in Bronckaers *et al* (2016), factors detected in BM-derived MSC secretome include VEGF, FGF, IL-6, angiopoietin-1/2, PGF, monocyte chemoattractant protein-1 and cysteine-rich angiogenic inducer 61 protein, which generally induce EC proliferation, survival, migration, and tube formation. Additionally, macrophage inflammatory protein-1alpha and beta are also secreted by BM-derived MSCs acting as pro-inflammation agents and chemoattractants of immune cells. Finally, MMP-2 and angiogenin were also detected in BM-MSC secretome and their angiogenic activity is ECM degradation and vessel stabilization, respectively.

Regarding other tissue sources, placental MSCs produce IL-6, adipose-derived MSCs secrete high amounts of VEGF, hepatocyte growth factor (HGF) and TGF-β and dental pulp MSCs express high levels of VEGF, monocyte chemoattractant protein-1 (or CCL2) and IL-8 (or CXCL8).[3,30]

Additionally, growing evidence suggest that MSC-derived exosomes play a significant role in angiogenesis, as they mediate intercellular communication between different cell types in the body, by bearing numerous paracrine factors that often contributes to this dynamic process.

For example, it was found that exosomes derived from human UC-MSC could enhance the growth and migration of normal and chronic wound fibroblasts and induce angiogenesis *in vitro*. Also, uptake of MSC exosomes by human umbilical vein endothelial cells (HUVEC) resulted in dose-dependent increase of tube formation by EC. Finally, these vesicles were shown to activate different

signalling pathways important in wound healing, such as Akt, extracellular signal-regulated kinase (ERK), and activators of transcription 3 (STAT3), and induce the expression of several growth factors including HGF and IGF-1.[35]

Another example was reported by Liang and colleagues, that found that exosomes generated by human AT-MSC enhanced EC tube formation both *in vitro* and *in vivo*, in part by the action of miRNA-125a that promotes tip cell specification through direct suppression of its target delta-like 4.[36]

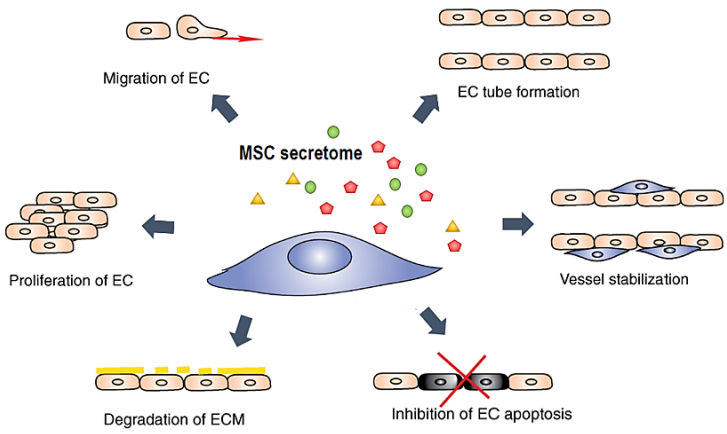

Figure 1.5 - MSCs secrete a broad range of growth factors, cytokines and other proteins with pro-angiogenic properties, inducing ECs proliferation and migration, stimulation of tube formation, enhancement of matrix degradation and blood vessel stabilization and maturation. Adapted from Bronckaers *et al* (2016)[3]

1.2.3. MSCs in tumour development

As previously mentioned, through chemoattraction, MSCs are able to migrate to a target tissue. Chemokines and other cytokines are extremely abundant in the tumour microenvironment, being produced not only by tumour cells but also its surrounding cells. These molecules include CCL2, CCL15, CCL20, CCL25, CXCL1 and CXCL8, being the primary reason for MSCs homing to tumour sites.[37,38] In addition, tumour treatment can contribute to MSCs recruitment into the tumour microenvironment, since irradiation of cancer cells increases the expression of several inflammatory mediators, including TGF-β, VEGF and PDGF-B.[39] Furthermore, upon interaction with cancer cells, MSCs will secrete cytokines such as CXCL1-2 or IL-6 and MMPs in which the latter will promote ECM degradation and favour migration.[38]

As reviewed in Lazennec *et al* (2016)[38], several studies in the field of tumour development have described the potential pro- or anti-tumorigenic action of MSCs. Considering its pro-tumorigenic features, MSCs are able to modulate the growth, response to the treatment (e.g. chemotherapy and/or radiotherapy), angiogenesis, invasion and metastasis of tumours, via direct contact or through the production of growth factors, cytokines and chemokines in a paracrine manner (*Figure 1.6*), thus supporting the replicative immortality, proliferative signal and metabolism of cancer cells.

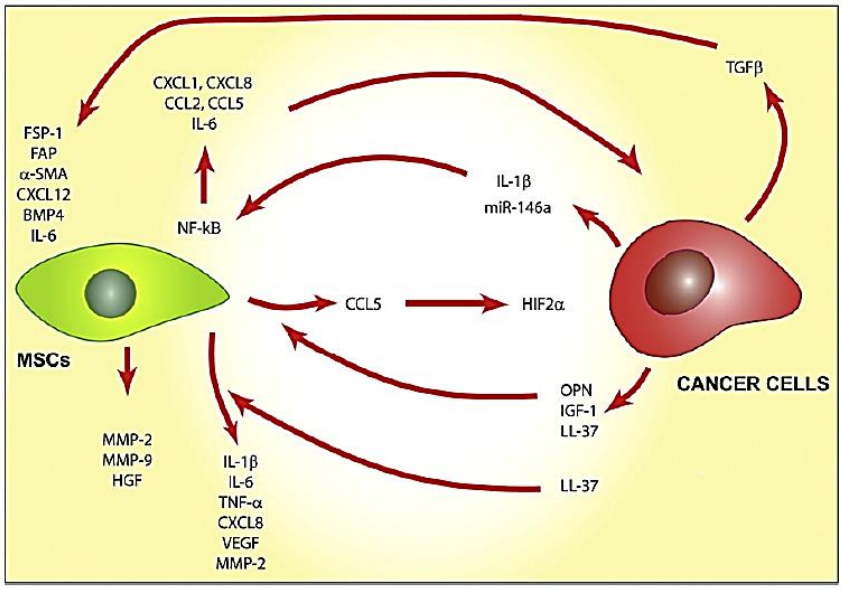

Figure 1.6 - Scheme of the some of the factors favouring tumour growth by MSCs, namely by sustaining proliferative and metastatic signal of cancer cells. From Lazennec *et al* (2016)[38]

Another mechanism by which MSCs can promote tumour development is by transiting to cancer associated fibroblasts (CAFs). CAFs are a component of the tumour that contributes to cancer progression by stimulating cancer cell growth, inflammation, angiogenesis and invasion, through specific communications with cancer cells. CAFs also secrete a variety of cytokines and growth factors such as CXCL1, CXCL2, IL-1β and IL-6. MSCs were found to home to tumours and transit into CAFs leading to the formation of a much more aggressive type of tumour.[40]

As referred previously, tumour angiogenesis is one of the hallmarks in cancer progression. Therefore, one of the tumour-promoting effects of MSCs is their ability to promote angiogenesis in tumour microenvironment, as described in the following studies.

Spaeth *et al* (2009), found that human BM-MSCs shows a significantly increased secretion of the angiogenic factors TGF-β, VEGF and IL-6 following 24 hour culture with human ovarian cancer Skov-3 conditioned medium (CM).[41] Similarly, Zhang and colleagues showed that human BM-MSCs, when exposed to human prostate cancer CM or in co-culture, overexpress markers associated with neovascularization (macrophage inflammatory protein-2, VEGF, TGF-β and IL-6). [42]

In another study, Beckerman and colleagues demonstrated that BM-MSC specifically migrate to tumour blood vessels of pancreatic carcinoma *in vitro* and *in vivo* when injected in nude mice. MSCs also support tumour angiogenesis *in vivo*, since vessel density was increased after MSCs injection. Additionally, MSC induce sprouting in endothelial cells *in vitro* due to the secretion of VEGF.[43]

Considering the alterations on the tumour microenvironment in reponse to treatment, a study showed that radiation therapy led to the increased release of stromal cell-derived factor 1 alpha (SDF1-α) and PDGF-B by tumour cells, which not only attract MSCs but also induces MSC to differentiation into pericytes and promote vasculogenesis.[44]

In another study, Huang and colleagues demonstrated that colorectal cancer cells, when mixed with MSCs, increase the tumour growth rate and angiogenesis by the production of IL-6 that increases the secretion of endothelin-1 in cancer cells, which induces the activation of Akt and ERK in ECs, thereby enhancing their capacities for recruitment endothelial cells to tumour.[40]

In Liu *et al* (2011) [45], MSCs stimulated by inflammatory cytokines, such as Interferon (IFN)-γ and tumour necrosis factor (TNF)-α,in the tumour microenvironment express higher levels of VEGF via the HIF-1α signalling pathway and promote tumour angiogenesis, leading to colon cancer growth in mice.

In Zhang *et al* (2018), it was found that colorectal derived MSCs enhance the growth and metastasis of colorectal cancer *in vivo* and identified IL-6 as the most secreted cytokine. Additionally, MSCs had a positive effect on colorectal cancer cell stemness, and promoted angiogenesis *in vitro* producing high levels of VEGF.[46]

In another study, Muehlberg and colleagues, demonstrated that murine AT-MSCs, when added to a murine breast cancer cell line, were responsible for a significantly faster tumour growth and enhance the AT-MSCs secretion of SDF1-α. Vascularity and capillary density were also found to be enhanced by AT-MSC.[47]

Regarding MSCs-vesicles, it was reported that exosomes derived from human BM-MSCs induce an increase in VEGF in gastric carcinoma cells, through activation of ERK1/2 and p38 MAPK pathways, that regulate the VEGF expression, resulting in enhanced tumour angiogenesis, which in turn promotes the tumour growth *in vivo.*[48] Furthermore, another study reported that human BM-MSC-exosomes facilitates nasopharyngeal carcinoma progression in terms of tumour proliferation, migration and angiogenesis through the FGF19-mediated activation of the FGF receptor 4 signalling cascade.[49]

1.3. RNA interference (RNAi) gene silencing

RNA interference (RNAi) discovery has revolutionized the understanding of gene regulation by revealing a collection of related pathways in which small (~20–30 nucleotide (nt)) non-coding RNAs and their associated proteins control the expression of genetic information. Two primary categories of these small RNAs – microRNAs (miRNAs) and small/short interfering RNAs (siRNAs) - act in both somatic and germline lineages in a broad range of eukaryotic species to regulate endogenous genes and to defend the genome from invasive nucleic acids, by a post-transcriptional gene-silencing pathway that mediates the degradation of a target mRNA.[50–52]

RNAi was initially discovered by Lee and colleagues in the form of a single miRNA in the *Caenorhabditis elegans* genome, in which the gene *lin-4* encoded small RNAs with antisense complementarity to *lin-14*.[53] Eventually, such miRNAs were found to be widespread: 5% of human genome is dedicated to encoding and producing the >1,000 miRNAs that regulate at least 30% of human genes. These endogenous and purposely expressed molecules regulate eukaryotic gene expression in vital processes such as cell growth, tissue differentiation, heterochromatin formation, and cell proliferation. Likewise, RNAi dysfunction has been linked to several diseases including cardiovascular diseases, neurological disorders, and many types of cancer.[52]

On the other hand, siRNAs are thought to be primarily exogenous in origin, derived directly from the virus, transposon, or artificially synthetizes and introduced into cells. A landmark study developed by Elbashir and colleagues, showed that transfection of mammalian cells with chemically synthesized 21-nucleotide siRNA molecules could result in sequence-specific target gene silencing via the RNAi pathway.[54] Since then, these molecules have been extensively used in for loss-of function studies clarifying enormous amounts of information relating to gene function. In addition, siRNAs have been applied in biomedical research in hopes of developing siRNA-based therapies to combat of a wide range of disorders including cancers and virus infections.[51,52]

Besides their origin, another characteristic that distinguish miRNAs and siRNAs reside in the double-stranded RNA (dsRNA) precursors of each: miRNAs appeared to be processed from stem-loop precursors with incomplete double-stranded character, whereas siRNAs were found to be excised from long, fully complementary dsRNAs.[50,52]

1.3.1. Biogenesis and Action of miRNA and siRNA

Despite their differences, the size similarities and sequence-specific inhibitory functions of miRNAs and siRNAs support their relatedness in biogenesis and mechanism (*Figure 1.7*).

Briefly, the biogenesis of mature miRNAs initiates by transcription of the encoding genes by RNA polymerase II (Pol II). This results in at least 1,000 nt long, capped and polyadenylated primary miRNAs (pri-miRNAs), with double-stranded stem-loop structure, containing single or clustered hairpins. These pri-miRNAs are cropped by the microprocessor complex composed by the ribonuclease (RNase) III Drosha and DiGeorge syndrome critical region 8 (DGCR8), a protein containing two double-stranded RNA-binding domains (RBDs), into double-stranded hairpin structure precursor miRNAs (pre-miRNAs) of 60–100 nucleotides.[50–52,55] DGCR8 directly interacts with the pri-miRNA flaking its single-stranded segments. This is a critical for processing since the Drosha cleavage site is determined by the distance from the single-stranded RNA-dsRNA junction (approximately ~11bp away).[56]

The resulting pre-miRNA are subsequently transported from the nucleus to the cytoplasm by Exportin 5 and RanGTP transport facilitators. [51,52,55]

Then, occurs a second processing step performed by a Dicer enzyme, large endoribonuclease containing a helicase domain and an internally dimerized pair of RNase III domains. This results in the excision of the terminal loop from the pre-miRNA. The PAZ domain of Dicer interacts with the 3' overhang and determines the cleavage site by positioning the RNase III catalytic sites two helical turns or approximately 22 bp away from the terminus/PAZ portion of the Dicer-RNA complex, leading to a mature miRNA duplex composed by 19- to 25-nt strands, bearing a 2-nt overhang at each 3' terminus and a phosphate group at each recessed 5' terminus.[50–52,55]

Similarly, long, perfectly base-paired dsRNAs precursors are also recognized and cleaved by Dicer resulting in siRNAs duplexes, once more with 19- to 25-nt strands with 2-nt 3' overhangs.[50–52]

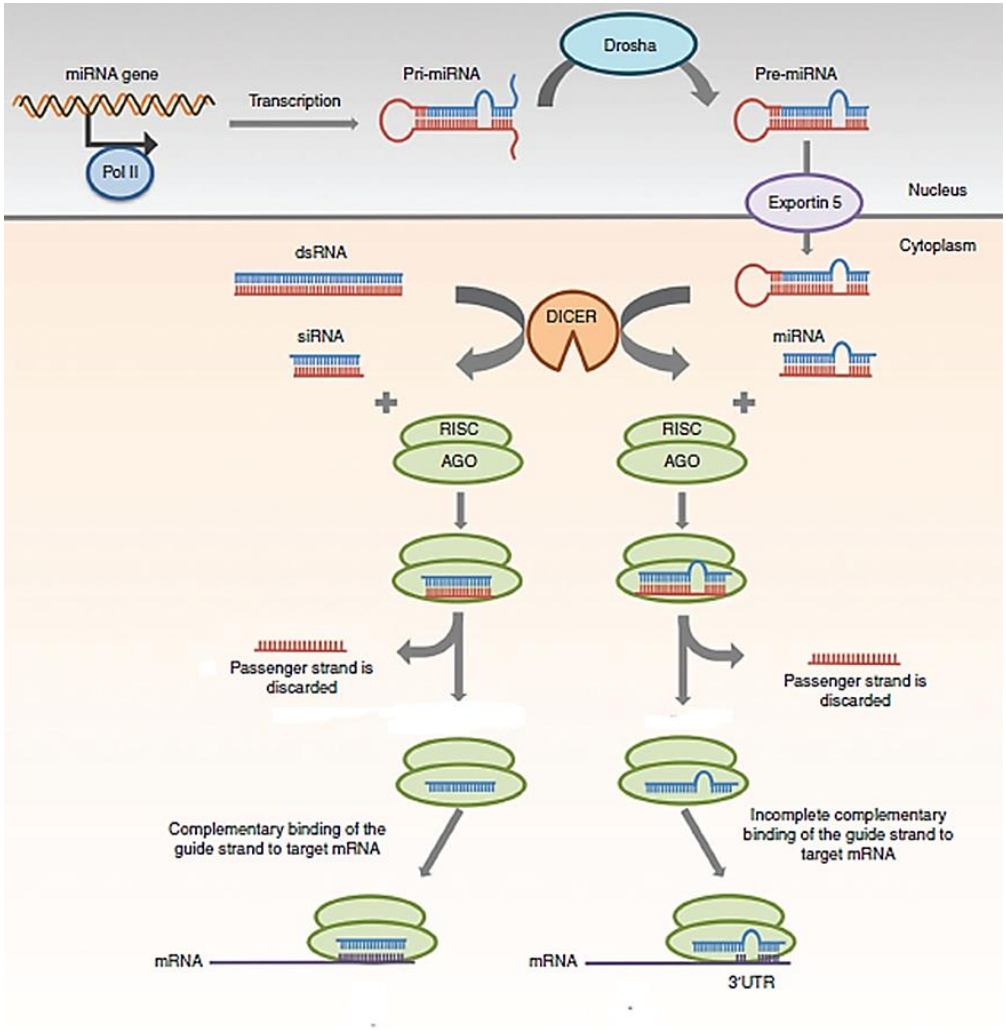

Figure 1.7 - Schematic representation of miRNA and siRNA biogenesis and gene silencing mechanisms. Endogenous or exogenous dsRNAs are processed by Dicer into siRNA which is loaded into Argonaute protein (AGO), generating the RNA-induced silencing complex (RISC). After cleavage of the passenger strand, the active RISC to the target mRNA complementary to the guide strand. The full complementary binding between the guide strand of siRNA and the target mRNA leads to the cleavage of mRNA, while partially complementary binding can induce different post-transcriptional silencing mechanisms. In the case of miRNAs, they are originated by RNA polymerase II in the nucleus, and after Drosha processing, they are transported to the cytoplasm and recognized by Dicer. Adapted from Lam *et al* (2015)[51]

After Dicer processing, dsRNA duplex of the appropriate size is loaded onto an Argonaute protein (AGO), that recognizes the 3' terminus and 5' phosphate of the guide strand through its PAZ and MID domains respectively, generating the RNA-induced silencing complex (RISC). RISC loading is coincident with the strand selection step, in which the passenger strand (sense strand) of the duplex is cleaved and discarded, while the guide strand (antisense strand) remains associated with the complex. Subsequently, RISC performs cellular surveillance, silencing single-stranded-RNA sequences complementary to its bound guide strand (target mRNA). [51,52,55]

Considering the different characteristics of their dsRNA precursors, the post-transcriptional gene-silencing response of miRNAs and siRNAs differ.

In the case of the siRNA-mediated pathway, the siRNA guide stand directs RISC to fully complementary RNA targets. The complementary binding between the guide stand and the target mRNA, activates the PIWI domain of AGO resulting in the cleavage of the phosphodiester backbone of the target at the nucleotides that are base paired to siRNA residues 10 and 11 from 5′ terminus. After cleavage, the target dissociated from the siRNA, releasing RISC to act on additional targets. After dissociation, the generated mRNA products with 5'-monophosphate and 3'-hydroxyl termini, are further degraded by cellular exonucleases. The newly generated 3' end of cleavage products is also a substrate for oligouridylation, which can promote exonucleolytic targeting. [50,51]

By contrast, the target recognition of miRNA is more complex, since miRNA only requires to be partially complementary to its target mRNA to induce RNAi mechanism. Therefore, miRNAs have the characteristic of having multiple targets since they are able to recognize an array of mRNAs with different binding sites and different degree of complementarity. For example, a microarray analysis showed that after the miRNA-124, which is preferentially expressed in brain tissues, can downregulate 174 annotated genes.[57] Typically, mature miRNAs regulate gene expression through sequence-specific binding to the 3′ untranslated region (UTR) of a target mRNA. However, several evidences indicate that miRNAs can also bind to other regions of a target mRNA, namely centered sites, 3′ supplementary sites and bulged sites, although a key feature of recognition involves Watson-Crick base pairing of miRNA nucleotides 2–8, representing the seed region.[50,51] The degree of miRNA-mRNA complementarity has been considered a key determinant of the regulatory mechanism. Due to the partially complementary base pairing between the miRNA and the target, the AGO of RISC is not activated. Instead, the silencing of the mRNA targets of miRNA occurs through: translation repression where miRNA-RISCs bind to target mRNA repressing initiation at the cap recognition stage or the 60S recruitment stage; deadenylation induction of the mRNA and thereby inhibit circularization of the mRNA before translation; repression of a post-initiation stage of translation by inducing ribosomes to drop off prematurely; mRNA degradation by inducing deadenylation followed by decapping.[50,51]

In rare cases, high level of complementary between mRNA and miRNA leads to the endonucleolytic cleavage of mRNA by AGO protein, a mechanism that is similar to siRNA-mediated gene silencing.[51] Similarly, siRNA-mediated post-transcriptional silencing can occur by translational repression or exonucleolytic degradation in a manner similar to miRNA silencing. This happens when mismatches near the center of the siRNA/target duplex suppress AGO endonucleolytic cleavage or targets are recognized by AGO proteins that lack endonuclease activity even with perfectly complementary complexes.[50]

Despite the understanding of miRNAs as negative regulators of gene expression, growing evidence suggest that miRNA can act as positive regulators. This includes evidence that miRNAs can also increase the translation of a target mRNA by recruiting protein complexes to the AU-rich elements of the mRNA. In addition, miRNAs can indirectly increase the target protein output by de-repressing mRNA translation by interacting with proteins that block the translation of the target gene. Furthermore,

miRNAs can cause global protein synthesis by enhancing ribosome biogenesis, or switch the regulation from repression to activation of target gene translation in conditions of cell cycle arrest.[55]

1.3.2. Challenges of siRNA-based therapeutics

As mentioned above, synthetic siRNAs have been widely used for loss-of function phenotype analyses in mammalian cells and extensively studied as their therapeutic potential by blocking the synthesis of disease-causing proteins. The potential of siRNA therapeutics was first demonstrated in Song *et al* (2003), where after injection of siRNAs targeting Fas expression, mice were protected from autoimmune hepatitis, and since then, drug development has been rapid.[58]

Despite the potential of siRNAs as therapeutics, many challenges remain, including rapid degradation, poor cellular uptake, off-target effects and other potential toxicities have been associated to these agents.

Regarding the off-target effect, through partial sequence complementarity of endogenous mRNAs, siRNAs can suppress the expression of non-target genes via a miRNA mechanism. Off-target effects are concentration dependent and can be reduced by chemical nucleotide modifications, careful sequence selection and the use of pools of oligonucleotides that dilute off-target effects by reducing the concentration of individual oligonucleotides.[59] Other factors contributing to these off-target effects include the incorporating passenger strand into AGO during loading and the competition for limiting resources of the endogenous miRNA pathway.[60]

Another setback is that the gene-silencing siRNAs is transient and is largely dependent on the rate of cell division, since mammalian cells lack the siRNA amplification mechanisms that confer RNAi potency and longevity in organisms, such as worms or plants.[59,61] However, various chemical modification have been introduced that that aim to increase the stability of the molecules while maintaining their gene-silencing potency. For example, direct modification of inter-nucleotide phosphate linkage is the simplest approach used to achieve nuclease resistance, and modification of the 2'-position of the ribose can decrease susceptibility of inter-nucleotide phosphate linkage to nuclease cleavage and increase stability of the duplex.[61]

siRNAs have other potential toxicities such as innate immune activation since dsRNA can activate innate immune receptors, triggering inflammatory and IFN responses, through recognition by Toll-like receptor 3 and 7 and retinoic acid-inducible gene I protein. A strategy to diminish this reaction are once again the use of specific chemical modifications largely restrict the binding and activation of these receptors.[59,60]

Another potential problem associated with the use of chemically synthesized siRNAs is related to the efficiency of delivery of the molecules to mammalian cells due to their negatively charged character. A widely used approach to deliver sufficient quantities of siRNAs into mammalian cells involves their encapsulation into cationic liposomes or polymers that are taken up into cells. Another approach employed is electroporation that leads to high transfection efficiency.[61,62] Additional methods have been developed for systemic delivery of siRNAs, since siRNAs are easily filtered from the

glomerulus being rapidly excreted from the kidney and they are highly susceptible to degradation by nucleases in the plasma. Some chemical modifications have been shown to protect siRNAs from nuclease degradation and contribute to increased protein binding and extend serum, such as phosphorothioate modification or hydrophobic ligands like cholesterol. Besides that, nanocarriers are also important tools during delivery of siRNAs to target tissues by providing protection against both rapid renal excretion and nuclease cleavage, facilitating siRNA cellular uptake, reducing siRNA related toxicities, preventing of off-target effects and improving in pharmacokinetic profiles of siRNA-based therapeutics. Based on surface charge, size (ranging from 1 to 300 nm) and hydrophobicity, nanocarriers have unique tissue biodistribution, toxicity and tumour cell uptake profiles and include natural or synthetic lipids (e.g., liposomes, micelles), polymers (e.g., chitosan, polylactic-co-glycolic acid, polylactic acid, polyethilenimine), carbon nanotubes, quantum dots, magnetic nanoparticles and others, in which the nanomaterials used in the fabrication process determine the attributes of the resulting carrier.[61]

Although the use of transfected siRNAs is appropriate in cases where transient gene silencing is sufficient, such as for many high-throughput cell-based gene-screening assays, it is not suitable in cases where prolonged inhibition of gene expression is necessary. Therefore, methods which enable the use of expression vectors that produce short RNAs continuously in mammalian cells have been developed,[62] and will be explained in detail in the next section.

1.3.3. Short-hairpin RNA (shRNA) expression systems

An alternative method for gene silencing in mammalian cells through a RNAi-related process has also been developed, involving the use of expression vectors that produce short-hairpin RNAs (shRNAs), that can silence gene expression as effectively as do synthetic siRNAs.

Such expression systems are based on plasmids or viral vectors that encode sequence composed complementary 19-22 nt sense and antisense segments of the target gene separated by a 6-11-nt spacer. Essentially, following transcription, a stem loop structure is produced, generating a shRNA into two complementary RNA sequences linked by a short loop similar to the hairpin found in naturally occurring miRNA (*Figure 1.8*). As such, after transcription, the shRNA sequence is exported to the cytosol where it is recognized by an endogenous enzyme, Dicer, which processes the shRNA into the siRNA duplexes that incorporates the RISC complex for target-specific mRNA degradation.[62,63] A variation of this method involves the use of vectors in which the sense and antisense short RNA strands are express individually by separate promoters.[64]

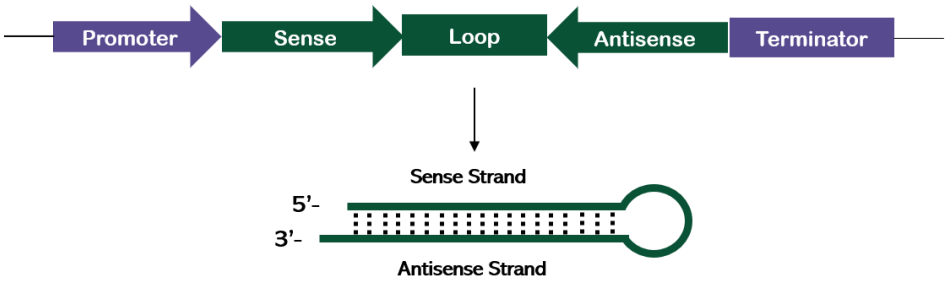

Figure 1.8- Schematic representation of the expression system cassette that encodes the short hairpin RNA and its predicted structure after transcription.

Typically, the shRNA sequence is expressed from Pol III promoters, such as U6 and H1 promoters, since they have a well-defined transcription start and end points producing a shorter, more predictable transcript. However, several studies have identified Pol II transcripts represents an effective alternative approach in designing shRNA-expression vectors.[65,66]

Since the hallmark study developed in Brummelkamp *et* al (2002)[67], in which the authors described a powerful new tool to stably suppress gene expression in mammalian cells using a retroviral vector pSUPER, viral vectors have been most extensively employed in shRNA-mediated approaches to study gene function in mammalian cells, including retroviruses, lentiviruses, adenoviruses, adeno-associated viruses (AAVs), herpesviruses, among others.[68–72] In the case of retroviruses, integrating viruses as lentiviruses and AAVs can lead to a long-term transgene expression after transduction of mammalian cells. Another beneficial characteristic of viral vectors is higher gene transfer efficiency both *in vitro* and *in vivo*, in contrary to most non-viral vectors are unable to effectively past the multiple biological barriers. In addition, unlike plasmids, viral vectors have the advantage of delivering shRNAs to non-dividing cells, such as neurons. However, despite these advantages, several limitations are associated with viral vectors, including carcinogenesis, immunogenicity, broad tropism, limited DNA packaging capacity and difficulty of vector production.[73,74]

Currently, different classes of non-viral vectors are available for promoting therapeutic transgene delivery and expression in eukaryotic cells, namely for the expression of shRNAs.[75–77] Among then, minicircles (MCs), classified as non-viral, episomal, circular gene expression vectors, emerged as a promising choice. These vectors consist in minimalistic backbones that lack the bacterial backbone sequence consisting of an antibiotic resistance gene, an origin of replication, and inflammatory sequences intrinsic to bacterial DNA, with potential to meet the clinical requirements for safe and long-lasting gene expression.[78,79] Minicircles are generally synthesized in recombinant bacteria and result from an *in vivo* site-specific recombination process: the parental plasmid (PP) carries the eukaryotic expression cassette flanked by two recognition sites of a site-specific recombinase, that upon induction originate a replicative miniplasmid (MP) carrying the undesired backbone sequences, and a MC carrying the therapeutic expression unit (*Figure 1.9*).[79,80]

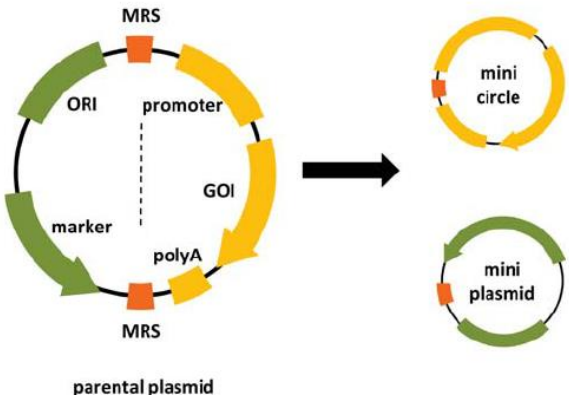

Figure 1.9 - Schematic representation of the recombination of a parental plasmid into a minicircle and a miniplasmid via the excision of the eukaryotic expression cassette flanked by two multimer resolution sites (MRS). Abbreviations: ORI, origin of replication; GOI, gene of interest. From Prazeres *et al* (2014)[80]

An example of the great potential of MCs encoding shRNA, is described in Zhao *et al*. (2011)[77], in which the authors demonstrated increased transfection efficiency and gene silencing capability of these minivectors compared to plasmids, and equivalence of gene silencing compared to siRNA. Overall, shRNA-encoding MCs were able to slow the growth of anaplastic large cell lymphoma cells *in vitro* by the efficient knockdown of anaplastic lymphoma kinase.

1.4. siRNA-mediated gene silencing in tumour angiogenesis

As mentioned previously, cancer is one of the main targets for RNAi-based therapy. siRNA can be used in the treatment tumours by targeting proteins related to several oncogenesis pathways, such as: (i) Bcl-2 which is involved in the apoptotic pathway; (ii) mutated oncogenic protein B-Raf which regulates the MAPK pathways, and (iii) CD31 that is a major constituent of ECs intercellular junctions or survivin, an anti-apoptotic gene overexpressed in tumour cells.[81]

Moreover, once angiogenesis is major player in the development and spread of tumours, RNAi targeting angiogenesis can serve as a potential target for cancer therapy. RNAi-based strategies are classically based on the inhibition of VEGF, VEGFRs and its signalling due to their critical role in the pathological angiogenesis that occurs in a number of cancers. Additionally, other angiogenesis-related targets have also been investigated. Examples of studies that support this evidence will be now presented.

For example, siRNA-targeting VEGF showed to effectively silence VEGF gene expression in a variety of human colon cancer cell lines, leading to decreased tumour proliferation.[82] Similarly, siRNA targeting VEGF dramatically suppressed tumour angiogenesis and growth in a human prostate cancer cell xenograft model.[83]

In a different study, lentiviral vectors-expressing shRNA targeting VEGF inhibited tumour angiogenesis and growth, and increased apoptosis of the pancreatic cancer cell line *in vitro* and *in vivo*.[84]

Furthermore, intravenous administration of polyethyleneimine (PEI) nanoparticles bearing siRNAs targeting VEGFR-2 into mice tumours led to decreased levels of VEGFR-2 within the tumours, as well as a reduction in both tumour angiogenesis and growth.[85]

Moreover, retrovirus-mediated transfer of a shRNA against Her-2/neu, an oncogene that belong to the EGF receptor tyrosine kinases family, was found to be associated with increased expression of the anti-angiogenic factor thrombospondin-1 and decreased expression of VEGF in models of human breast or ovarian cancer.[86]

In Donlinsek et al (2013), it was found that siRNA targeting Endoglin, a TGF- β co-receptor, is a promising anti-angiogenic therapy, since after the *in vivo* silencing with triple electrotransfer of siRNA-endoglin into mice mammary adenocarcinoma, the Endoglin-mRNA levels, number of tumour blood vessels and the growth of tumours, were significantly reduced.[87]

Another study showed that the delivery of a plasmid vector system encoding a shRNA targeting human c-Src, a non-receptor protein tyrosine kinase overexpressed in many solid tumours, into pancreatic carcinoma cell line, was able to inhibit tumour angiogenesis *in vivo.*[88]

Additionally, Huang and colleagues reported that siRNA targeting signal transducers and activators STAT3, a central cytoplasmic transcription factor that regulates a number of important pathways in tumorigenesis, significantly suppressed tumour growth and angiogenesis of pancreatic cancer cells *in vivo*. Furthermore, STAT3 gene silencing also led to a decrease of VEGF and MMP-2 at the mRNA and protein levels.[89]

In Zhang *et al* (2017)[90] it was found that Net1, a guanine nucleotide exchange factor implicated in cancer cell invasion, promotes the angiogenesis of cervical squamous cell carcinoma, and siRNA targeting Net1 can effectively reduce the angiogenesis in part through downregulation of VEGF, thus inhibiting the tumour growth *in vivo.*

Overall, the use of siRNA targeting angiogenesis showed significant results on several types of cancer. As such, siRNA-based therapeutics would most likely continue to be developed to achieve the treatment of tumours and abnormal angiogenesis, and the possible synergistic effects with chemotherapy and radiotherapy should be investigated.

2. Aims and Scope of the study

Tumour angiogenesis is important for delivering oxygen and nutrients to growing tumours, and therefore considered an essential pathologic feature of cancer, while also playing an important role in enabling other aspects of tumour pathology such as metabolic deregulation and tumour dissemination.

Vascular endothelial growth factor (VEGF), which is a protein involved in stimulation of endothelial cells' (ECs) functions, is a key player in angiogenesis. VEGF is present in tumour microenvironment being secreted by cancer and surrounding cells such as Mesenchymal Stem/Stromal Cells (MSCs). Thus, blocking VEGF production seems a plausible approach to slow down tumour growth.

MSCs are present in perivascular locations, from nearly all tissues in the adult body, providing stromal support in the maintenance of a dynamic and homeostatic tissue microenvironment, by the secretion of a broad range of biologically active molecules including growth factors (namely VEGF), chemokines and cytokines. In addition, MSCs have tropism to tumour sites mainly by the chemoattractants secreted from cancer and surrounding cells. Furthermore, upon interaction with cancer cells, MSCs became active participants in tumour development namely by promoting angiogenesis.

Overall, a promising tool for blocking VEGF production by MSCs and cancer cells is by small interfering RNA (siRNA)-mediated silencing, which involves the double-stranded RNA (dsRNA)-mediated degradation of a specific target mRNA at a post-transcriptional level. Despite the challenges with delivery and possible harmful off-target effects, many efforts have been made towards the development of siRNA-based therapies to tackle various diseases.

In this context, this project involves the transfection of human bone marrow MSCs and MCF-7, a human breast adenocarcinoma cell line, with specific siRNAs targeting VEGF expression.

siRNAs will be designed and synthesized outsourced with specific chemical modifications to increase their half-lives. Additionally, minicircle (MC) vectors encoding a short hairpin RNA (shRNA), targeting the same location of VEGF-mRNA, will be also constructed, produced and purified for further transfection. Unlike the synthetic siRNA, which is degraded with gene silencing, the MC continues to deliver the transcribed shRNA to the transfected cells.

Moreover, to assess VEGF silencing, VEGF-mRNA and VEGF-protein will be quantified by real time quantitative PCR and ELISA, respectively. Finally, the effect on blood vessel formation will be addressed by performing a functional *in vitro* assay, in which the capacity of human umbilical vein endothelial cells (HUVECs) to form tubes in the presence of the conditioned media of transfected MSCs and MCF-7 will be evaluated.

3. Materials and Methods

3.1. *In silico* design of a siRNA and vector-expressed shRNA to silence VEGF expression

The oligonucleotide sequence of siRNA targeting VEGF-A chosen was: Passenger/Sense: AUGUGAAUGCAGACCAAAGdTdT; Guide/Antisense: CUUUGGUCUGCAUUCACAUUU (*Supplementary Data 1*), which is shown to efficiently silence VEGF expression in different mammalian cells.[91–93] The inclusion of the deoxythymidine dinucleotide overhangs in the passenger strand should improve strand selection, since RISC exhibit a distinct preference in favour of a strand with an RNA overhang (guide strand).[94]

Additionally, siRNA will be expressed as an shRNA encoded in a minicircle DNA vector. The inserted fragment must contain the sequence of the passenger strand followed by a loop sequence and finally the sequence of the guide strand, allowing the transcript to fold back on itself forming a shRNA, analogous to natural miRNA.[95] For the loop sequence the 9-nt loop 5'-TTCAAGAGA -3' was selected since is one of the most commonly used hairpin loops and is based on a naturally occurring miRNA sequence.[96] A graphical representation of the annealed insert, the transcript and its hairpin structure can be observed in *Figure 3.1.*

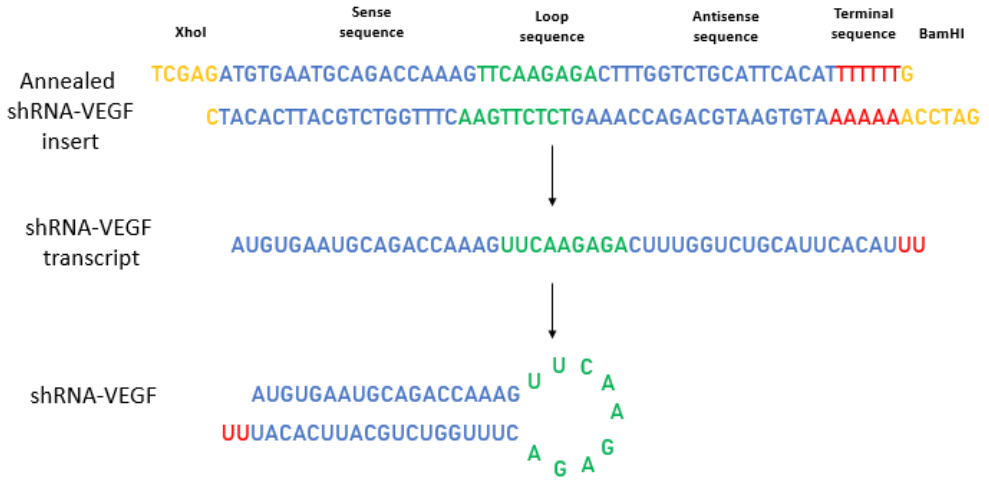

Figure 3.1 - Graphical representation of the annealed insert, the transcript and its hairpin structure originating the shRNA.

3.2. *Escherichia coli* competent cells and transformation

Escherichia coli DH5α and BW2P cells were made competent by a chemical method. Firstly, an inoculum was prepared from frozen cells in 15 mL Falcon tubes containing 5 mL of LB medium (pH 7.4) and incubated overnight at 37 °C and 250 rpm. Cells were used to inoculate 100 mL Erlenmeyer flasks containing 20 mL of LB medium at an $OD_{600nm} \approx 0.1$. Cultures were grown at 37 °C and 250 rpm until

OD_{600nm} ≈ 1 has been reached. At that point, the culture was centrifuged at 1000xg and 4ºC for 10min in two 15mL falcon tubes and resuspended in 2 mL of cooled TSS medium (20 g/L LB, 5% DMSO, 50mM $MgCl_2$, 10% PEG 8000 (w/v), pH 6.5). After a 10min incubation on ice, 100µL aliquots were stored at -80ºC.

The transformation of *E. coli* DH5α and BW2P was performed by heat shock, in which one 100µL aliquot of chemically competent cells was mixed with the appropriate amount of plasmid DNA (pDNA). First, the mixture was incubated for 20 min on ice, and then submitted to 42ºC for 90 secs followed by 2 min on ice. Finally, cells were resuspended with 900 µL of LB medium, allowed to recuperate for 1 hour at 37ºC and then plated on LB agar supplemented with 30 µg/mL kanamycin (Sigma-Aldrich) and 0.5% (w/v) of glucose (only for *E. coli* BW2P), and incubated overnight at 37ºC.

3.3. Construction of parental plasmids expressing a shRNA targeting VEGF

pshRNA

A pair of DNA oligonucleotides (STABVIDA) (Forward: TCGAGATGTGAATGCAGACCAAAGTTCAAGAGACTTTGGTCTGCATTCACATTTTTTTG; Reverse: GATCCAAAAAAATGTGAATGCAGACCAAAGTCTCTTGAACTTTGGTCTGCATTCACATC) were resuspended in 10 mM Tris, pH 8.0; 50 mM NaCl; 1 mM EDTA [97], each obtaining a final concentration of 10µM.

The annealing was performed by incubation of 20µL of each oligonucleotide at 95°C for 2 min, then it was gradually cooled to 25 °C during 45 min, and finally cooled to 4°C for temporary storage.[97] After the annealing, the dsDNA oligonucleotide exhibit overhangs of the XhoI and BamHI digested sequence, as shown in Figure 3.1.

The parental plasmid pVEGF-GFP (*Figure 3.2*), previously constructed at BioEngineering Research Group (BERG) laboratory[98], was digested with XhoI (*Thermo* Fisher Scientific) and BamHI (Promega) restriction enzymes for 3 hours at 37°C. The digested pDNA was separated by a 1% agarose gel electrophoresis and the correct fragment was extracted from the gel with NZYGelpure kits (Nzytech) accordingly to the manufacturer's instructions. The concentration pDNA was assayed by spectrophotometry at 260nm, using Nanodrop Spectrophotometer (GE Healthcare).

Afterwards, the annealed dsDNA oligonucleotide (insert) was ligated to the XhoI/BamHI digested vector pVEGF-GFP. The ligation mixture was performed with 0.4 µL of T4 DNA Ligase (3U/ µL; Promega), 1x T4 ligase buffer and 50 ng of vector and vector/insert ratio of 1:5 and 1:7 (*Equation 1*) to a final volume of 20 µL.

$$ng\ of\ insert = \frac{ng\ of\ vector\ \times kb\ size\ of\ insert}{kb\ size\ of\ vector} \times molar\ ratio\ of\ insert/vector$$

(Equation 1)

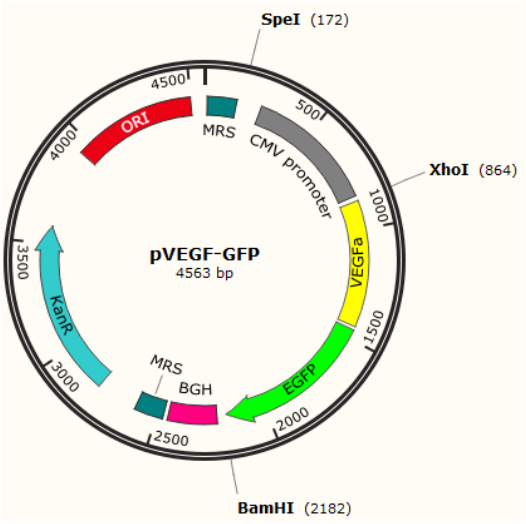

Figure 3.2 - Schematic representation of the parental plasmid pVEGF-GFP (4,563 bp).

After 3 hours of incubation at room temperature, 10µL of the ligation mixture was used to transform 100µL chemically competent *E. coli* DH5α by heat shock as described previously. Then, cells were plated in a LB agar medium supplemented with 30 µg/mL kanamycin (Sigma-Aldrich) which is the selection marker of the plasmid, and incubated overnight at 37°C.

The process was repeated for the remaining 10µL of the ligation mixture, after overnight incubation at 4°C.

E. coli DH5α colonies were picked from plates and grown overnight in 15 mL Falcon tubes containing 5 mL of LB medium supplemented with 30 µg/mL kanamycin (Sigma-Aldrich). The pDNA was extracted by NZYMiniprep kit (Nzytech) accordingly to the manufacturer's instructions. To verify the insertion, the pDNA was digested with the restriction enzymes SpeI (Fermentas) and BamHI (Promega) during 3 hours at 37°C and the restriction pattern was evaluated through a 1% agarose gel separation. To further validate the insertion, DNA sequencing was performed on the construct (STABVIDA) using primers for Cytomegalovirus (CMV) promotor (CMV-F) and bovine growth hormone (BGH) polyA signal (BGH-R) (*Table 3.1*). The confirmed parental plasmid was named pshRNA.

Table 3.1- List of primers used for sequencing.

Name	Size (bp)	Sequence (5'-3')
CMV-F	21	CGCAAATGGGCGGTAGGCGTG
BGH-R	18	TAGAAGGCACAGTCGAGG
MP_R3	20	ATTCCGGTTCGCTTGCTGTC

Finally, 25 ng of purified pshRNA was used to transform 100µL chemically competent *E. coli* BW2P by heat shock as described above. Cells were plated in a LB agar medium supplemented with 30 µg/mL kanamycin (Sigma-Aldrich) and 0.5% (w/v) of glucose, and incubated overnight at 37°C. A colony was grown overnight in 5mL LB medium supplemented with 30 µg/mL kanamycin (Sigma-Aldrich) and 0.5% (w/v) of glucose until and an optical density at 600nm (OD_{600nm}) of approximately 1. Aliquots of 35µL of 35% (w/v) glycerol and 65µL of culture were made and kept at -80ºC.

pshRNA_2

In addition to pshRNA, a parental plasmid with a different sequence for the CMV promoter and a synthetic polyA signal instead of the BGH polyadenylation signal, was also constructed.

Firstly, PCR amplification of the insert was performed using the KOD Hot Start DNA Polymerase kit (Novagen), by mixing 0.02 U/µL of KOD Polymerase, 1mM of $MgSO_4$, 1x Buffer, 0.2 mM of dNTPs, 0.3 µM of each DNA oligonucleotides (STAVIDA) (Forward: CCAGAGCTCGGTTTAGTGAACCGTCTCGAGATGTGAATGCAGACCAAAGTTCAAGAGACTTTGGTCTGCATTCACATTTTTTTACTAGTAATAAAGGAT; Reverse: CTGATGCATCCGCGGGGACTAGAGTCGACGCGGCCGCACACAAAAAACCAACACACGGATCCAATGAAAATAAAGGATCCTTTATTACTAGTAAAA) and completed with PCR-grade water to a final volume of 25 µL. The cycling conditions were an initial denaturation at 95ºC for 2 min, followed by 35 cycles of 1 min at 95ºC, a cooling ramp of 1.10 min from 60ºC to 44ºC and 1 min at 70ºC.

After amplification, the PCR product was separated by a 1% agarose gel electrophoresis and the fragment was extracted with NZYGelpure kits (Nzytech) accordingly to the manufacturer's instructions, and its concentration was assayed by spectrophotometry at 260nm, using Nanodrop Spectrophotometer (GE Healthcare).

Afterwards, the PCR product was digested with SacI (*Thermo* Fisher Scientific) and NsiI (Promega) restriction enzymes for 3 hours at 37°C. The digested fragment (insert) was purified with NZYGelpure kits (Nzytech) according with the manufacturer's instructions.

Parallelly, the previously constructed parental plasmid pshRNA (*Figure 3.*3) was digested with SacI (*Thermo* Fisher Scientific) and NsiI (Promega) restriction enzymes for 3 hours at 37°C. The digested pDNA was separated by a 1% agarose gel electrophoresis and the fragment was extracted with NZYGelpure kits (Nzytech) accordingly to the manufacturer's instructions.

The ligation mixture was performed with 0.5 µL of T4 DNA Ligase (3U/ µL; Promega), 1x T4 ligase buffer and 100 ng of vector and vector/insert ratio of 1:5 (*Equation 1*) to a final volume of 20 µL.

After 3 hours of incubation at room temperature and overnight incubation at 4ºC, 10µL of the ligation mixture was used to transform 100µL chemically competent *E. coli* DH5α by heat shock as above described.

E. coli DH5α transformants were grown overnight in in 15 mL Falcon tubes containing 5 mL of LB medium supplemented with 30 µg/mL kanamycin (Sigma-Aldrich). The pDNA was extracted by NZYMiniprep kit (Nzytech) accordingly to the manufacturer's instructions. To verify the insertion, the

pDNA was digested with the restriction enzyme SacII (Thermofisher) during 2 hours at 37°C and the restriction pattern was evaluated through an 1% agarose gel separation.

To validate the insertion, DNA sequencing was performed on the construct (STABVIDA) using primers for CMV promotor and before the multimer resolution sites (MRS) (MP_R3) (*Table 3.1*). The confirmed parental plasmid was named pshRNA_2.

Finally, 25 ng of purified pshRNA_2 was used to transform *E. coli* BW2P and aliquots of the transformants were performed as described before.

3.4. Parental plasmid and minicircle production

The producer strain *E. coli* BW2P was constructed by the insertion of the PBAD/*araC-parA* cassette in the *endA* gene in the genome of the *E. coli* strain BW27783 (The Coli Genetic Stock Center at Yale). The cassette contains the ParA resolvase gene under a PBAD promoter with an optimized ribosome binding site and the AraC repressor gene in opposite direction.[99] ParA catalyzes to recombination of parental plasmid (PP) into miniplasmid (MP) and minicircle (MC)[79] in which the activity is induced by arabinose and repressed by glucose. Thus, this strain was used to produce the minicircle vectors.

As a first step, an inoculum was prepared from frozen *E. coli* BW2P cells harbouring the PPs pshRNA, pshRNA_2 or pVEGF-GFP in 15 mL Falcon tubes containing 5 mL of LB medium (pH 7.4) supplemented with 30 µg/mL kanamycin (Sigma-Aldrich) and 0.5 % (w/v) of glucose to block ParA resolvase expression.

After overnight incubation at 37 °C and 250 rpm, cells were used to inoculate 100 mL Erlenmeyer flasks containing 30 mL of the previously described medium at an $OD_{600nm} \approx 0.1$. Cultures were incubated at 37 °C and 250 rpm until $OD_{600nm} \approx 2.5$ has been reached. At that point, an appropriate volume was used to inoculate 2 L Erlenmeyer flasks containing 250 mL of LB medium (pH 7.4) supplemented with 30 µg/mL kanamycin (Sigma-Aldrich) at an $OD_{600nm} \approx 0.1$.

The OD_{600nm} was monitored during the growth and recombination induction was performed at an OD_{600nm} of approximately 2.5 (late exponential phase). The recombination was induced by adding 0.01% (w/v) L-(+)-arabinose directly to the culture and recombination was allowed to proceed for 1 and 2 hours. Culture samples at the induction time and during induction were collected to monitor recombination profile by agarose gel electrophoresis.

The final culture was centrifuged for 15 minutes at 4ºC under 6000xg. The cell pellets were stored at -20ºC for further purification.

3.5. Purification of minicircles

Primary purification

The process was based in the method described by Silva-Santos *et al* (2017)[100]. Firstly, an alkaline lysis was performed to the cell pellets stored at -20ºC. Briefly, the pellets were resuspended in P1 buffer (50 mM glucose, 25 mM Tris-HCl, 10 mM EDTA, pH 8) by vortex. The volume of P1 (V_{P1}): was calculated to have a cell suspension with an OD_{600nm}= 60. The following equation was used, considering the final optical density of the culture (OD_{600nm}) and volume of the respective cellular growth (V_{cg}):

$$V_{P1} = \frac{OD_{600nm} \times V_{cg}}{60}$$

(Equation 2)

The resuspended cells were mixed gently with P2 buffer (0.2 M NaOH, 1% (w/v) SDS) at a 1:1 volume ratio and incubated at room temperature for 10 minutes. Finally, the P3 buffer (5 M acetate; 3 M potassium, pH 5) at a 1:2 volume ratio was added. The mixture was gently homogenized and placed on ice for 10 minutes.

After neutralization, the mixture was centrifuged twice at 18250xg and 4ºC for 30 minutes. The nucleic acids of the clarified lysate obtained were precipitated with 0.7% (v/v) isopropanol at -20ºC for 2 hours. Afterwards, a centrifugation at 18250xg and 4ºC for 30 minutes was performed. The resulting pellets were left to dry overnight at room temperature.

The pellets were resuspended in 10mM Tris-HCl, and then conditioned with ammonium acetate salt for a final concentration of 2.5M. After salt dissolution, the lysate was placed on ice for 15 minutes and centrifuged at 15000xg and 4ºC for 30 minutes. The supernatant was recovered and 30% (w/v) PEG-8000 in 1.6 M NaCl at a 1:2 volume ratio was added and left overnight at 4ºC. Afterwards, the mixture was centrifuged at 15000xg, 4ºC for 30 min, and the pellet containing the nucleic acids were washed with 70% ethanol and centrifuged again. The pellet was left to dry and finally resuspended in PCR-grade water.

Digestion with endonuclease Nb.BbvCI

The digestion step was carried out as described in Alves *et al* (2016)[101] with endonuclease Nb.BbvCI to nick of one of the strands of the MP and of the non-recombined PP, since this enzyme recognizes a specific target sequence strategically placed in the MP molecule. As a result, supercoiled (sc) MP and non-recombined PP were converted into the corresponding open-circular (oc) forms, whereas sc MC remain unaffected. The sample obtained previously was divided in two and the digestion was performed in a total reaction volume of 290 µL, using 5-10 µL of Nb.BbvCI (1U/ µL, New England Biolabs), 1x CutSmart buffer (New England Biolabs), for 1 to 3 hours at 37ºC. The digested samples were analyzed by agarose gel electrophoresis.

Multimodal chromatography

The Multimodal chromatography based in the method described by Silva-Santos *et al* (2017)[100] was performed using a Tricorn 10/50 column (GE Healthcare) packed with 5 mL of Capto^{TM} adhere resin connected to an ÄKTApurifier10 system (GE Healthcare) under the control of UNICORN 5.11 software. This matrix contains an immobilized ligand that can mediate anion-exchange (with the charged nitrogen), hydrophobic (with the phenyl ring) and hydrogen bonding (with the hydroxyl groups) interactions with the solutes in the feed stream.

The samples were conditioned with a buffer containing 830 mM NaCl in 10 mM TE, prior to column loading. The mobile phase consisted of mixtures of buffer A (10 mM Tris-HCl, 1 mM EDTA, pH 8) and buffer B (2 M NaCl in 10 mM Tris-HCl, 1 mM EDTA, pH 8). The absorbance of the eluate was continuously measured at 254 nm by a UV detector positioned after the column outlet and the system was operated at 1 mL/min. The column was equilibrated with 3 column volumes (CV) of 41.5% buffer B (approximately 69 mS/cm).

Then, 1 mL of the conditioned sample was injected into the column by washing the loop with 3 mL of 41.5% buffer B. All unbound material was washed out of the column with 2 CV of 41.5% buffer B. Elution steps were then performed with 3 CV of 46% B (approximately 75 mS/cm) and 3 CV of 100% B (approximately 140 mS/cm). The eluate was collected (fractions of 1.5 mL) during the chromatographic run in 2 mL Eppendorf tubes with a fraction collector. The fractions collected were analyzed by agarose gel electrophoresis.

Dialysis and Concentration

Finally, MC purified fractions were processed in Amicon® Ultra-4, MWCO 30 kDa (*Thermo* Fisher Scientific), according to the respective protocol, to diafiltrate and concentrate the sample. Afterwards, the purified pDNA remained approximately in 100 µL of PCR-grade water and was stored at 4ºC. The concentration pDNA was assayed by spectrophotometry at 260nm, using Nanodrop Spectrophotometer (GE Healthcare), and pDNA integrity and purity was assessed through a 1% agarose gel electrophoresis separation.

3.6. Synthetic siRNA annealing

The siRNA strands were individually synthesized (STABVIDA) including the specific chemical modifications described previously, to increase their half-lives and silencing efficacy.

The oligonucleotides were resuspended in 10 mM Tris, pH 8.0; 50 mM NaCl; 1 mM EDTA [97], each obtaining a final concentration of 10µM. The annealing was performed as previously by incubation of 20 µL of each oligonucleotide at 95°C for 2 min, then gradually cooled to 25 °C during 45 min, and finally cooled to 4°C. The siRNA complexes (5 µM) were stored at -20ºC.

3.7. Bone Marrow Mesenchymal Stem/Stromal Cells thawing and expansion

Bone Marrow Mesenchymal Stem/Stromal Cells (BM-MSCs) (M79A15 and M48A08 donors) kept cryopreserved in liquid/vapor phase nitrogen tanks at the Stem Cell Engineering Research Group (SCERG), iBB, were thawed by submerging the cryovials in a 37ºC water bath and resuspended in low-glucose Dulbecco's Modified Eagle's Medium (DMEM) supplemented with 20% fetal bovine serum (FBS) *(Thermo* Fisher Scientific). After a centrifugation at 1500xg for 7 min, the pellet was resuspended in DMEM supplemented with 10 % FBS MSC qualified *(Thermo* Fisher Scientific) and 1 % Antibiotic-Antimycotic (A/A, Gibco). The determination of total cell number (TCN, *Equation 3*) and viabilities (CV, *Equation 4*) was estimated by the 0.4% Trypan Blue dye exclusion method using a hemocytometer under an optical microscope.

$$TCN = \frac{Number\ of\ viable\ cells}{Number\ of\ squares} \times 1000\ cells/mL \times Dilution factor \times Final\ volume$$

(Equation 3)

$$CV(\%) = \frac{Number\ of\ viable\ cells}{Total\ number\ of\ cells} \times 100$$

(Equation 4)

According to number of cells recovered, the cells were plated in T-Flasks at the appropriate cell density (3,000 – 6,000 cells/cm^2) in the previously described culture medium. Cells were incubated at 37ºC, 5% CO_2 and >95% humidity and the culture medium was replaced every 3-4 days.

Cell passages were performed when 70-80% confluence was observed by microscope. Briefly, the exhausted medium was removed, and cells were washed with Phosphate Buffered Saline (PBS) buffer. After PBS removal, cell detachment was accomplished by adding accutase (*Thermo* Fisher Scientific) solution, for 7 min at 37ºC. Inactivation of the accutase enzymatic activity was achieved by adding DMEM supplemented with 10% FBS MSC qualified in a proportion of 1:1. Collected cells were concentrated by centrifugation at 1500xg for 7 min and resuspended in DMEM supplemented with 10 % FBS MSC qualified *(Thermo* Fisher Scientific) and 1 % A/A (Gibco). TCN and CV were accessed by the Trypan Blue dye exclusion method and the appropriate cell densities were plated.

3.8. MCF-7 thawing and expansion

MCF-7 (human breast adenocarcinoma cell line) cryopreserved cells, obtained from ECACC (European Collection of Authenticated Cell Cultures), were thawed using the same procedure as BM-MSCs thawing above described. Vials containing 1 x 10^6 cells were plated on a T-Flask with 25 cm^2 in high glucose DMEM supplemented with 10 % FBS *(*Thermo Fisher Scientific) and 1 % A/A (Gibco). Cells were incubated at 37ºC, 5% CO_2 and >95% humidity. Typically, part of the cells remained detached and were removed by replacing medium in the following day.

Cell passages were performed when 90-100% confluence was observed by microscope. Firstly, the exhausted medium was removed, the cells were washed with PBS buffer and detached by adding 0.05% trypsin (Coring) for 3 min at 37ºC. Inactivation of the trypsin enzymatic activity was achieved by adding DMEM supplemented with 10% FBS in a proportion of 2:1. Collected cells were concentrated by centrifugation at 1500xg for 7 min and resuspended in 3 mL fresh medium. Finally, 1 mL of the medium was plated on a T-Flask with the same area.

TCN and CV were accessed by the Trypan Blue dye exclusion method and the appropriate cell densities were plated when used in transfection experiments.

3.9. Microporation of BM-MSC and MCF-7

Microporation experiments were performed with the Neon™ Transfection System, in which 1.5x10^6 BM-MSC cells/MCF-7 were resuspended in resuspension buffer supplied by the microporator (MP100µL) manufacturer's and incubated with the appropriate amount of MC, followed by microporation. Cells were also microporated without pDNA as a control.

The BM-MSCs microporation procedure was adapted from Serra *et al* (2018)[102]. The microporation conditions used were: 1 pulse; 1000 V of pulse voltage and 40ms of width. After microporation, each 100 µL of cell suspension was introduced into an Eppendorf containing 900µL of Opti-MEM® medium (Thermo Fisher Scientific). Then, the microporated cells were divided and plated on T75- flasks coated with 1:200 CELLStart (Thermo Fisher Scientific) using StemPro MSC SFM XF *(*Thermo Fisher Scientific) medium and kept in an incubator at 37ºC, 5% CO_2 and >95% humidity.

Cells and culture supernatants were collected after 24h or 48h post-transfection. Before storage at -80ºC, growth medium was centrifugated at 1750xg for 10 min and cells were centrifugated at 1500xg for 7min.

In the case of MCF-7, the process was identical except the microporation conditions (2 pulses; 1,100 V; 30ms) and the culture medium used, that was high glucose DMEM supplemented with 10 % FBS (Thermo Fisher Scientific) and 1 % A/A (Gibco).

Besides the previous described calculations of the TCN and CV, for each transfection sample (*t*), cell recovery (*CR*) was calculated by Equation 5, where *CA* is the number of viable cells and *c* is the non-transfected control cells. After centrifugation at 1500xg for 7min, the cell pellets were kept at -80ºC to further experiments.

$$CR_t(\%) = \frac{CA_t}{CA_c} \times 100$$

(Equation 5)

3.10. Liposome-mediated transfection of BM-MSCs and MCF-7

The process was based in the method described by Boura *et al* (2013)[103]. BM-MSCs from P4-P7 were plated at a cell density of 4,000 cells/cm^2 on 12-well plates and cultured DMEM supplemented with 10 % FBS MSC qualified *(Thermo* Fisher Scientific) and 1 % A/A (Gibco). Alternatively, for MCF-7

transfection, cells were plated at an optimized cell density of 25,000 cells/cm^2. Additionally, some preliminary experiments were performed using Chinese hamster ovary (CHO) cells.

After 72 hours of culture, with cells at 70-80% confluency, transfection was carried out using the 1 mg/mL Lipofectamine 2000 reagent (Lipofectamine; Invitrogen) according to the manufacturer's instructions. Briefly, the appropriate amount of MC (MC-VEGF-GFP; MC-shRNA; MC-shRNA_2) or synthetic siRNA and 1 µL of Lipofectamine were diluted in 50 µL of Opti-MEM® medium *(Thermo* Fisher Scientific). Then, solutions were combined to allow complex formation to occur during 20 minutes at room temperature. After the 20 minutes incubation, the transfection mixture was added to the cells in which the medium was replace to 400 µL of serum- and antibiotic-free DMEM. Five hours after transfection, the medium was replaced by 1 mL of fresh DMEM supplemented with 10% FBS and 1% A/A (Gibco).

Cell pellets and culture supernatants were collected to further experiments at different time points, namely 24, 48 and 72 hours after transfection. Before -80ºC storage, culture supernatants were centrifuged at 2000xg for 10 min and cells were centrifuged at 1500xg for 7min.

Both non-transfected cells and cells treated only with Lipofectamine (i.e. no vector or siRNA) were used as a control. For each transfection, TCN, CV, and CR were calculated as described previously.

3.11. Flow cytometry

After transfection of CHO cells with pVEGF-GFP, for monitoring of the GFP-expressing viable cells, cells were harvested after the incubation for 7 min with Accutase (*Thermo* Fisher Scientific), centrifuged and resuspended in 1% paraformaldehyde (PFA, Sigma-Aldrich), a cell fixative solution.

Then, considering the acquisition of a minimum of 10,000 events, the percentage of GFP positive cells was determined using a BD FACSCalibur™ equipment (BD Biosciences). The level of GFP protein expression was given by mean fluorescence intensity also measured during the flow cytometry procedure. Non-transfected cells were used to determine the control cell population and the non-specific fluorescence. The results from flow cytometry were analyzed using FlowJo® (LLC) software.

3.12. RNA extraction, conversion to cDNA and VEGF-mRNA quantification by RT-qPCR

Total RNA was extracted from the cell pellets with RNeasy Mini Kit (Qiagen), according to the manufacturer's instructions. The concentration RNA was assayed by spectrophotometry at 260nm, using Nanodrop (GE Healthcare).

Afterwards, 250-500 ng of RNA were converted to cDNA with iScript™cDNA Synthesis Kit (BIORAD), using an equal RNA mass for all the samples within an experiment. The PCR conditions included a single cycle of 5 minutes at 25ºC, 30 minutes at 42°C and 5 minutes at 85ºC. As an alternative, the High Capacity cDNA Reverse Transcription Kit (*Thermo* Fisher Scientific) was used, in

which the PCR conditions were a single cycle of 10 minutes at 25ºC, 120 minutes at 37°C and 5 minutes at 85ºC. cDNA samples were stored at -20ºC

Real-time quantitative PCR (RT-qPCR) was performed using Applied Biosystems StepOne Real-Time PCR System (Applied Biosystems), using NZY qPCR Green ROX plus kit (Nzytech) with a reaction mixture composed by either 0.4 µM of primers for VEGF (Forward: CGAGGGCCTGGAGTGTGT, Reverse: CGCATAATCTGCATGGTGATG) or for the control GAPDH (Forward:ACGACCCCTTCATTGACCTCA, Reverse:ATATTTCTCGTGGTTCACACC), 25 ng of cDNA template and 1x NZY qPCR Green Master Mix to a final volume of 20 µL.

Each PCR run was followed by a no-template control to confirm the specificity of the amplification and the absence of primer dimers.

The relative gene expression from quantification cycle (Ct) values obtained by RT-qPCR was calculated by the ΔΔCt method using Equation 6. Overall, this is accomplished by normalization of a target gene (VEGF) with experimental treatment, to an endogenous control gene (Glyceraldehyde 3-phosphate dehydrogenase; GAPDH) whose expression remains unchanged. Subsequently, this value is normalized to the targeted gene expression detected in a separate control sample.

$$\Delta\Delta\mathrm{Ct} = \left(Ct_{target\ gene} - Ct_{control\ gene}\right)_{treatment\ sample} - \left(Ct_{target\ gene} - Ct_{control\ gene}\right)_{control\ sample}$$

(Equation 6)

To calculate the fold change (FC) and percentage of knockdown ($\%KD$) of the target gene in the treated cells, the following equations were used:

$$FC = 2^{-\Delta\Delta\mathrm{Ct}}$$

(Equation 7)

$$\%KD = (1 - 2^{-\Delta\Delta\mathrm{Ct}}) \times 100$$

(Equation 8)

3.13. VEGF quantification by ELISA

BM-MSC and MCF-7 culture supernatants collected 48 hours post-transfection were centrifuged as previously described and stored at -80ºC to further VEGF quantification by Enzyme-Linked Immunosorbent Assay (ELISA).

VEGF quantification was performed using RayBio® Human VEGF ELISA kit (RayBiotech), accordingly to manufacturer's instructions. Briefly, the reagents and standard solutions were prepared as described in the protocol. First, 100µL of each standard and samples (without dilution) were added to the plate wells and incubated for 2 hours. The next step was 1 hour of incubation with 100µL of biotinylated antibody. Then, 100µL of Streptavidin solution was added to each well and incubated for 45min. Afterwards, 100µL of TMB One-Step Substrate reagent was added to each well and incubated 15min in the dark. Finally, the reaction was stopped by the addition of 50µL of Stop Solution and OD_{450nm} was measured on Infinite® 200Pro microplate reader (Tecan).

All steps of incubation were performed at room temperature and with gentle shaking. Between each step of the procedure a washing step was performed four times by 300µL of washing buffer, except for the Stop solution step in which the reagent was added directly.

The standard curve was generated, and the concentration of each sample was determined based on that calibration curve. VEGF secretion (VGF pg/1000 cells) in each sample was assessed considering its initial volume, and TCN of the correspondent culture supernatant. The values were expressed as the mean of duplicates for one single experiment.

3.14. *In vitro* tube formation assay

As an attempt to evaluate the MSC angiogenic potential after transfection, a functional assay with HUVEC was performed – Tube formation assay.

For that, 24 hours after BM-MSCs or MCF-7 transfection, the medium was replaced by Endothelial Growth Basal Medium -2 (EBM-2, Lonza) and cells were allowed to condition the medium for 48 hours. The conditioned medium (CM) was then collected, centrifugated for 10 min at 2000xg and stored at -80ºC until used in the *in vitro* tube formation assays. CM was produced from at least $1.0x10^5$ cells and collected 72 hours after transfection.

In order to obtain HUVECs to perform this assay, these cells (P4-P7) were expanded in Endothelial Cell Growth Medium-2 (EGM-2, Lonza) at 37ºC, 5% CO_2 and >95% humidity, and the assay was performed when 80-90% confluence was observed by optical microscope. Accutase (*Thermo* Fisher Scientific) was used for cell detachment as previously described, and DMEM+ 10% FBS was used to stop the reaction. After centrifugation at 1500xg for 7 min, cells were resuspended in EBM-2, and TCN and CV were assessed as previously.

For the *in vitro* tube formation assay using CM from BM-MSC or MCF-7 cultures to cultivate HUVECs, each condition required 20,000 cells that were centrifugated at 1500xg for 7 min. Afterwards, cells were resuspended in 200 µL of CM, EBM-2 as negative control, EGM-2 as positive control (each condition was performed in duplicate). The CM was normalized to the cell number with EBM-2.

Finally, cells were plated onto the wells of a 96-well plate previously coated with 50 µL of Matrigel (100mg/mL, Corning) and allowed to grow for 6 hours at 37ºC, 5% CO_2 and >95% humidity. Afterwards, images were collected using bright field microscopy and HUVECs tube formation was evaluated (tube length, tube connections and number of tubes), using the ImageJ (NIH) software.

4. Results and Discussion

The present work aims to provide insights regarding the implementation of an siRNA-based system that specifically targets VEGF expression with the aim of diminishing the angiogenic potential of cells present in tumour microenvironment, and consequently slow down cancer progression. In this context, it involves the transfection of human BM-MSCs and MCF-7, with specific siRNAs targeting VEGF expression. Despites being synthesized outsourced, MC vectors encoding a shRNA targeting the same location of VEGF-mRNA, will be also constructed, produced and purified for further transfection. In order to assess VEGF silencing, VEGF-mRNA and VEGF-protein will be quantified by RT-qPCR and ELISA, respectively. Finally, a functional *in vitro* assay, in which the capacity HUVECs to form tubes in the presence of the CM of transfected MSCs and MCF-7 will be evaluated, in order to assess the silencing effect on blood vessel formation.

4.1. Construction of a parental plasmid expressing a shRNA targeting VEGF (pshRNA)

Despite the majority of studies that developed short-hairpin RNA expressing systems used viral vectors, mainly due to their high delivery efficiencies and stable gene expression, safety concerns are still a limitation[74] and thus, in the present work, a non-viral system was selected.

One of the major challenges of non-viral vectors is the short-lived transgene expression. Evidences suggest that the primary mechanism limiting long-term episomal transgene expression is gene silencing, instead of loss of the DNA vector. The immunogenic CpG dinucleotides in the bacterial backbone of plasmid and its interaction with a variety of cytokines have been suggested to play a key role in episomal gene silencing. Additionally, the bacterial backbone is highly rich in sequences associated with biosafety concerns, such as antibiotic resistance markers, due to their possible dissemination via horizontal gene transfer. Furthermore, it has been found that smaller plasmids lead to higher transfection efficiencies and have better bioavailability characteristics compared to larger ones, providing smaller plasmids with an advantage to overcome cellular barriers.[78,79,104] As such, minicircle DNA vectors, free of plasmid bacterial DNA sequences, capable of persistent high level of transgene expression *in vivo*, seemed to be a promising choice.[78,79]

In the present work, a parental plasmid containing the bacterial backbone to allow bacterial replication, and the eukaryotic expression cassette (short-hairpin RNA sequence) flanked with MRS to the further minicircle isolation, was constructed – pshRNA. In order to construct the parental plasmid expressing a shRNA targeting VEGF, pVEGF-GFP (*Figure 3.2*), a PP previously developed at iBB-BERG laboratory[98], was used as a template in which the fusion between VEGF and GFP genes was replaced by the annealed dsDNA oligonucleotides. The selected targeting sequence of shRNA was chosen based on its efficiency in silencing VEGF expression in different mammalian cells.[91–93]

Firstly, the pVEGF-GFP was digested for 3 hours at 37ºC with XhoI and BamHI. After that, the digested samples, were separated by agarose gel electrophoresis (*Figure 4.1*).

After double digestion, the resulting fragments should have 3,245 and 1,318bp length, in which the latter corresponds to the VEGF+GFP portion of the pVEGF-GFP. As shown in Figure 4.1, the

restriction pattern matches the expected one, so the desired band (highlighted with an arrow) was extracted and purified from the gel. Since the dsDNA oligonucleotide exhibit overhangs of the XhoI and BamHI digested sequence (*Figure 3.1*), its digestion was not required.

After ligation of the desired fragment from pVEGF-GFP with the annealed dsDNA oligonucleotides, with a vector:insert ratio of 1:5 or 1:7, *E. coli* DH5α transformation was performed. Six *E. coli* DH5α colonies that resulted from the transformation were selected from the plate to further evaluation. After pDNA extraction and digestion with SpeI and BamHI restriction enzymes, the pDNA was separated on an agarose gel electrophoresis (*Figure 4.2*).

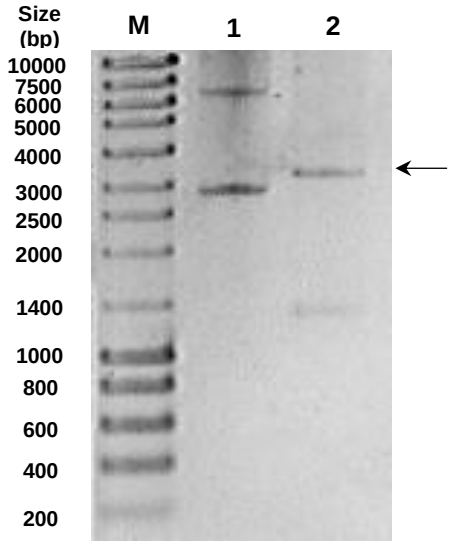

Figure 4.1 - Agarose gel electrophoresis analysis of the digested parental plasmid pVEGF-GFP. pDNA was purified from *E. coli* cells before (lane 1) and after restriction with XhoI and BamHI (lane 2) for 3 hours at 37ºC. The desired band is highlighted with an arrow. Lane M - molecular weight marker NZYDNA Ladder III (Nzytech).

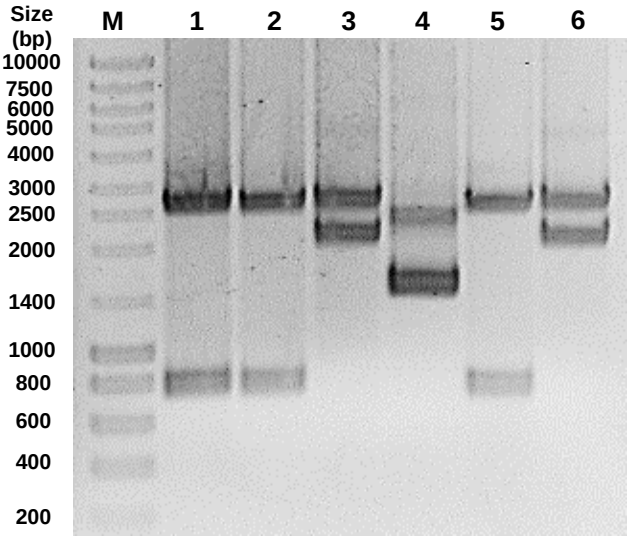

Figure 4.2 - Agarose gel electrophoresis analysis of pshRNA candidates. pDNA purified from *E. coli* colonies resulting from the transformation with the ligation mixture with a vector:insert ratio of 1:5 (lane 1 to 3) or 1:7 (lane 4 to 6). The samples were digested with SpeI and BamHI for 3h at 37ºC. Lane M - molecular weight marker NZYDNA Ladder III (Nzytech)

The restriction pattern of the transformants 1, 2 and 5 matches the one expected for the digestion of the newly constructed PP (pshRNA) with SpeI and BamHI (2,553 bp + 751 bp), while transformants 3 and 6 match the restriction pattern of double digested pVEGF-GFP (2,553 bp + 2,010 bp) (*Figure 4.2*). The transformant 1 inserted sequence was confirmed by DNA sequencing (*Supplementary Data 2A*), in which the result validated the correct insertion of the shRNA sequence and consequently successful construction of the parental plasmid pshRNA (*Figure 4.3*).

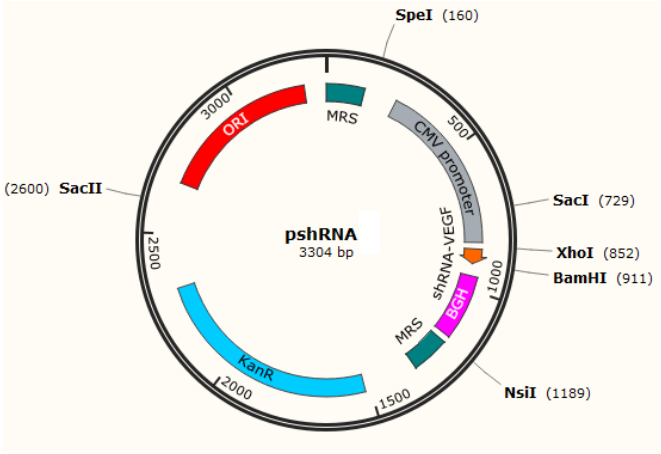

Figure 4.3- Schematic representation of the constructed parental plasmid pshRNA (3,304 bp).

4.2. Minicircle production and purification

For this project, purified minicircles of pVEGF-GFP and pshRNA (MC-VEGF-GFP and MC-shRNA, respectively) are required to further transfect different types of cells. First, it is required the production and *in vivo* recombination of the parental plasmid. Afterwards, minicircle isolation and purification is accomplished.

4.2.1. Cell growth and recombination

For the production and *in vivo* recombination of the parental plasmid, the producer strain *E. coli* BW2P was used. This strain contains the ParA resolvase gene under transcriptional control of the arabinose promoter/operator system, induced by arabinose and repressed by glucose. ParA catalyzes the recombination of parental plasmid (PP) into miniplasmid (MP) and minicircle (MC).[79]

E. coli BW2P cells harbouring the different parental plasmids were grown and OD_{600nm} was monitored throughout time allowing the construction of growth curves (*Figure 4.4*). The recombination into MC plus MP was induced by the addition of L-(+)-arabinose at an $OD_{600nm} \approx 2.5$ (*Figure 4.4*), corresponding to the late exponential phase to allow cell number and PP maximization before induction.

As shown in Figure 4.4, the *E. coli* BW2P harboring different PP grown similarly, reaching approximate OD_{600nm} values after 1 hour of recombination, which is expected since the plasmid size is similar.

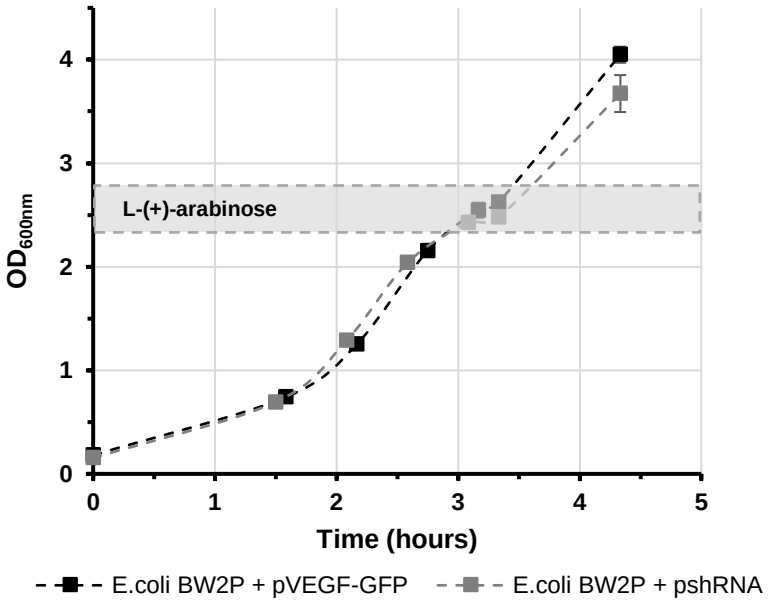

Fi**gure 4.4 -** Growth curves of *E. coli* BW2P harbouring different parental plasmids. Bacterial growth was performed in 250mL LB medium supplemented with 30 µg/mL kanamycin, at 37ºC and 250 rpm. The range of OD_{600nm} values in which recombination in MP plus MC was induced is shown.

To evaluate the recombination efficiency of newly constructed PP pshRNA, samples were collected after recombination induction, every 30 minutes for 2 hours. The pDNA was extracted from the samples and separated by an agarose gel electrophoresis (*Figure 4.5*).

This analysis showed that before induction, open-circular (sc) PP form predominate (lane 1, *Figure 4.5*). The fact that MC and MP species are absent is a clear indication that no recombination occurs before L-(+)-arabinose induction. On the other hand, after 30 min, 60 min, 90 min, and 120 min of recombination, the production of MP and MC is detected by the presence of the corresponding bands of sc MP at ~1,500bp and of sc MC at ~900bp and absence of the PP bands (lane 2 to 5, *Figure 4.5*). From this result, it is possible to confirm the recombination efficiency of the producer system used to express the ParA resolvase, since PP species are almost undetectable after 30min of recombination (lane 2, *Figure 4.5*). As such, for the following minicircle productions, 1 hour of recombination seemed appropriate.

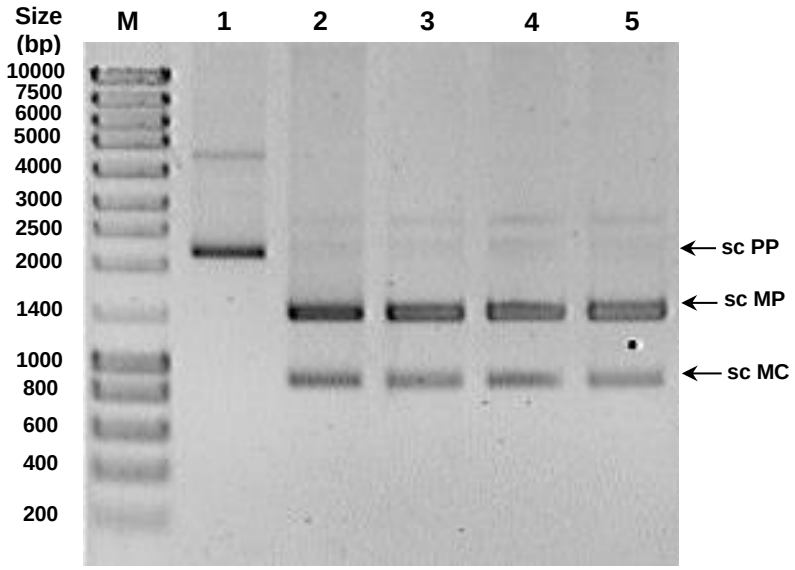

Figure 4.5 - Agarose gel electrophoresis analysis of pshRNA recombination *in vivo*. pDNA purified from *E. coli* cells collected before (lane 1) and after (lane 2: 30min, lane 3: 60min, lane 4: 90min, lane 5: 120min) induction of recombination with L-(+)-arabinose. Lane M - molecular weight marker NZYDNA Ladder III (Nzytech). Abbreviations: sc PP- supercoiled parental plasmid; sc MC- supercoiled minicircle; sc MP- supercoiled miniplasmid.

4.2.2. Minicircle purification

After *E. coli* BW2P growth and recombination of PP into target MC, cell harvesting followed by alkaline lysis were performed, to release the intracellular contents and denature genomic DNA and proteins. Then, a tandem precipitation process was performed with isopropanol, ammonium acetate and PEG-8000, in order to remove the RNA and protein impurities of the solution and concentrated the pDNA. Samples were collected after each precipitation step to monitor the primary purification of pVEGF-GFP (*Figure 4.6A*) and pshRNA (*Figure 4.6B*) minicircles.

Through the gel electrophoresis analysis, it was possible to verify that the two isoforms of MPs and MCs and RNA are the major components in the samples (*Figure 4.6*). Additionally, the RNA load was substantially reduced after ammonium acetate precipitation (lane 3, *Figure 4.6*). However, it is possible to note that, in the case of pshRNA, high amounts of RNA molecules from various sizes appear to remain in the sample (lane 3, *Figure 4.6B*), that could lead to complications in the following purification steps. The significant amount of RNA might be due to an inadequate RNA degradation during cellular lysis or some precipitation step poorly executed, namely during the precipitation with ammonium acetate where RNA and protein impurities in this solution should be excluded in the pellet.[100]

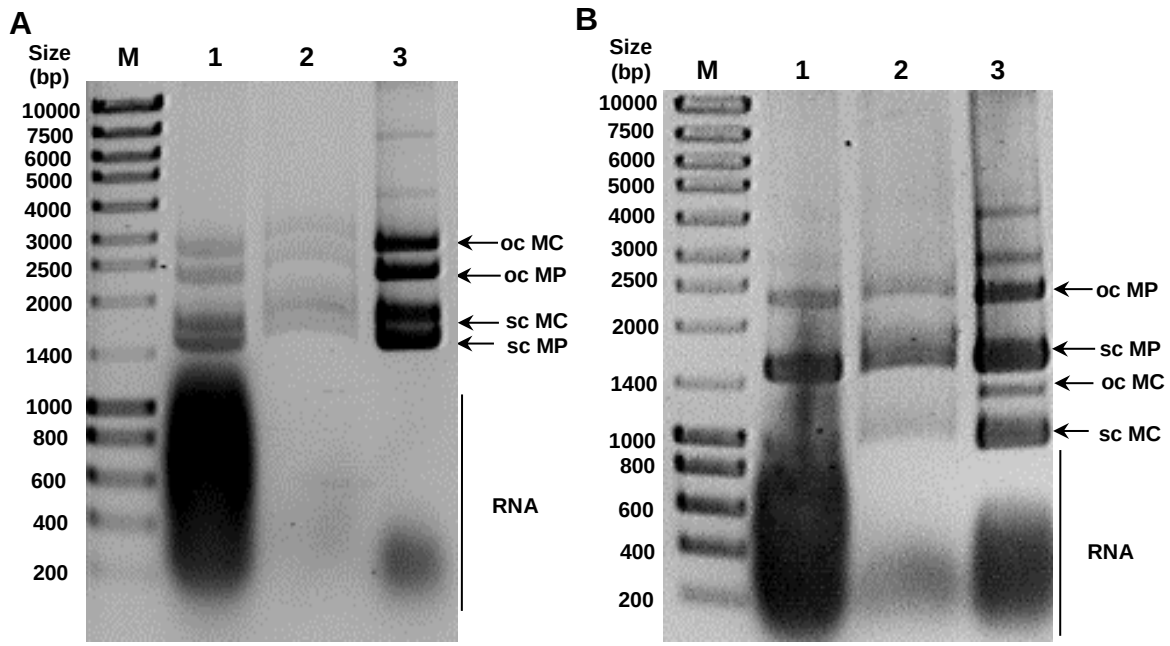

Figure 4.6 - Agarose gel electrophoresis was used to analyse samples collected after each step of the primary purification of pVEGF-GFP (**A**) and pshRNA (**B**) minicircles. Samples were collected after alkaline isopropanol precipitation (lane 1, 3µL of sample), ammonium acetate precipitation (lane 2, 6µL of sample) and PEG-8000 precipitation (lane 3, 1µL of sample). Lane M - molecular weight marker NZYDNA Ladder III (Nzytech). Abbreviations: oc MC- open-circular minicircle; sc MC- supercoiled minicircle; oc MP- open-circular miniplasmid; sc MP- supercoiled miniplasmid.

After the primary purification, enzymatic digestion with Nb.BbvCI, that recognizes a specific target sequence located on the bacterial back-bone of the PP, was used to convert sc molecules into the corresponding oc forms by nicking one of the MP and non-recombined PP strands at the target site.[101] MC plus MP samples of pVEGF-GFP and pshRNA collected before and after digestion with Nb.BbvCI for 1 hour at 37ºC, were analysed through agarose gel electrophoresis (*Figure 4.7*).

The results show that sc MP (lane 1, *Figure 4.7*) were readily converted into its oc counterpart (lanes 2, *Figure 4.7*), whereas sc MC remained intact (lanes 1 and 2, *Figure 4.7*). After digestion, the sample comprised a mixture of sc MC, oc MC and oc MP (lanes 2, *Figure 4.7*).

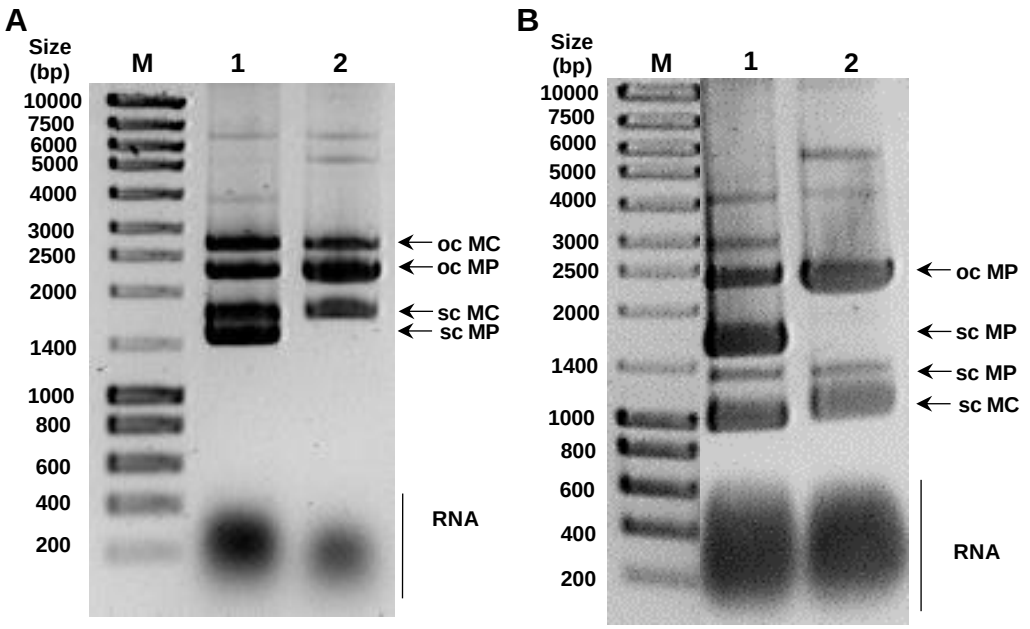

Figure 4.7 - Agarose gel electrophoresis analysis of MC plus MP samples of pVEGF-GFP (**A**) and pshRNA (**B**) before and after digestion with endonuclease Nb.BbvCI. Samples were collected before (lane 1, 1µL of sample) and after (lane 2, 1µL of sample) digestion with endonuclease Nb.BbvCI, that nick one of the MP and non-recombined PP strands, for 1-3 hours at 37ºC. Lane M - molecular weight marker NZYDNA Ladder III (Nzytech). Abbreviations: oc MC- open circular minicircle; sc MC- supercoiled minicircle; oc MP- open circular miniplasmid; sc MP- supercoiled miniplasmid.

As such, in order to isolate the sc MC from the other species, multimodal chromatography was completed using a 5 mL chromatographic column packed with Capto^{TM}adhere resin. Runs were performed at 1 mL/min, unbound material was washed with 2 CV of 41.5% B (830 mM, ≈ 69 mS/cm) and elution was accomplished using two steps with increasing salt concentration, the first at 46% B (920 mM, ≈75 mS/cm) and the second at 100% B (2 M, ≈140 mS/cm).

The chromatogram obtained when samples containing MC plus MP of pVEGF-GFP were run in the column, under the referred conditions, is shown in Figure 4.8A. Moreover, some of the fractions collected were analysed by agarose gel electrophoresis (*Figure 4.8B*).

The results show that the first peak, at 41.5%B, contains oc forms of MP and MC (lanes 2–5), the second peak, at 46%B contains sc MC (lanes 13–17) and a last peak at 100%B contains RNA (lane 25). The fraction 13 to 17, containing sc MC appear to be free from oc species, however it is possible to verify the presence of RNA molecules. Despite the chromatographic profile matches the one expected[100], 400 mAU in the third peak (*Figure 4.8A*) indicates the presence of high amounts of RNA in the sample, which was then verified in both feed stream and fraction 25 (lane F and 25, *Figure 4.8B*). High amounts of RNA may have resulted in an overload of the column, leading to the elution of RNA in the sc MC fractions.

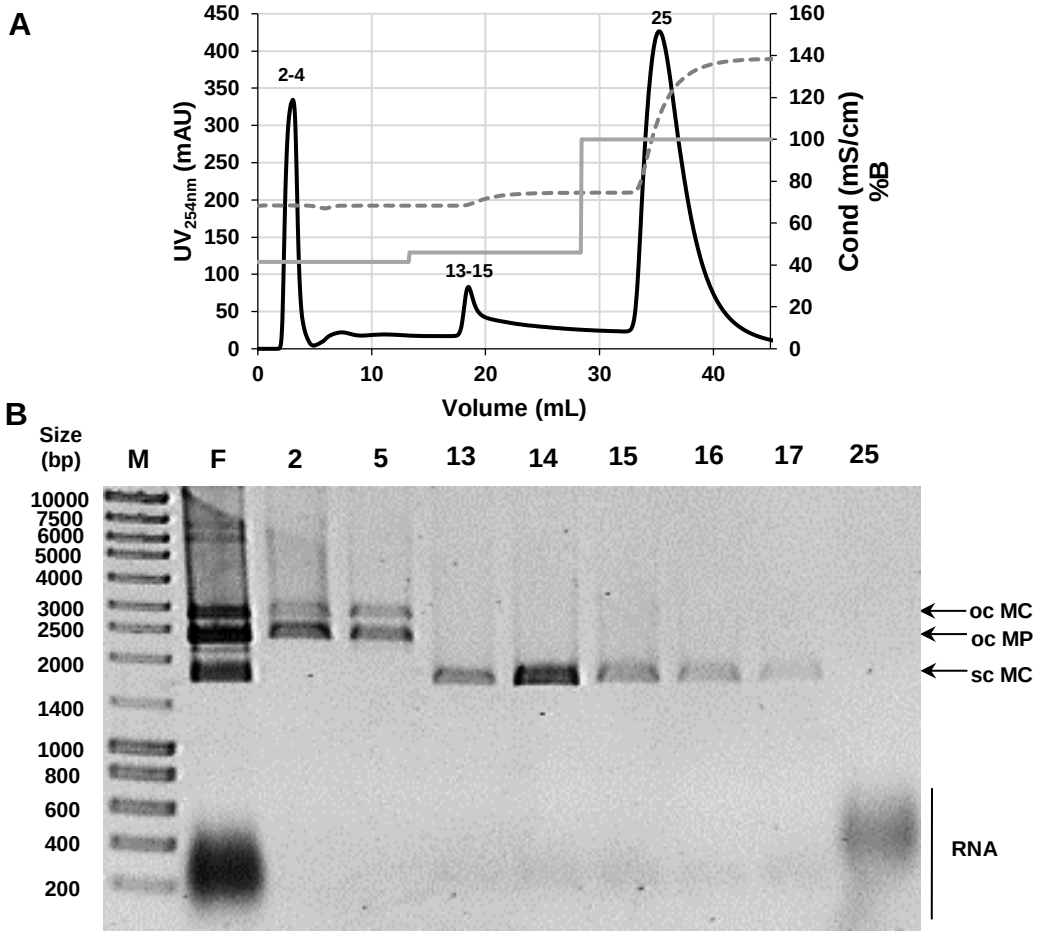

Figure 4.8 - Multimodal chromatography purification of sc MC from pVEGF-GFP from a feed stream containing also oc pDNA and RNA. **(A)** Chromatogram obtained using a Capto^{TM}Adhere column and a series of elution steps with increasing NaCl concentrations. Numbers over peaks correspond to collected fractions. Black continuous line: absorbance at 254 nm; grey dashed line: conductivity (mS/cm); grey continuous line: percentage of buffer B (%B). **(B)** Agarose gel electrophoresis analysis of fractions collected during the chromatographic run. The numbers above each lane correspond to fractions collected (10 µL of sample for fractions 2–17; 30 µL of sample for fraction 25). Lane M - molecular weight marker NZYDNA Ladder III (Nzytech). Abbreviations: oc MC- open circular minicircle; sc MC- supercoiled minicircle; oc MP- open circular miniplasmid; sc MP- supercoiled miniplasmid.

Finally, after dialysis and concentration of the fractions 13-15 of the chromatographic runs of the two samples resulted from pVEGF-GFP primary purification, using Amicon® Ultra-4 MWCO 30 kDa, an agarose gel electrophoresis separation was completed to evaluate the integrity and purity of the sample (*Figure 4.9*). It is possible to note the presence of an individual band that corresponds to the sc form of the MC of pVEGF-GFF (MC-VEGF-GFP; 2 457 bp). Additionally, the sample appeared to be free from RNA which indicates that the RNA molecules were smaller than 30kDa and pass through the membrane while sc MC was retained.

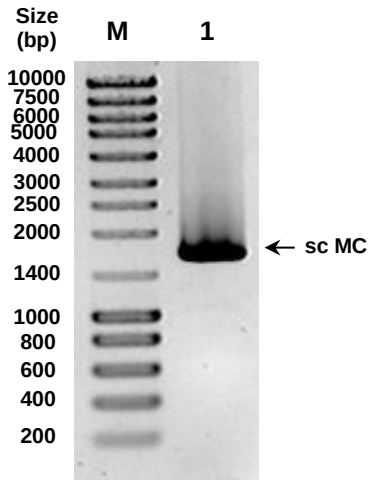

Figure 4.9 - Agarose gel electrophoresis analysis of pVEGF-GFP minicircle sample after dialysis and concentration of the corresponding fractions, using Amicon® Ultra-4 MWCO 30 kDa (1µL, lane 1). Lane M - molecular weight marker NZYDNA Ladder III (Nzytech). Abbreviations: sc MC- supercoiled minicircle.

Regarding the isolation of the sc MC of pshRNA, a multimodal chromatography was performed under the same conditions previously described. The chromatogram and agarose gel electrophoresis analysis of some fractions collected after the run are shown in Figure 4.10A and 4.10B, respectively.

Once again, the results show that the first peak, at 41.5%B, contains oc forms of MP and MC (lanes 2–5), the second peak, at 46%B contains sc MC (lanes 13–17) and a last peak at 100%B contains RNA (lane 25). The fraction 13 to 15, appear to be free from oc species and RNA, containing only sc MC. The chromatographic profile obtained (*Figure 4.10A*) is similar to the one expected [100], however is possible to note that the second peak is very reduced indicating low amounts of pDNA. Moreover, it is possible to verify that the bands that corresponds to sc MC of pshRNA (lane 13-17, *Figure 4.10B*) are fainter compared to the sc MC of pVEGF-GFP ones (lane 13-17, *Figure 4.8B*), confirming that the sc MC is present in lower amounts. In fact, throughout the purification steps sc MC bands appeared to be fainter, indicating lower pDNA amounts. This might be related to its smaller size, which make it more susceptible to destabilisation and degradation during the several purification steps.

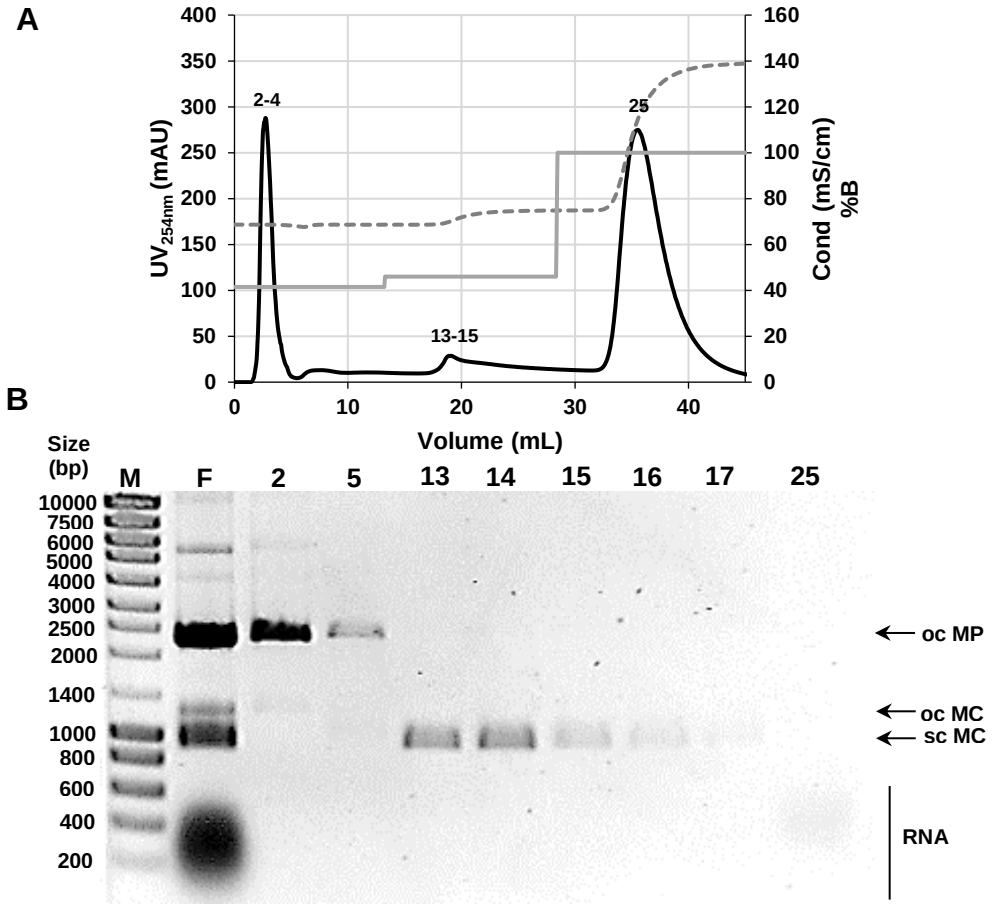

Figure 4.10 - Multimodal chromatography purification of sc MC from pshRNA from a feed stream containing also oc pDNA and RNA. **(A)** Chromatogram obtained using a Capto^{TM}Adhere column and a series of elution steps with increasing NaCl concentrations. Numbers over peaks correspond to collected fractions. Black continuous line: absorbance at 254 nm; grey dashed line: conductivity (mS/cm); grey continuous line: percentage of buffer B (%B). **(B)** Agarose gel electrophoresis analysis of fractions collected during the chromatographic run. The numbers above each lane correspond to fractions collected (10 µL of sample for fractions 2–17; 30 µL of sample for fraction 25). Lane M - molecular weight marker NZYDNA Ladder III (Nzytech). Abbreviations: oc MC- open circular minicircle; sc MC- supercoiled minicircle; oc MP- open circular miniplasmid; sc MP- supercoiled miniplasmid.

Finally, after dialysis and concentration of the fractions 13-15 of the chromatographic runs of one sample resulted from pshRNA primary purification, using Amicon® Ultra-4 MWCO 30 kDa, an agarose gel electrophoresis separation was completed to assess the integrity and purity of the sample (*Figure 4.11).* It is possible to note that the isolation of the sc form of the MC of phRNA (MC-shRNA; 1 198 bp) was successful, by the presence of a single band at ~900 bp.

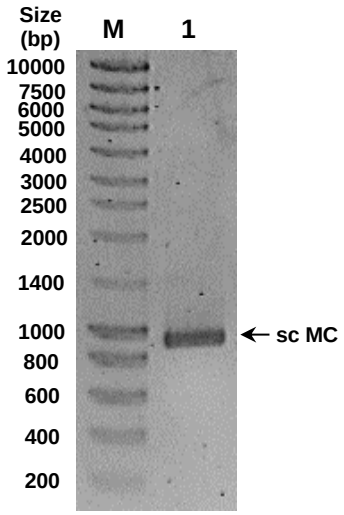

Figure 4.11- Agarose gel electrophoresis analysis of pshRNA minicircle sample after dialysis and concentration of the corresponding fractions, using Amicon® Ultra-4 MWCO 30 kDa (1µL, lane 1). Lane M - molecular weight marker NZYDNA Ladder III (Nzytech). Abbreviations: sc MC- supercoiled minicircle.

4.3. Microporation of BM-MSCs and MCF-7 with the MC-shRNA targeting VEGF

In order to confirm that the recombinant plasmid obtained in the present work is successfully recognized by cellular machinery, leading to the expression of the short-hairpin RNA (*Figure 3.1*) that after processing results into a functional siRNA that silences VEGF expression, some preliminary experiments were performed by transfecting BM-MSCs (donor M79A15) and MCF-7 by microporation. Microporation was the chosen method since growing evidence reveal that electroporation is one of the most efficient non-viral methods for transferring exogenous DNA into mammalian cells, namely using the Neon Transfection System device.[105] In fact, microporation demonstrated to be a reliable and efficient method to genetically modify BM-MSCs by the delivery of minicircles[102] and also larger conventional vectors.[106]

A microporation experiment of BM-MSC was performed as previously optimized[102,107], in which 1.5×10^6 cells were microporated with 3 µg of MC-VEGF (the equivalent number of molecules of 10 µg of pVAX-VEGF[102,107]). In this experiment, non-microporated MSCs and MSCs microporated without pDNA were used as controls. Cells were plated at 8.0×10^3 cells/cm^2 and collected 48 hours after microporation. Cell density and viability were determined in order to evaluate the impact of the delivery system on the proliferative capacity of MSCs (*Figure 4.12*). Additionally, cell recovery (CR) of the microporated samples were also determined in which non-microporated cells were considered to have a recovery of 100% (*Figure 4.12*).

From the results presented in Figure 4.12, it is possible to verify that after 48 hours the cell densities of the microporated cells were lower relatively to the non-microporated control. Regarding the CR, the microporated conditions showed lower values than the control condition (MSC; 100%). In contrast to the expected, cells microporated without pDNA (MSC micro) showed lower recoveries compared with cells microporated with MC-shRNA (55.9% and 79.0%, respectively). In fact, it was

reported that the presence of pDNA seems to slow down BM-MSC proliferation and cell mortality in most cases seems to be related to the presence of pDNA inside the cells and not, at least significantly, with the gene delivery process itself.[106] However, high viabilities (≥ 95%) can be observed even when few cells are recovered from electroporation process.

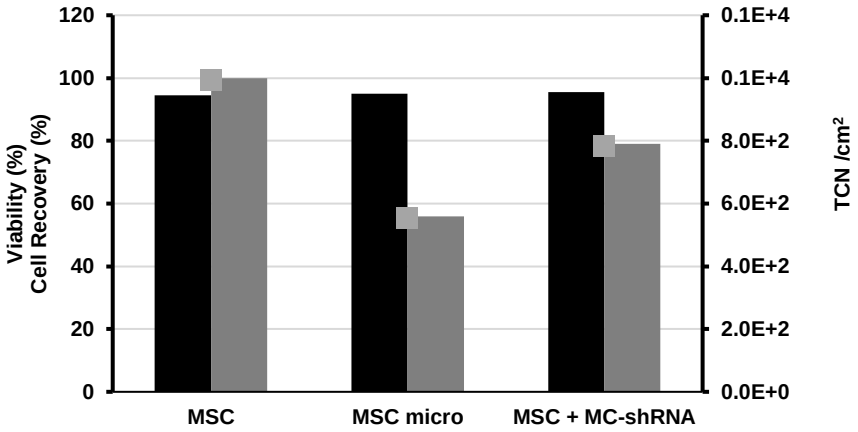

Figure 4.12 - Analysis of the BM-MSC behaviour 48 hours after microporation with MC-shRNA. Viability and cell recovery after microporation are presented as the black and grey bars, respectively. Cell densities (TCN/cm^2) are shown in squares. After microporation, cells were plated at 8.0x10^{3}cell/cm^2. Non-microporated cells (MSC) and microporated without pDNA (MSC micro) were used as controls.

Subsequently, in order to evaluate the effect of the shRNA on the expression levels of VEGF, RT-qPCR was performed. For that, the RNA from the collected cells was extracted, converted into cDNA and finally the determination of the fold change (FC) in VEGF-mRNA expression applying the $2^{-\Delta\Delta CT}$ method was accomplished. GAPDH was used as the housekeeping gene and non-microporated MSC as baseline, as performed elsewhere.[102]

Figure 4.13 shows the effect of MC-shRNA on VEGF relative expression from BM-MSCs 48 hours post-transfection. MSC microporated with MC-shRNA (MSC + MC-shRNA) showed no alteration on the mRNA copies of VEGF when compared to non-microporated cells (MSC). As such, from this

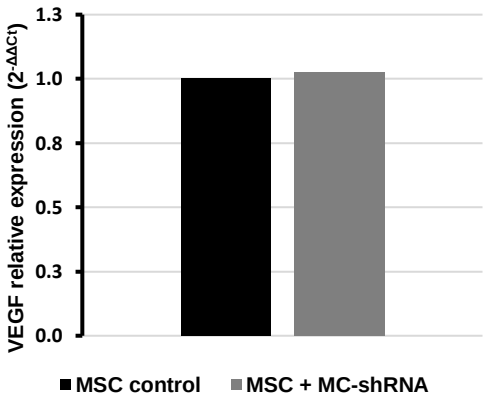

Figure 4.13 - Evaluation of transgene delivery 48 hours after microporation with MC-shRNA, by analysis of BM-MSC VEGF-mRNA expression by RT-qPCR. The fold change values were obtained using the $2^{-\Delta\Delta Ct}$ method, with GAPDH as the endogenous control gene and non-transfected MSC as baseline.

preliminary experiment, MC-shRNA appeared to have no effect on diminishing BM-MSC VEGF expression at the mRNA level.

MCF-7, a widely studied fast growing non-invasive breast cancer cell line was selected to further test the effect of MC-shRNA on VEGF expression. VEGF is not only responsible for monitoring the angiogenic process in the tumour microenvironment but also exerts several the autocrine functions in breast tumour cells such as MCF-7, including cell proliferation, survival and migration/invasion.[108]

A single MCF-7 transfection experiment was performed by microporation, in which 1.5×10^6 cells were microporated with 10 µg of MC-shRNA (standard amount[109] since no previous studies using the Neon transfection system are described). In this experiment, it was only possible to use non-microporated MCF-7 as control. Cells were plated at 3.0×10^4 cells/cm^2 and collected 24 h and 48 h post-transfection. To evaluate the impact of the pDNA delivery on the proliferative capacity of MCF-7, cell density, viability and cell recovery (CR) were determined (*Figure 4.14*). Once again, CR of the microporated samples were also determined in which non-microporated cells were considered to have a recovery of 100%.

Regarding the cell density of cells non-microporated (MCF-7) and cells microporated with the MC-shRNA (MCF-7 + MC-shRNA) (*Figure 4.14A*) it is possible to verify that 24 hours post-transfection, the number of cells is lower even in the control condition, indicating that not all the plated cells successfully adhered and grew. Nevertheless, the microporated cells showed even lower cells numbers after 24 hours and, unlike the control cells, were not able to achieve a higher population density even after 48 hours in culture.

The CR, which reflects the level of cell death in microporated samples, showed that microporation MCF-7 with MC-shRNA strongly disturb the cells, reaching a value of 26% (*Figure 4.14B*)

The viability of microporated MCF-7 (79%: *Figure 4.14B*) was lower than the one obtained for BM-MSC (96%: *Figure 4.12*), but considering that the CR was extremely low, this result further support that microporation does not affect the viability of the cells, consistent with data from literature.[105]

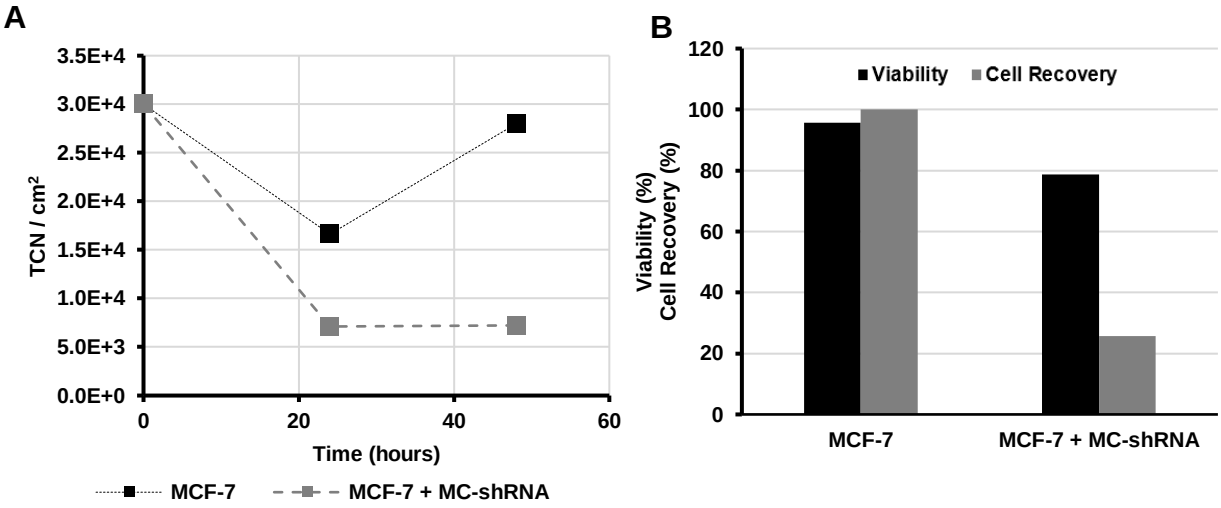

Figure 4.14 - Analysis of the MCF-7 behaviour 48 hours after microporation with MC-shRNA. **(A)** MCF-7 cell density for non-microporated (black) and microporated with MC-shRNA (grey) after 24 and 48 hours. Cells were plated after microporation at $3.0\text{x}10^4$cell/cm^2. **(B)** Viability and cell recovery of MCF-7 48 hours after microporation are represented as black and grey bars, respectively. Non-microporated cells (MCF-7) were used as control.

In order to evaluate the impact of the MC-shRNA presence on MCF-7 cell proliferation, recovery and viability, an experiment including MCF-7 microporated without pDNA should be included as control.

Afterwards, the MCF-7 cells collected 24h and 48h after microporation were used to quantify the VEGF-mRNA by RT-qPCR using the $2^{-\Delta\Delta CT}$ method as described above (*Figure 4.15*).

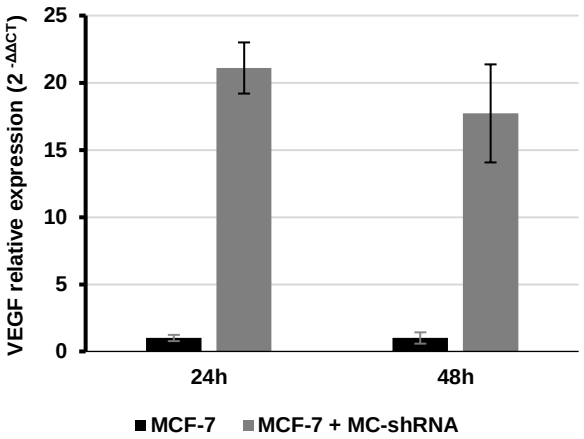

Figure 4.15 - Evaluation of transgene delivery 24h and 48 h after microporation with MC-shRNA, by analysis of MCF-7 VEGF-mRNA expression by RT-qPCR. The fold change values were obtained using $2^{-\Delta\Delta Ct}$ method, with GAPDH as the endogenous control gene and non-transfected MCF-7 as baseline. Values are presented as mean ± SD of sample duplicates.

Through the analysis of Figure 4.15, it is possible to note that the transfection of the MC-shRNA (MCF-7 + MC-shRNA) exhibited 21- and 17-fold higher mRNA copies of VEGF than non-microporated cells (MCF-7), 24h and 48h after transfection respectively.

These results were not expected, since the transcribed shRNA should be processed into a siRNA that recognizes a specific region of the VEGF-mRNA targeting it for degradation, leading to reduced levels of VEGF, instead of inducing its expression as observed in these preliminary experiments. A possible explanation could be that the transcribed shRNA is acting as transcriptional activator of VEGF, as a consequence of off-target effects.

siRNA off-target effects can result in the suppression of non-target genes via a microRNA mechanism by partial sequence complementarity of other endogenous mRNAs.[59] Hypothetically, by silencing non-target genes that downregulate VEGF, the siRNA might be inducing VEGF expression, leading to the increased mRNA levels observed.

Additionally, growing evidence report that miRNA and siRNA can also serve as activators of gene expression by targeting gene regulatory sequences.[110] For example, Long-Cheng and colleagues have identified several dsRNAs that activate gene expression by targeting non-coding regulatory regions promoters of human genes, namely VEGF, in which the transfection of dsRNA targeting its promoter at position −706, into HeLa cells resulted in a 4-fold increase in VEGFA-mRNA levels.[111] As such, the transcribed shRNA might be acting as a transcriptional activator of VEGF as result of an off-target effect by partial sequence complementarity with VEGF regulatory regions, rather than the target region.

However, more experiments should be performed to validate this effect, namely by transfecting the synthetic siRNA targeting the same sequence (identical guide strand) as MC-shRNA to verify if the increased expression of VEGF persists.

4.4. Microporation of BM-MSCs with the synthetic siRNA targeting VEGF

As previously mentioned, a microporation experience including a siRNA synthetize outsource, that represent the product originated after the MC-derived shRNA processing, was performed. This way, it is possible to verify if the increased levels of VEGF-mRNA are related to the target sequence.

Microporation of BM-MSC with MC-shRNA was performed according to Materials and Methods, however a higher amount of pDNA (10 µg MC-shRNA) was used since no significant effect in the BM-MSC VEGF-mRNA levels was detected previously (1-fold, compared to MSC control; *Figure 4.13*). Regarding the microporation with synthetic siRNA, a concentration of 50 nM was used[109,112]. In this experiment, non-microporated MSCs and MSCs microporated without pDNA were used as controls. Cells were collected 24 h and 48 h after microporation. BM-MSC cell density over 48h post-transfection and viability/CR 48h after microporation are shown in Figure 4.16A and 4.16B, respectively.

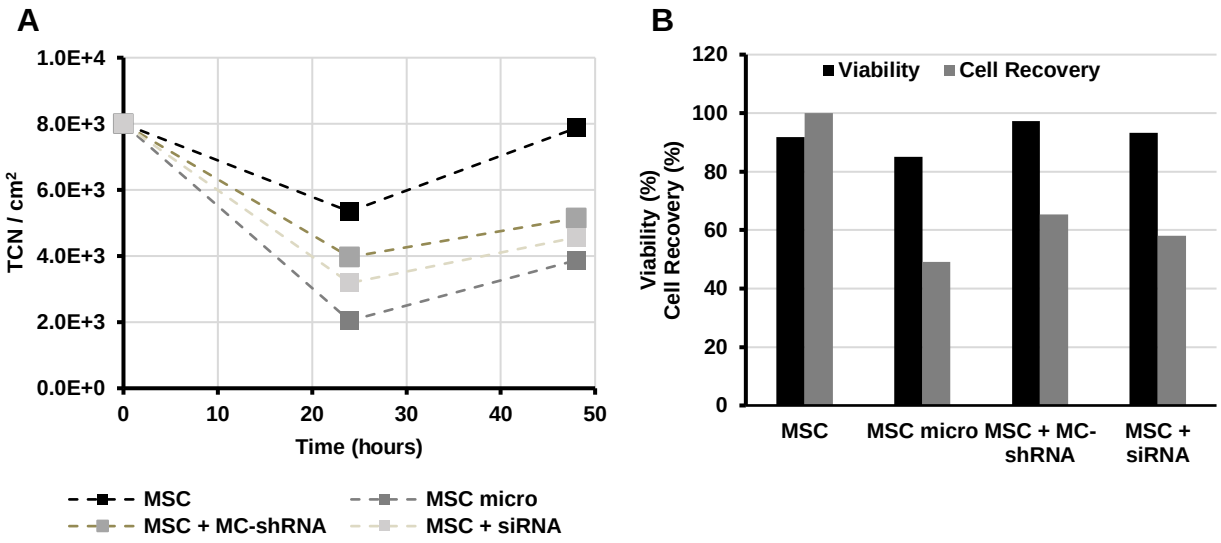

Figure 4.16 - Analysis of the BM-MSC behaviour 48 hours after microporation with MC-shRNA or synthetic siRNA. **(A)** MSC cell density 24 and 48 hours after microporation. Cells were plated after microporation at 8.00x10^{3}cell/cm^2. **(B)** Viability and cell recovery of MSC 48 hours after microporation are represented as black and grey bars, respectively. Non-microporated cells (MSC) were used as control.

From the results presented in Figure 4.16, it is possible to verify that, as obtained previously (*Figure 4.12*), cells number for microporation conditions were lower relatively to the non-microporated control, 48 hours after microporation. Additionally, CR of the microporated conditions showed lower values than the control condition (MSC; 100%). Once again, cells microporated without pDNA/siRNA showed lower recoveries (MSC micro; 49%). Comparing the cells microporated with pDNA (MSC +MC-shRNA; *Figure 4.16B*) and siRNA (MSC + siRNA; *Figure 4.16B*), it is possible to see that CR was lower

in the siRNA condition (65% and 58%, respectively). Cell viabilities were high in all conditions, with the lowest condition being the cells microporated without pDNA/siRNA (MSC micro; 85%).

Afterwards, the collected cells were used to quantify the VEGF-mRNA 24 h and 48 h after microporation, by RT-qPCR using the $2^{-\Delta\Delta CT}$ method (*Figure 4.17*).

Through the analysis of Figure 4.17 it is possible to verify that 24 h post-transfection with the MC-shRNA (MSC + MC-shRNA), BM-MSC express 0.85-fold of mRNA copies of VEGF than non-microporated cells (MSC) that corresponds to a percentage of knockdown (%KD) of 15%, whereas 48 hours post-transfection the VEGF-mRNA were slightly higher (1.0-fold) than the control, as obtained before (*Figure 4.13*). These results are not consistent compared to the ones obtained previously after MCF-7 transfection with 10µg of MC (*Figure 4.15*), in which an significant increase in VEGF-mRNA was observed. As such, further experiments need to be performed in order to determine if this up-regulation effect only occurs in transfected MCF-7.

On the other hand, the effect of the siRNA (MSC + siRNA) is more evident 48 hours post-transfection in which BM-MSC express 0.75-fold of mRNA copies of VEGF than non-microporated MSC, corresponding to a knock-down of 25%, while at 24h post-transfection was only 5.7%. Although, further experiments are required, siRNA appears to have a positive silencing effect on BM-MSC VEGF expression at mRNA level.

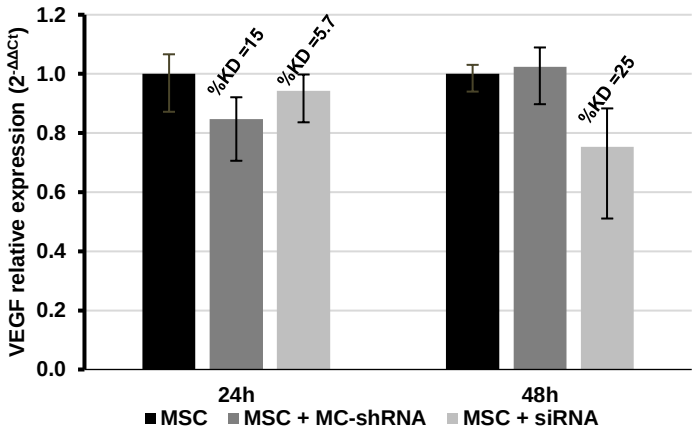

Figure 4.17 - Evaluation of transgene delivery 24 and 48 hours after microporation with MC-shRNA or synthetic siRNA, by analysis of BM-MSC VEGF gene expression by RT-qPCR. The values were obtained using $2^{-\Delta\Delta Ct}$ method, with GAPDH as the endogenous control gene and non-transfected MSC, collected after 24 h and 48 h, as baseline. The percentagens of VEGF knockdown (%KD) are also shown. Values are presented as mean ± SD of sample duplicates.

Due technical limitations with the microporator, the following experiments were performed using Lipofectamine, a widely used reagent tested in numerous gene delivery studies with different agents and cell types, some developed at iBB-SCERG.[73,103]

4.5. Co-transfection of CHO cells with MC-VEGF-GFP and MC-shRNA/synthetic siRNA targeting VEGF

A preliminary experiment was performed using CHO cells, an easily transfected cell line, to access the efficacy of siRNA/shRNA in silencing VEGF expression. The experiment involved the co-transfection of CHO cells with MC-VEGF-GFP and MC-shRNA/synthetic siRNA using Lipofectamine. The protocol to transfect these cells was adapted from La Vega *et al* (2013)[113], in which 1,000,000 cells/ well were platted in 12w-plate and grown 24 hours. In this experiment, 2 µL of LF was used to transfect 600ng of MC-VEGF-GFP, 600ng of MC-VEGF-GFP plus 1,200ng of MC-shRNA and 600ng of MC-VEGF-GFP plus 20pmol of synthetic siRNA, accordingly to the manufacturer's instructions.

The rationale behind this experiment was that the efficacy of siRNA/shRNA sequences could be monitored by their ability to reduce the expression of target-reporter fusion with easily quantified readouts[114]. In the present study, VEGF is the target gene, which is fused to Green Fluorescent Protein (GFP) reporter gene (MC-VEGF-GFP). Therefore, the efficacy to siRNA/shRNA in silencing VEGF will be monitored using fluorescent microscopy and flow cytometry.

The fluorescence intensity for the different conditions 24 hours post-transfection was observed through bright field and fluorescence microscopic images (*Figure 4.18*).

It is possible to observe that in the condition in which cells were transfected with MC-VEGF-GFP in combination with the synthetic siRNA targeting VEGF appeared to have less GFP^+ cells than cells transfected with MC-VEGF-GFP alone (CHO + MC-VEGF-GFP + siRNA and CHO + MC-VEGF-GFP, respectively) indicating that the siRNA could be preventing the expression of VEGF-GFP protein. On the other hand, the number of GFP^+ cells transfected with MC-VEGF-GFP in combination with the MC-shRNA (CHO + MC-VEGF-GFP + MC-shRNA) seems to be slightly lower to one obtained for cells transfected with MC-VEGF-GFP alone. Moreover, fluorescence intensity appears to be lower in the case of the co-transfection.

Afterwards, cells were collected for flow cytometry analysis in order to assess the percentage of GFP+ cells, as well as the mean GFP-fluorescence intensity for each condition (*Figure 4.19*).

The viability and CR of CHO cells in the different condition 24h post-transfection was determined (*Figure 4.20*). The results in Figure 4.20 show that cell viabilities are similar to the control of non-transfected cells (CHO). Regarding CRs, it is possible to verify that cells transfected without pDNA/siRNA (CHO lipofectamine) showed a CR higher than the non-transfected control (CR=100%) indicating that Lipofectamine itself is not toxic to the cells. Also as expected, cell recoveries for cells transfected with genetic material were lower, due to cellular toxicity associated with pDNA.[106] Additionally, cells transfected with MC-VEGF-GFP in combination with MC-shRNA or siRNA exhibited lower CRs (approximately 50%) than cells transfected with MC-VEGF-GFP alone (64%).

Considering the results of flow cytometry, it is possible to verify that the percentage of GFP^+ cells obtained for the cells transfected with MC-VEGF-GFP was 12% (*Figure 4.19*), which was not excepted. In the work developed by Liliana Brito[98], the percentage of GFP^+ CHO cells was approximately 80%[98], which is higher than the one obtained in the present project. However, the transfection method

differ since microporation was used instead of Lipofectamine, which can be the reason for the discrepancy in the results. Additionally, cell recovery for microporation with MC-VEG-GFP was 10%[98],which could led to the higher percentage of GFP^+ cells since few cells survived microporation.

Despite that, it is possible to note a decrease in the $\%GFP^+$ cells in the conditions of cells transfected with MC-VEGF-GFP in combination with MC-shRNA (11%; *Figure 4.19*) and with the synthetic siRNA (6.7%; *Figure 4.19*), as suggested by the microscopy images (*Figure 4.18*). Although this difference is not completely evident for co-transfection with MC-shRNA, in the case of siRNA co-transfection, the molecule appears to have a silencing effect on VEGF-GFP protein expression, decrease $\%GFP^+$ cells by 56%. Additionally, mean of intensity values also shows than siRNA molecules not only led to a reduction of $\%GFP^+$ cells but also to a decreasing in GFP-intensity relatively to cells transfected with MC-VEGF-GFP alone (17 AU and 6.5 AU, respectively), which indicates that GFP-expressing cells could be producing lower amounts of VEGF-GFP protein.

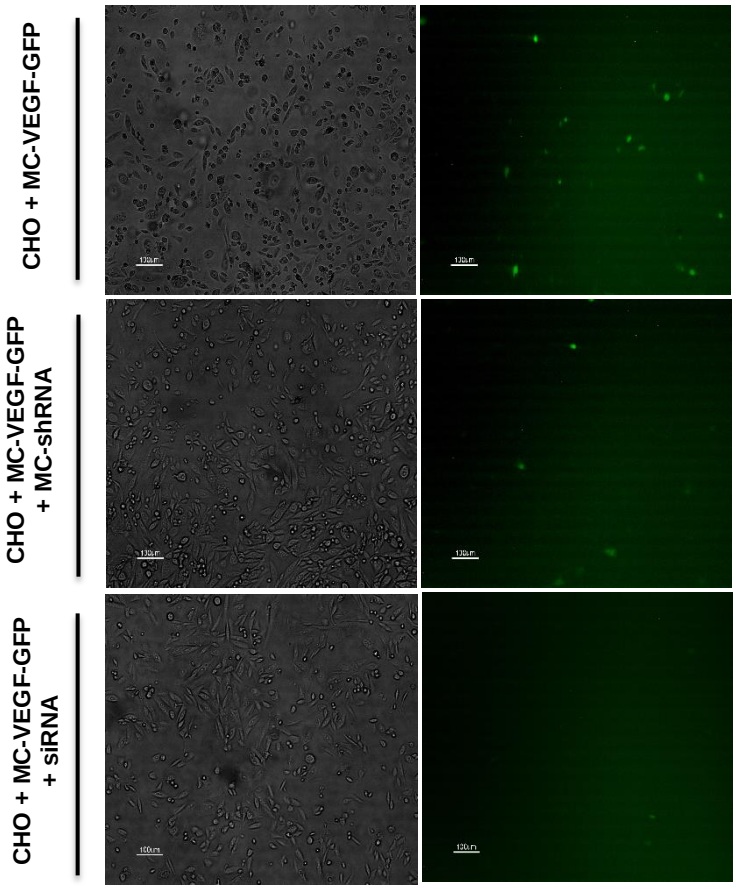

Figure 4.18 - Bright field and fluorescence microscopic images (100X) of CHO cells 24h after transfection with Lipofectamine harbouring MC-VEGF-GFP alone or in combination with the MC-shRNA or synthetic siRNA.

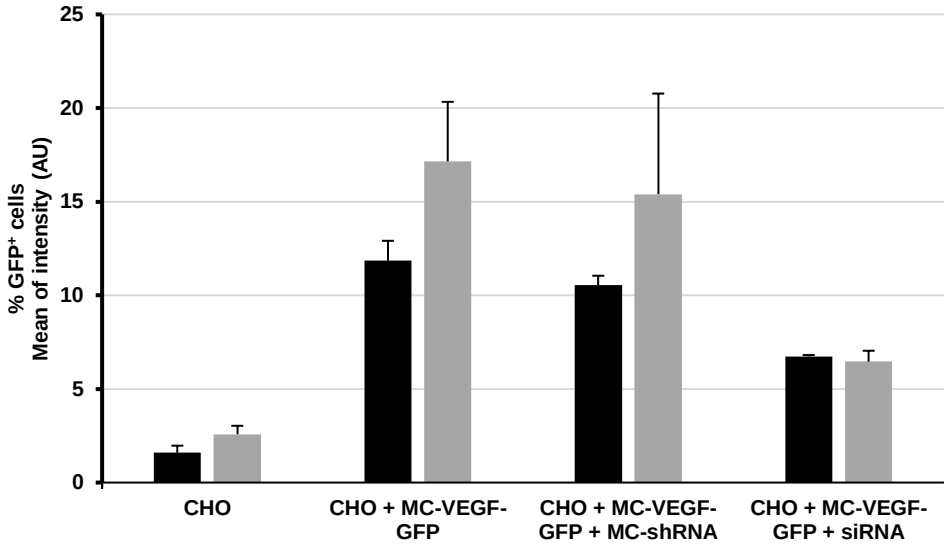

Figure 4.19 - The outcome of the transfected CHO cells with Lipofectamine harbouring MC-VEGF-GFP alone or in combination with the MC-shRNA or synthetic siRNA. After 24h, cells were collected and analysed by flow cytometry and analysed in terms of percentage of GPF-fluorescent cells (black bars) and mean GFP-fluorescence intensity (grey bars). CHO cells transfected only with Lipofectamine were used as control. Values are presented as mean and standard deviation of duplicate samples. Values are presented as mean ± SEM of samples from two individual experiments.

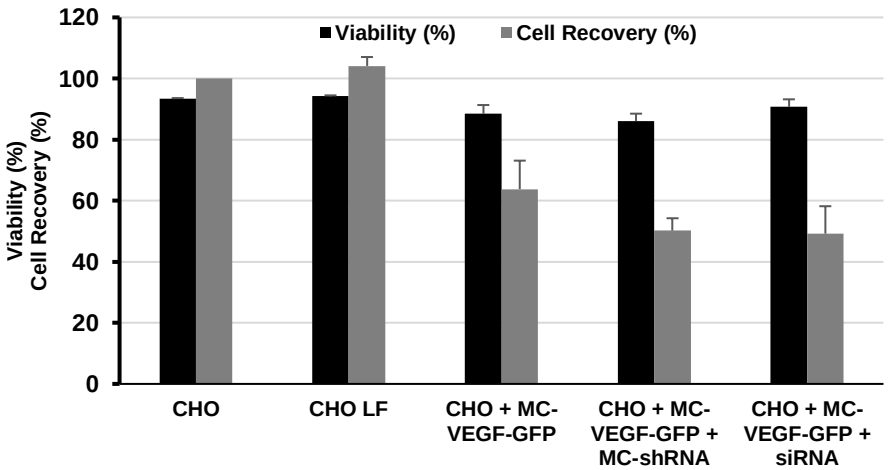

Figure 4.20 - Analysis of the CHO cells behaviour 24 hours after transfection with Lipofectamine harbouring MC-VEGF-GFP alone or in combination with the MC-shRNA or synthetic siRNA. Viability and cell recovery after microporation are presented as the black and grey bars, respectively. Non-transfected cells (CHO) and transfected without pDNA/siRNA (CHO lipofectamine) were used as controls. Values are presented as mean ± SEM of samples from two individual experiments.

4.6. Lipofection of BM-MSCs with the MC-shRNA and synthetic siRNA

In order to further evaluate the silencing potential of the siRNA and MC-derived shRNA, a transfection experiment of BM-MSCs using Lipofectamine was performed.

BM-MSCs were lipofected as described in Boura *et al* (2013)[103], in which cells were plated at a cell density of 4,000 cells/cm^2 in 12-well plates. After 72 hours in culture, with cells at 70-80% confluence (*Figure 4.21*), transfection was carried out using Lipofectamine according to the manufacturer's instructions. This approach was used as in order to minimize surface area limitation to the cultured cells and to ensure that the most of the cells were actively proliferating at the time of transfection, maximizing the transfection efficacy.[103]

In this experiment, 1 µg MC-shRNA/ 50nM synthetic siRNA and 1 µL of Lipofectamine (1 mg/mL) were used to transfect BM-MSCs. Non-transfected cells and cells transfected without pDNA/siRNA were used as control. After 24 h and 48 h in culture, cells were collected from 2 wells (duplicates), in order to reach the required cell numbers to further experiments.

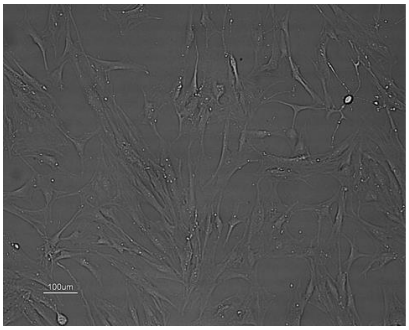

Figure 4.21 - Bright field image of BM-MSCs (100X) before transfection with Lipofectamine, at 70-80% confluence.

Through the CR results of transfected BM-MSCs (*Figure 4.22*), it is possible to confirm that the Lipofectamine itself does not lead to cellular toxicity (>100%; MSC LF), as seen for CHO cells (*Figure 4.20*). Additionally, transfection with the MC-shRNA appears to have a stronger impact in CR compared to the synthetic siRNA, since values of 57% and 69% were obtained. Moreover, Lipofectamine

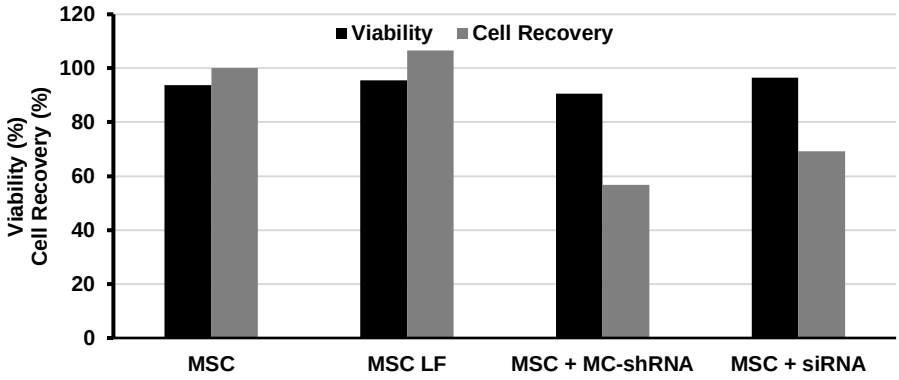

Figure 4.22 - Analysis of the BM-MSC behaviour 48 hours after lipofection with MC-shRNA or synthetic siRNA. Viability and cell recovery after microporation are presented as the black and grey bars, respectively. Non-transfected cells (MSC) and cells transfected without pDNA/siRNA (MSC LF) were used as controls.

transfection does not affect BM-MSC viability, since high values were obtained for all conditions (>90%; *Figure 4.22*).

Afterwards, the collected cells were used to quantify the VEGF-mRNA 24h and 48h after lipofection, by RT-qPCR using the $2^{-\Delta\Delta Ct}$ method (*Figure 4.23*).

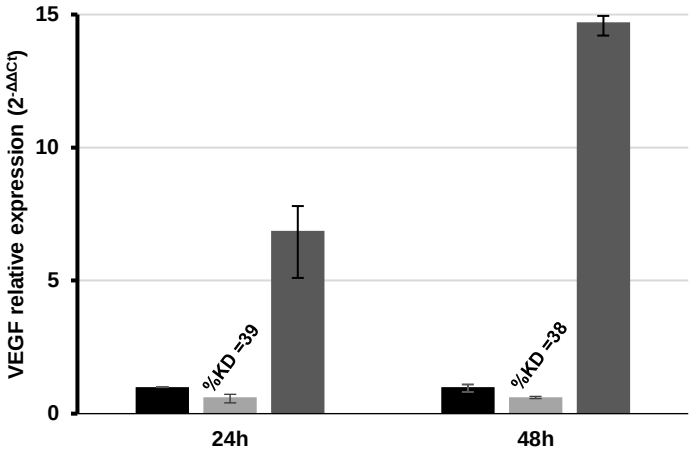

Figure 4.23 - Evaluation of transgene delivery 24 and 48 hours after lipofection with MC-shRNA or synthetic siRNA, by analysis of BM-MSC VEGF gene expression by RT-qPCR. The values were obtained using $2^{-\Delta\Delta Ct}$ method, with GAPDH as the endogenous control gene and MSC transfected without pDNA/siRNA, collected after 24h and 48h, as baseline. The percentagens of VEGF knockdown (%KD) are also shown. Values are presented as mean ± SD of sample duplicates.

The results showed that transfection of BM-MSC with MC-shRNA using Lipofectamine further evidence the unexpected effect on VEGF-mRNA expression, exhibiting 6.7- and 15-fold higher mRNA copies of VEGF than the control cells (MSC LF), 24h and 48h after transfection respectively. Moreover, it was also possible to verify that the transfection with the synthetic siRNA induces a strong effect in silencing VEGF-mRNA expression, with a knockdown of approximately 38%, then the maximum obtained after microporation of BM-MSC (%KD=25%; *Figure 4.17*).

By confirming that the synthetic siRNA successfully leads to the silencing of VEGF-mRNA, it is possible to conclude that the selected target's region is not the cause for the increased levels of VEGF-mRNA associated with MC-shRNA transfection. Additionally, the opposite effects indicate that the transcribed shRNA does not result in the theoretical siRNA molecule (identical to the synthetic siRNA) after processing. Thus, a problem involving the correct processing of the transcript might be causing the observed discrepancies. In fact, polyadenylation coupled with Pol II transcription abolishes its ability to express RNA with clear-cut ends, originating long, undefined shRNAs molecules.[60] Therefore, pre-miRNA-like shRNAs driven by Pol II might not recognized by Dicer, which is responsible for the processing of the shRNA into functional siRNA duplexes that will incorporate the RISC complex for target-specific mRNA degradation.[60,62,63] An approach to minimize this possible effect will be discussed in the next section.

Moreover, a transfection experiment with a gradient of siRNA concentrations was performed in order to assess if the %KD is proportional to siRNA concentration. Cells were collected 24h after

lipofection. Cell viabilities and CR were similar to the ones obtained before (~70%; *Figure 4.22*) indicating that higher siRNA concentration does not lead to increasing cellular toxicity.

The VEGF-mRNA was quantified by RT-qPCR 24 hours post-transfection (*Figure 4.24*). The results showed that a higher %KD was obtained when using the same concentration as before (39%; *Figure 4.23*), reaching 51% (MSC + siRNA (50nM); *Figure 4.24*). The observed difference between the %KD using the same siRNA concentration might be associated to the use of distinct annealed siRNA stock solutions that, although the same procedure is applied, can add variability.

Additionally, the results demonstrate that the %KD remains relatively constant regardless of the siRNA concentration transfected, indicating that all concentrations might be in the gene-knockdown efficacy plateau. As such, for the following experiments involving BM-MSC transfection, a concentration of 50nM seemed appropriate.

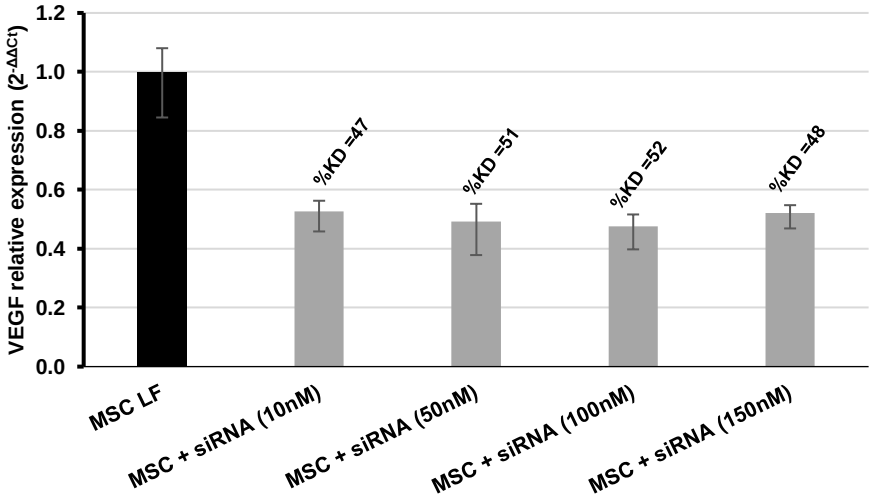

Figure 4.24 - Evaluation of transgene delivery 24 hours after lipofection with different concentrations of synthetic siRNA, by analysis of BM-MSC VEGF gene expression by RT-qPCR. The values were obtained using $2^{-\Delta\Delta Ct}$ method, with GAPDH as the endogenous control gene and MSC transfected without pDNA/siRNA, as baseline. The percentagens of VEGF knockdown (%KD) are also shown. Values are presented as mean ± SD of sample duplicates.

The silencing efficiency of siRNA targeting a particular sequence varies depending on the cell type and expression level of the target gene.[115] Additionally, different transfection methods/delivery systems or experimental procedures result in distinct transfection efficiencies and consequent siRNA silence efficiency. Comparing the obtained results on VEGF gene expression with the ones found in previous studies, it is possible to note some discrepancies. In the study by Wang et al (2010)[92], the authors showed that the selected siRNA was able to efficiently silence VEGF-A expression in BTT-T739-GFPcells, a mouse bladder cancer cell line. The RT-qPCR results revealed a %KD of approximately 75%, 48h after transfection with Lipofectamine. Moreover, Zuo and the colleagues found that this siRNA result in a %KD of 66% after transfecting ARPE-19 cells, a human retinal pigment epithelial cell line, with Lipofectamine.[91] Additionally, in Qazi *et al* (2012)[116], nanoparticle-mediated delivery of plasmid-derived shRNA targeting the same region of VEGF-mRNA, showed to silence its expression with a mRNA %KD of approximately 50%, after corneal intrastromal injection of mice.

4.7. Construction of a novel parental plasmid expressing a shRNA targeting VEGF

As mentioned previously, the opposite set of results obtained for the transfections with the synthetic siRNA and MC-derived shRNA, might due to the incorrect processing of the latter. In fact, due to the lack of a well-defined transcription initiation and termination signal, the originated shRNA might be too long, leading to the formation of secondary structures which might restrain Dicer recognition or/and correct processing. In fact, many commonly used systems for expressing shRNA in cells use an RNA pol III promoter such as U6 or H1, since they have a well-defined transcription start and end points producing a shorter, more predictable transcript.[60] However, RNA pol II promoters such as Cytomegalomavirus (CMV), are also capable of expressing high levels of functional pre-miRNA-like shRNA in cells.[117]

p*Silencer*™ adeno 1.0-CMV System, is an example of a shuttle vector that employs a modified CMV promoter to drive expression with RNA pol II, and includes a modified simian virus-40 (SV40) polyadenylation signal downstream of the siRNA template to terminate transcription.[118] It has been shown that this vector is capable of expressing functional siRNAs that enter the RNAi pathway and reduce target gene expression in both tissue culture cells and animals.[119–121] For example, in Das *et al* (2008)[120], p*Silencer*™ adeno 1.0-CMV System was used to target PKG expression and it was found to significantly knockdown PKG expression in H9C2 cells and adult rat cardiomyocytes after infection.

As such, in order to test this hypothesis, a parental plasmid mimicking the expressing unit of p*Silencer*™ adeno 1.0-CMV System and encoding the same shRNA, was constructed – pshRNA_2. For that, the terminal sequence for the pshRNA CMV promoter was modified and the BGH polyadenylation signal was replaced by the synthetic polyA signal of the p*Silencer*™ adeno 1.0-CMV System (text-based sequence present at the manufacturer's website[118]). Therefore, to construct the novel parental plasmid expressing the shRNA targeting VEGF, the previously developed PP pshRNA was used as a template in which a final portion of the CMV promoter and BGH polyadenylation signal will be replaced. The differences in the expression unit sequences between the two vectors are presented in Supplementary Data 3. A schematic representation of those differences is shown in Figure 4.25.

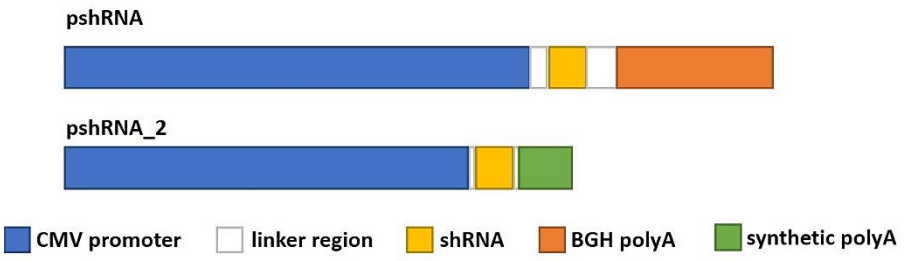

Figure 4.25- Schematic representation of the different expression cassettes of pshRNA and pshRNA_2.

Firstly, the pshRNA was digested for 3 hours at 37ºC with SacI and NsiI. After that, the digested samples, were separated by agarose gel electrophoresis (*Figure 4.26*). The double digestion should result in two fragments with 2,844 and 460 bp of length. From the Figure 4.26, it is possible to verify that the double digestion was accomplished, and the restriction pattern matches the one expected. The desired band (highlighted with an arrow; *Figure 4.26*) was extracted and purified from the gel to further use.

Parallelly, PCR amplification of the insert, composed by a portion of the CMV promoter, shRNA sequence and synthetic polyA signal, was performed. Subsequently, the PCR product was separated by agarose gel electrophoresis (*Figure 4.27*). It is possible to note the presence of a fainted band with less than 200 bp (highlighted by an arrow in *Figure 4.27)*, which matches the length of the predicted PCR product (167 bp). Therefore, the desired fragment was extracted from the gel and digested with SacI and NsiI restriction enzymes for 3 hours at 37°C.

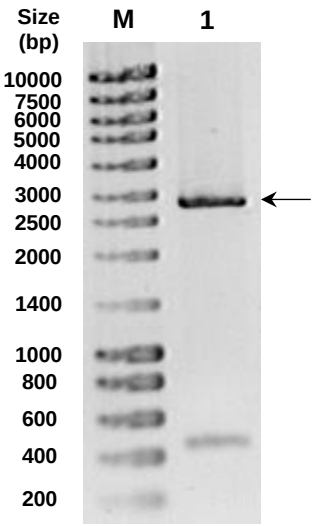

Figure 4.26 - Agarose gel electrophoresis analysis of the parental plasmid pshRNA purified from *E. coli* after restriction SacI and NsiI for 3 hours at 37ºC. The desired band is highlighted in with an arrow. Lane M - molecular weight marker NZYDNA Ladder III (Nzytech).

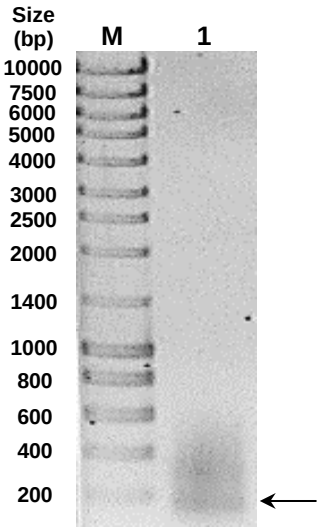

Figure 4.27 - Agarose gel electrophoresis analysis of the PCR product obtained PCR amplification using the KOD Hot Start DNA Polymerase kit. The cycling conditions were an initial denaturation at 95ºC for 2 min, followed by 35 cycles of 1 min at 95ºC, a cooling ramp of 1.10 min from 60ºC to 44ºC and 1 min at 70ºC. The desired PCR product is highlighted with an arrow. Lane M - molecular weight marker NZYDNA Ladder III (Nzytech).

After ligation of the desired fragment of pshRNA and PCR product for 3 hours at room temperature, with a vector:insert ratio of 1:5 or 1:7, *E. coli* DH5α transformation was performed. Eight *E. coli* DH5α colonies that resulted from the transformation were selected from the plate to further evaluation. For that, pDNA extraction and digestion with SacII restriction enzyme for 2 hours at 37ºC were carried out. Finally, the pDNA was separated on an agarose gel electrophoresis (*Figure 4.28*).

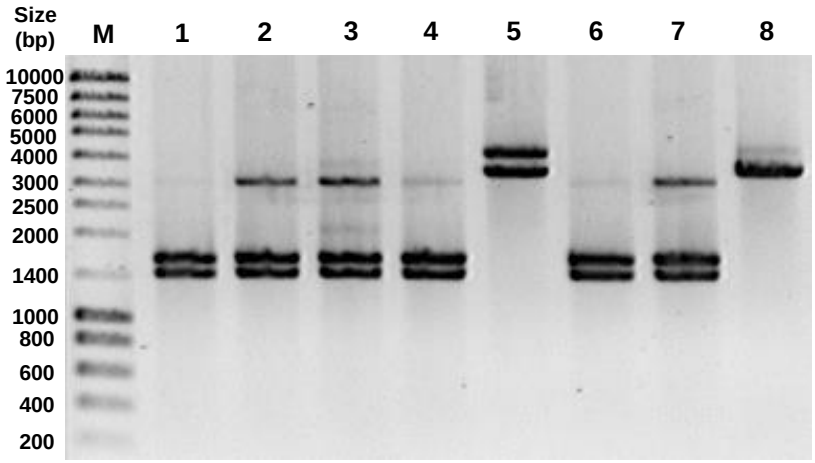

Figure 4.28 - Agarose gel electrophoresis analysis of pshRNA_2 candidates. pDNA purified from *E. coli* colonies resulting from the transformation with the ligation mixture with a vector:insert ratio of 1:5 (lane 1 to 6) or 1:7 (lane 7 and 8). The samples were digested with SacII for 2 hours at 37ºC. Lane M - molecular weight marker NZYDNA Ladder III (Nzytech).

The restriction pattern of the transformants 1-4 and 6-7 matches the one expected for the digestion of the newly constructed PP with ScaII (1,589 bp + 1,418 bp). The presence of an extra band of approximately 3,000 bp should correspond to the linearized form of the novel 3,007 bp-long PP.

The transformant 1 inserted sequence was confirmed by DNA sequencing (*Supplementary Data 2B*), in which the result validated the correct insertion of the sequence and consequently successful construction of the parental plasmid pshRNA_2 (*Figure 4.29*).

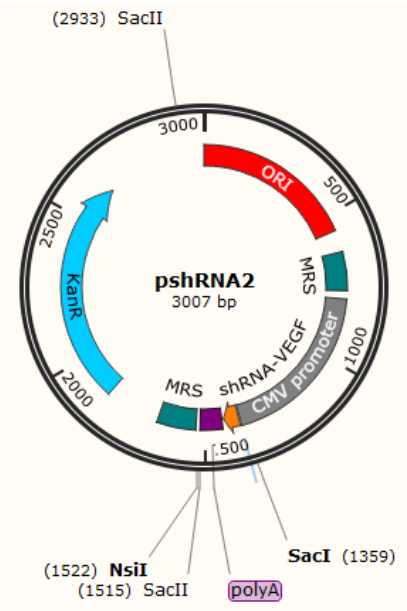

Figure 4.29- Schematic representation of the constructed parental plasmid pshRNA_2 (3,007 bp).

4.8. Production and purification of the novel minicircle

4.8.1. Cell growth and recombination of the novel PP

E. coli BW2P cells harbouring the novel PP pshRNA_2 were grown as previously. The OD_{600nm} was monitored throughout time allowing the construction of growth curves for *E. coli* BW2P harbouring pshRNA_2. The recombination into MC plus MP was again induced with the addition of L-(+)-arabinose at an $OD_{600nm} \approx 2.5$ (*Figure 4.30*). Interestingly, *E. coli* BW2P harbouring pshRNA_2 appears to have grown faster than harbouring other PPs, reaching higher OD_{600nm} values after 1 hour of recombination ($OD_{600nm} \approx 5.0$ after 3.6 hours in culture).

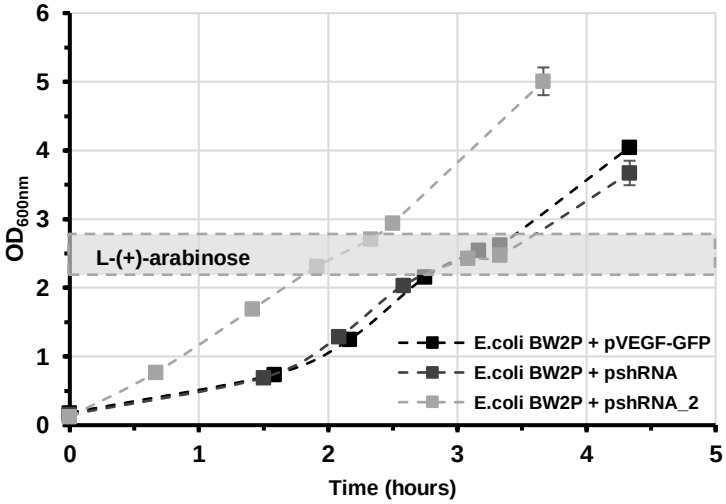

Figure 4.30 - Growth curves of *E. coli* BW2P harbouring different parental plasmids. Bacterial grow was performed in 250mL LB medium supplemented with 30 µg/mL kanamycin, at 37ºC and 250rpm. The range of OD_{600nm} values in which recombination in MP plus MC was induced is shown.

In order to evaluate the recombination efficiency of pshRNA_2 into MP and MC, samples were collected before and after 1 hour of recombination. The pDNA was extracted from the samples and separated by an agarose gel electrophoresis (*Figure 4.31*).

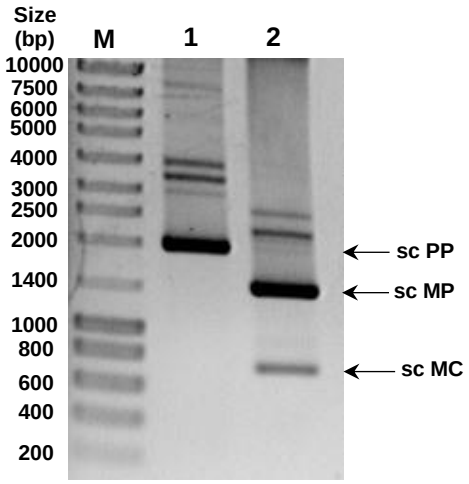

Figure 4.31 - Agarose gel electrophoresis analysis of pDNA purified from *E. coli* cells collected before (lane 1) and after (lane 2; 1 hour) induction of recombination with L-arabinose. Lane M - molecular weight marker NZYDNA Ladder III (Nzytech). Abbreviations: sc PP- supercoiled parental plasmid; sc MC- supercoiled minicircle; sc MP- supercoiled miniplasmid.

This analysis showed that before induction, open-circular (oc) PP bands predominate (lane 1, *Figure 4.31*), and MC and MP species are absent indicating that recombination occurs only after L-(+)-arabinose induction. Moreover, it is possible to confirm the recombination efficiency of the producer system since after 1h of recombination, the production of MP and MC is detected, by the presence of and bands of sc MP at ~1,500bp and of sc MC at ~900bp respectively, and absence of the PP bands (lane 2, *Figure 4.31*). The difference in intensities noted between the MP and MC bands is explained by the fact that, contrary to MC, the MP counterparts continues undergoing replication after recombination (lane 2, *Figure 4.31*).

4.8.2. Purification of the novel minicircle

Finally, purification of pshRNA_2 minicircle (MC-shRNA_2) was performed as previously, with the exception that RNase was added to the P1 lysis buffer as an attempted to eliminate the problem of excess RNA in the samples, as seen before. The primary purification was completed with isopropanol, ammonium acetate and PEG-8000 precipitations. Samples were collected after each precipitation step and analysed by the gel electrophoresis (*Figure 4.32A*). The results showed that the two isoforms of MPs and MCs are the major components in the samples. Additionally, the RNA load was substantially reduced by the addition of RNase during cell lysis, since lower amounts were observed even after isopropanol precipitation (lane 1, *Figure 4.32A*). As a result, the RNA load was not altered after ammonium acetate precipitation (lane 3, *Figure 4.32A*).

After the primary purification, enzymatic digestion with Nb.BbvCI was performed and MC plus MP samples collected before and after digestion, were analysed through agarose gel electrophoresis (*Figure 4.32B*). The results show that, contrarily to sc MC, the sc MP (lane 1, *Figure 4.32B*) is completely converted into its oc counterpart (lanes 2, *Figure 4.32B*). As expected, after digestion, the sample comprises a mixture of sc MC, oc MC and oc MP (lanes 2, *Figure 4.32B*).

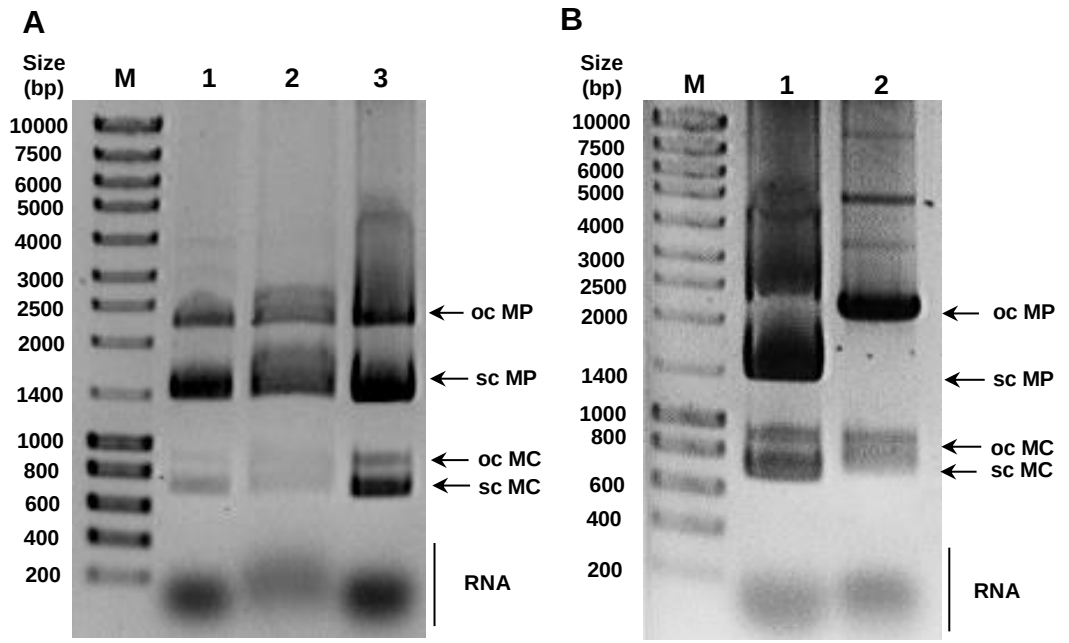

Figure 4.32 - Agarose gel electrophoresis was used to analyse each step of the primary purification of pshRNA_2 minicircle and subsequent digestion with endonuclease Nb.BbvCI. (**A**) Samples were collected after each step of the primary purification: alkaline isopropanol precipitation (lane 1, 3µL of sample), ammonium acetate precipitation (lane 2, 6µL of sample) and PEG-8000 precipitation (lane 3, 0.5 µL of sample). **(B)** Samples were collected before (lane 1, 1µL of sample) and after (lane 2, 1µL of sample) digestion with endonuclease Nb.BbvCI, that nick one of the MP and non-recombined PP strands, for 1 hour at 37ºC. Lane M - molecular weight marker NZYDNA Ladder III (Nzytech). Abbreviations: oc MC- open-circular minicircle; sc MC- supercoiled minicircle; oc MP- open-circular miniplasmid; sc MP- supercoiled miniplasmid.

Afterwards, to isolate the sc MC, multimodal chromatography was completed as described previously. The chromatogram obtained when samples containing MC plus MP of pshRNA_2 were run in the column is shown in Figure 4.33 A. The chromatographic profile did not match the one expected[100], since instead of a defined peak at 46%B, a peak with tailing is observed. Additionally, a peak with >2,500 mAU indicates the presence of extremely high amounts of RNA in the sample. As a result, column overload may have led to the elution of RNA in the sc MC fractions.

Some of the fractions collected were analysed by agarose gel electrophoresis, shown in Figure 4.33B. The results show that the first peak, at 42%B, contains oc forms of MP and MC (lanes 2 and 6), the second peak at 46%B contains sc MC (lanes 13–17) and a last peak at 100%B contains RNA (lane 25). As expected, the fractions 13 to 17, comprising sc MC free from oc species, also contains RNA molecules. Additionally, by the analysis of both feed stream and fraction 25 (lane F and 25, *Figure 4.33B*) is possible to confirm the significant amounts of RNA. This high RNA load was not anticipated since, throughout the purification process, the samples appear to have reduced amounts of RNA (*Figure 4.32 A* and *B*).

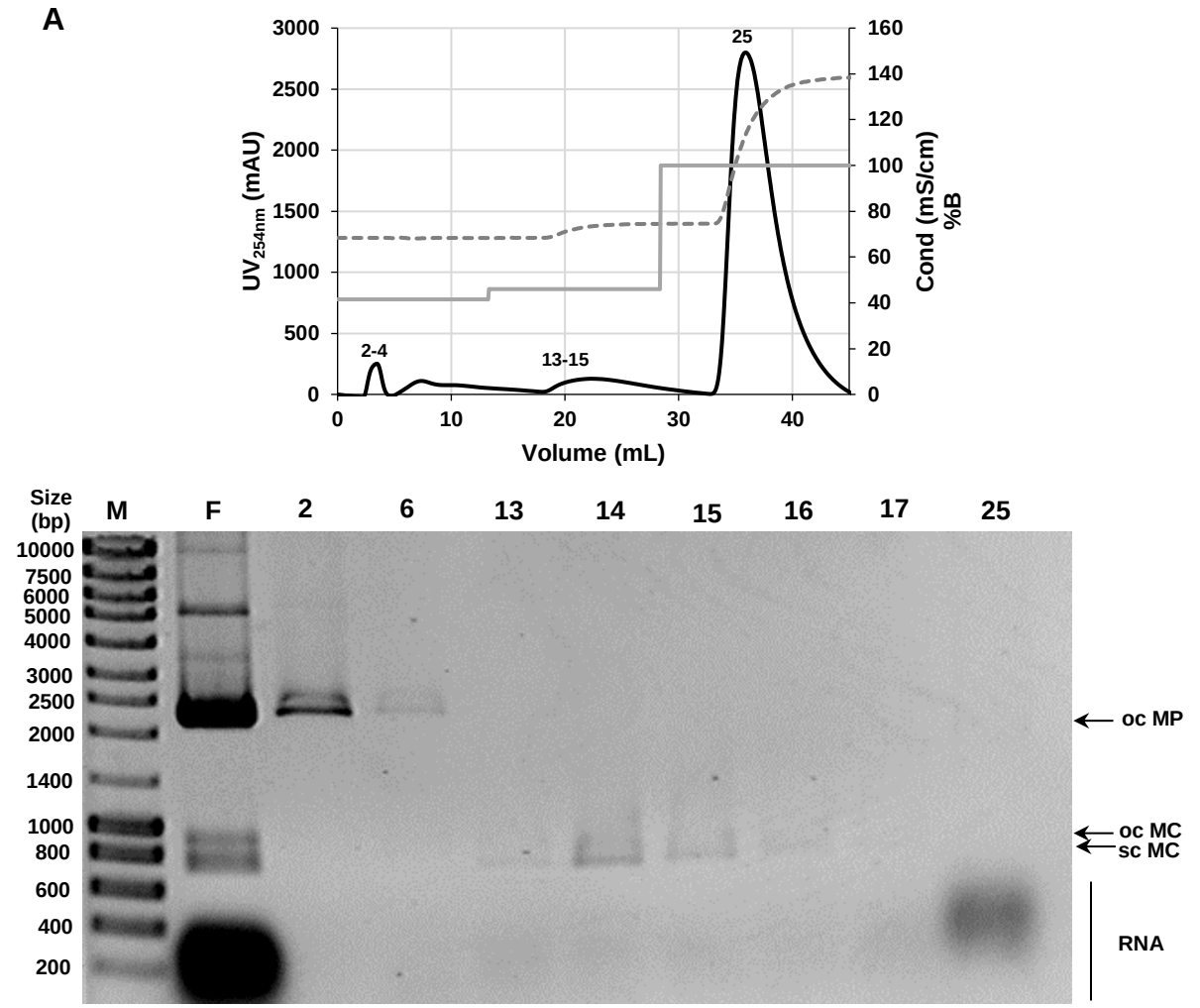

Figure 4.33 - Multimodal chromatography purification of sc MC from pshRNA_2 from a feed stream containing also oc pDNA and RNA. **(A)** Chromatogram obtained using a Capto™Adhere column and a series of elution steps with increasing NaCl concentrations. Numbers over peaks correspond to collected fractions. Black continuous line: absorbance at 254 nm; grey dashed line: conductivity (mS/cm); grey continuous line: percentage of buffer B (%B). **(B)** Agarose gel electrophoresis analysis of fractions collected during the chromatographic run. The numbers above each lane correspond to fractions collected (10 µL of sample for lanes 2–17; 30 µL of sample for lane 25). Lane M - molecular weight marker NZYDNA Ladder III (Nzytech). Abbreviations: oc MC- open circular minicircle; sc MC- supercoiled minicircle; oc MP- open circular miniplasmid; sc MP- supercoiled miniplasmid.

Despites that, dialysis and concentration of the fractions 13-15 of the chromatographic runs of the one sample resulted from pshRNA_2 primary purification was performed, using Amicon® Ultra-4 MWCO 30 kDa. An agarose gel electrophoresis was completed to evaluate the integrity and purity of the sample (*Figure 4.34*). It is possible to note that once again the RNA molecules were eliminated from the sample and an individual band of ~700bp, corresponding to the sc MC-shRNA_2 (901 bp), was present.

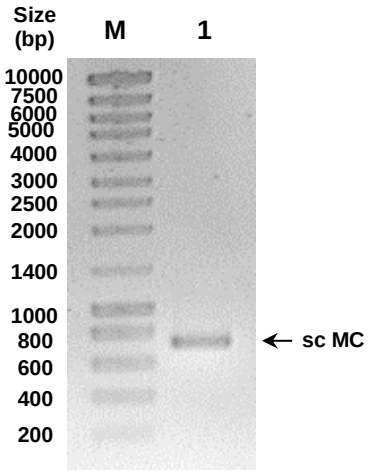

Figure 4.34 - Agarose gel electrophoresis analysis of pshRNA_2 minicircle sample after dialysis and concentration of the corresponding fractions, using Amicon® Ultra-4 MWCO 30 kDa (1µL, lane 1). Lane M - molecular weight marker NZYDNA Ladder III (Nzytech). Abbreviations: sc MC- supercoiled minicircle.

4.9. Lipofection of BM-MSCs and MCF-7 with the new minicircle MC-shRNA_2

In order to evaluate the effect of the synthetic siRNA and MCs encoding a shRNA targeting VEGF (MC-shRNA and MC-shRNA_2) on MCF-7 cells, cells were transfected with Lipofectamine. The synthetic siRNA and MC-shRNA were used as controls. In this experiment, two different amounts of MC-shRNA/MC-shRNA_2 and synthetic siRNA were used to transfect MCF-7 cells, that were collected 48 hours post-transfection. Through the transfected MCF-7 CR results (*Figure 4.35*) it is possible to confirm that once again Lipofectamine itself does not significantly affect MCF-7 cells recovery (95%; MCF-7 LF). Additionally, transfection with the high amounts of MCs/siRNA appears to constantly have a stronger impact in MCF-7 CR. It is possible to note that the conditions transfected with the MC-shRNA have the lowest CR, reaching values of 32% and 20%, once transfected with 500ng and 1,000ng of vector, respectively.

Despites that, Lipofectamine transfection *per se* does not affect MCF-7 viability, since high values were obtained for all conditions. However, conditions transfected with high amounts of MC revealed lower viabilities, indicating that the pDNA might be toxic to cells (~83%; *Figure 4.35*).

Afterwards, the collected cells were used to quantify the VEGF-mRNA by RT-qPCR using the $2^{-\Delta\Delta Ct}$ method (*Figure 4.36*).

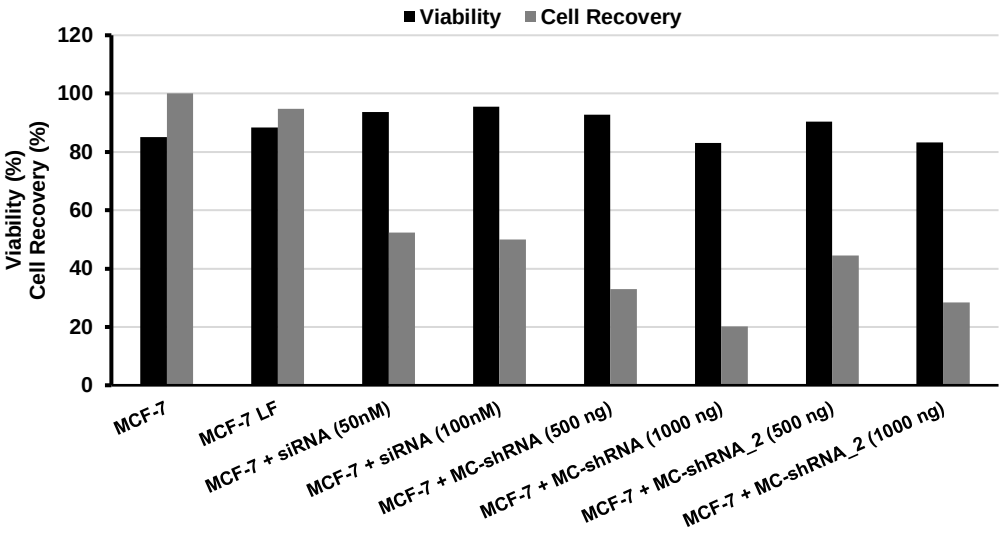

Figure 4.35 - Analysis of the MCF-7 cells behaviour 48 hours after lipofection with MCs or synthetic siRNA. Viability and cell recovery after microporation are presented as the black and grey bars, respectively. Non-transfected cells (MSC) and cells transfected without pDNA/siRNA (MSC LF) were used as controls.

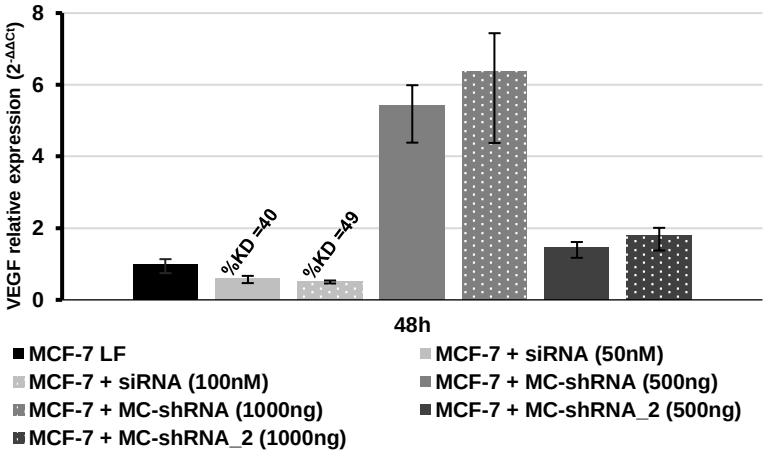

Figure 4.36 - Evaluation of transgene delivery 48 hours after lipofection of MCF-7 with different amounts of MC-shRNA, MC-shRNA_2 or synthetic siRNA, by analysis of VEGF gene expression by RT-qPCR. The values were obtained using $2^{-\Delta\Delta Ct}$ method, with GAPDH as the endogenous control gene and MCF-7 transfected without pDNA/siRNA, as baseline. The percentagens of VEGF knockdown (%KD) are also shown. Values are presented as mean ± SD of sample duplicates.

The results further confirm the silencing potential of the synthetic siRNA showed previously after BM-MSC transfection (*Figure 4.23* and *4.24*), reaching a knockdown of 40% and 49% at a concentration of 50nM and 100nM, respectively (*Figure 4.36*). It is possible to note that, despite the silence efficiency variability associated to the transfection of different cell types, the %KD obtained are relatively similar.

Regarding the MC-shRNA transfection, the results support the previously obtained data since it leads to increased levels of VEGF-mRNA relatively to the control cells (MCF-7 LF). In addition, it is possible to note that higher amounts of MC lead to higher levels of VEGF-mRNA, reaching 5.4- and 6.3-fold when transfected with 500ng and 1,000ng of MC-shRNA, respectively (*Figure 4.36*).

Furthermore, the results of transfection with the new minicircle MC-shRNA_2, revealed that the effect of increased expression appears to be conserved; however, the up-regulation seems to be attenuated relatively to MC-shRNA, since a 1.5- and 1.8-fold increase was observed after transfection with 500ng and 1,000ng, respectively (*Figure 4.36*).

To further validate the effect of the new minicircle MC-shRNA_2 on VEGF expression, BM-MSC were also transfected. A second BM-MSCs donor (M48A08) was used to further support the results, since MSCs are characterized as heterogeneous cell populations and donor variability throughout the expansion process is often reported.[122] The lipofection was performed as before with two different amounts of MC-shRNA/MC-shRNA_2 and 50 nM of synthetic siRNA as control. Cells were collected 24h and 48h post-transfection.

Through the results of cell recoveries and viabilities of transfected BM-MSCs (*Figure 4.37*) it is possible to note that two BM-MSC donors appeared to have a similar proliferative behaviour after transfection in all conditions. Additionally, the results were comparable to the ones obtained previously for BM-MSCs lipofection (*Figure 4.22*) and cells transfected with MC-shRNA_2 behaved similarly to the ones transfected with the other MC (*Figure 4.37*).

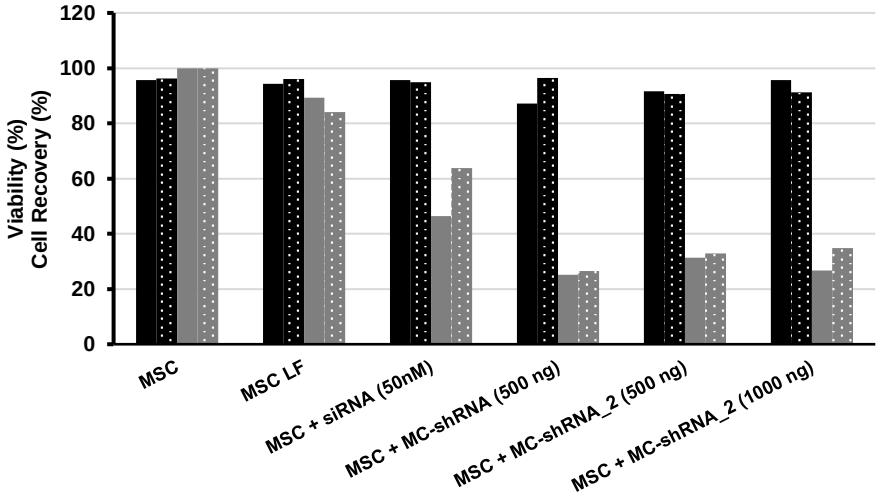

Figure 4.37- Analysis of the BM-MSC behaviour 48 hours after lipofection with MC-shRNA or synthetic siRNA. Viability and cell recovery after microporation are presented as the black and grey bars, respectively. BM-MSC M79A15 donor and M48A08 donor values are presented as the solid and dotted bars, respectively. Non-transfected cells (MSC) and cells transfected without pDNA/siRNA (MSC LF) were used as controls.

Afterwards, the VEGF-mRNA of the collected cells were quantified by RT-qPCR using the $2^{-\Delta\Delta Ct}$ method (*Figure 4.38*).

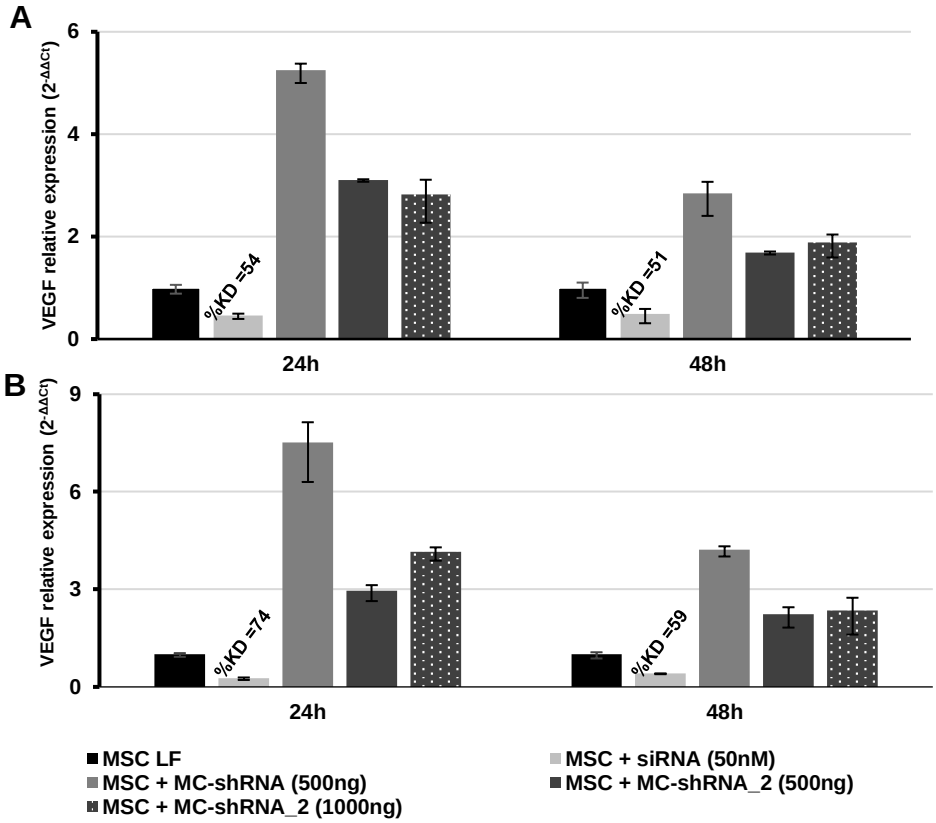

Figure 4.38 - Evaluation of transgene delivery 24 and 48 hours after lipofection of two BM-MSC donors (**(A)** M79A15; **(B)** M48A08) with MCs or synthetic siRNA, by analysis of VEGF gene expression by RT-qPCR. The values were obtained using $2^{-\Delta\Delta Ct}$ method, with GAPDH as the endogenous control gene and MSC transfected without pDNA/siRNA, collected after 24h and 48h, as baseline. The percentagens of VEGF knockdown (%KD) are also shown. Values are presented as mean ± SD of sample duplicates.

Through these results it is possible to verify that MC-shRNA_2 did not silence VEGF expression, since increased levels of VEGF-mRNA were obtained compared to the control (MSC LF), both 24h and 48 h post transfection. As seen in MCF-7 cells transfection, MC-shRNA_2 up-regulation effect appeared to be weaker than for MC-shRNA, reaching values of ~3- fold and ~2-fold higher VEGF-mRNA molecules than the control, at 24 h and 48 h post-transfection, respectively. Additionally, as previously seen, cells collected 48 h after MCs transfection expressed higher levels of VEGF-mRNA than the ones collected after 24 h.

Regarding the transfection with synthetic siRNA, the silencing effect appears to be stronger after 24 h, being more evidenced in the case of the second BM-MSC donor, exhibiting a knockdown of 74 and 59%, 24 h and 48 h post-transfection respectively (*Figure 4.38B*). Interestingly, the siRNA %KD reached when transfecting this donor were the highest obtained until now. Besides that, the two BM-MSC donors appeared to behave similarly in terms of transfection efficiency.

Overall, these experiments revealed that MC-shRNA_2 appears to induce a similar cellular response. As such, the modifications performed in the MC promoter and termination signal might not be

enough to originate a well-defined pre-miRNA-like shRNA capable of being processed by Dicer. Therefore, a different promoter with a well-defined transcription initiation and termination, such as U6 promoter, could be a promising option to be tested in future studies.

Nevertheless, an alternative hypothesis for the observed MC-derived overexpression of VEGF, might be the saturation of RNAi machinery. Considering that the RNAi machinery used to process the transcribed shRNA is common to the one for miRNA, shRNA overexpression could cause unintentional miRNA inhibition leading to unknown side effects by impelling the latter function.

In fact, it has been reported that exogenous expression of shRNAs has been associated with severe side effects due to the saturation of the miRNA pathway.[123,124] For example, in the study by Gestel *et al* (2014)[124], the authors demonstrated that the presence of adverse tissue response after shRNA expressing adeno-associated viral (AVV) vector administration to rats brains is likely to be caused by shRNA-induced saturation of the miRNA pathway, since neurons transduced with the AAV vector displayed a decrease in miRNA-124 expression, which was used as a marker. Nevertheless, the risk of oversaturating endogenous small RNA pathways can be minimized by optimizing shRNA dose and/or sequence.[123]

Therefore, considering this hypothesis, a transfection experiment with reduced amounts of shRNA-expressing MCs was accomplished in order evaluate if VEGF-overexpression is associated with a saturation of the miRNA pathway side effect.

4.10. Lipofection of BM-MSCs and MCF-7 with reduced amounts of MCs

As mentioned above, a transfection experiment with reduced amounts of MC-shRNA_2 was performed in order evaluate if VEGF-overexpression is connected to a side effect associated to the saturation of the miRNA pathway. For that, BM-MSCs and MCF-7 were transfected with Lipofectamine as described before, with 20 ng and 100 ng of MC. Cells were collected 48h post-transfection and VEGF expression was assessed by RT-qPCR using the $2^{-\Delta\Delta Ct}$ method (*Figure 4.39*).

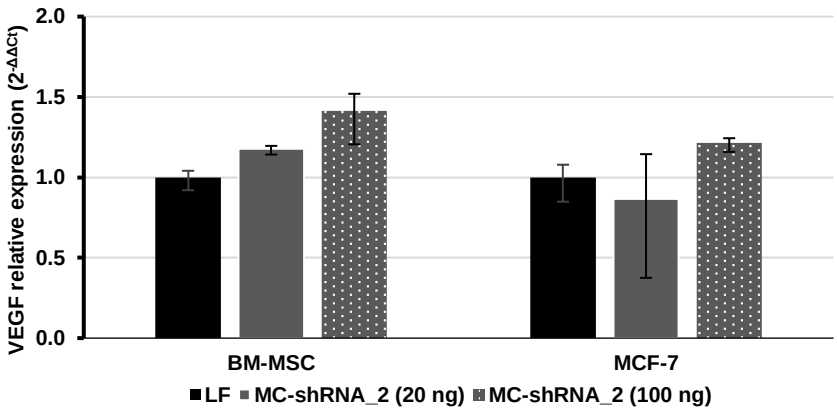

Figure 4.39 - Evaluation of transgene delivery 48 hours after lipofection of BM-MSC and MCF-7 with reduced amounts of MC-shRNA_2, by analysis VEGF gene expression by RT-qPCR. The values were obtained using $2^{-\Delta\Delta Ct}$ method, with GAPDH as the endogenous control gene and cells transfected without pDNA, as baseline. The percentagens of VEGF knockdown (%KD) are also shown. Values are presented as mean ± SD of sample duplicates.

The results showed that, even when transfected with 25x and 50x le ss the lower MC amount tested, MC-shRNA_2 fails to decrease VEGF expression after transfection of BM-MSC and MCF-7. In fact, BM-MSC transfection with 20ng and 100ng of MC-shRNA_2 led to 1.2- and 1.4-fold higher mRNA copies of VEGF than the control cells (LF), respectively (*Figure 4.39*). Additionally, MCF-7 transfection with 100ng of MC-shRNA_2 led to an increase in VEGF-mRNA of 1.2-fold relatively to the control cells. The apparent decrease after MCF-7 transfection with 20ng of MC-shRNA_2 is probably the result of experimental error in the RT-qPCR sample duplicates. As such, a side effect associated to the saturation of the RNAi machinery common to shRNA and miRNA, did not appear to be the cause for the MC-related increase VEGF-mRNA levels, since the overexpression effect is conserved when reduced amounts are used. Nevertheless, it is possible to verify once more that the amount of MC is proportional to the increase in VEGF expression. However, in order to exclude this hypothesis an experiment with even lower amounts of MC, such as 1ng or 0.1ng, should be performed.

Lastly, another possible explanation for the observed increase in mRNA levels could be the fact that, instead of promoting its degradation, the originating shRNAs are blocking the target translation. As mentioned previously, endogenous miRNAs often silence their mRNA targets by translation repression through a series of different mechanisms.[50,51] Thus, due to the possible incorrect shRNA processing, it might resemble the endogenous miRNAs in terms of structure and overall pathway, and consequently silence VEGF by impelling its translation. Hence, shRNA could be recognizing and stabilizing the target but not degrading it. As such, since the target does not follow for translation, the accumulation of VEGF-mRNA would occur. This hypothesis will be addressed in the next section, in which VEGF secretion to the culture medium by transfected cells will be quantified by ELISA.

4.11. ELISA quantification of VEGF secretion by transfected cells

To further validate the efficacy of siRNA/shRNA in silencing VEGF production and consequent secretion, a final VEGF quantification at the protein level was performed using an ELISA assay.

For that, cell supernatants collected 48h after transfection of BM-MSC and MCF-7 with the synthetic siRNA or shRNA-expressing MCs were tested. Supernatants from cultured cells transfected only with Lipofectamine were used as controls and all samples were tested in duplicate. In order to determine the concentration of VEGF (pg/ml) in the supernatant, a calibration curve was performed with the standard concentrations of VEGF (*Supplementary Data 4*). After normalization with the corresponding cell number and volume of the culture supernatant of the different conditions, the mass of VEGF produced was determined (*Supplementary Data 5*; *Figure 4.40*).

Through the analysis of the results from transfected BM-MSC (*Figure 4.40A*) it is possible to observe that cells transfected with the synthetic siRNA secrete lower amounts of VEGF (12.3±0.8 pg/1000 cells) relatively to the control (20.5±0.2 pg/1000 cells) exhibiting a 40% decrease in protein production. This result is consistent with the ones obtained for VEGF expression at the mRNA level through RT-qPCR. On the other hand, cells transfected with shRNA-expressing MCs produced more VEGF than the control and that increase, as seen at the mRNA level, is proportional to the amount of MC transfected, reaching a ~4-fold increase in protein production when transfected with 500 ng of MC (approximately 88 pg/1000 cells). The basal levels of VEGF secreted by the control cells is similar to the one reported in Serra *et al* (2018)[102], in which a VEGF production rate of 11.1±3.4 pg/1000 cells.day was obtained for non-transfected BM-MSCs.

Regarding the results from transfected MCF-7 (*Figure 4.40B*), it is possible to confirm that silence efficacy of the synthetic siRNA is inferior to the one obtained for BM-MSCs, as previously seen in the RT-qPCR results, showing a maximum of 25% decrease in VEGF production relatively to the control. A higher decrease in the VEGF protein was expected since the cells that produced that supernatant showed a KD of approximately 50% at the mRNA level. Once again, cells transfected with the MC induce VEGF production which is consistent with the increase levels of mRNA obtained in the RT-qPCR results. However, the maximum fold increase in protein production is inferior to BM-MSCs, being ~2-fold when transfected with the 100ng and 500ng of MC-shRNA_2 and MC-shRNA, respectively. Interestingly, despite being a cancer cell line, the overall levels of VEGF secreted by MCF-7 cells are approximately 10 times lower than BM-MSCs (2.38 pg/1000 cells vs 20.5±0.2 pg/1000 cells). In fact, Guo and colleagues reported that parental MCF-7 cells only secreted 3–6 pg/ml/1000 cells of VEGF into the supernatant.[125] This value is at least 3 times higher than the one obtained for the control cells in this work (1.2 pg/ml/1000 cells), which might be associated to the culture medium and/or the result of the LF transfection. Additionally, the low values of MCF-7 basal VEGF secretion might be diminishing the difference between the conditions tested and consequent siRNA actual silencing effect.

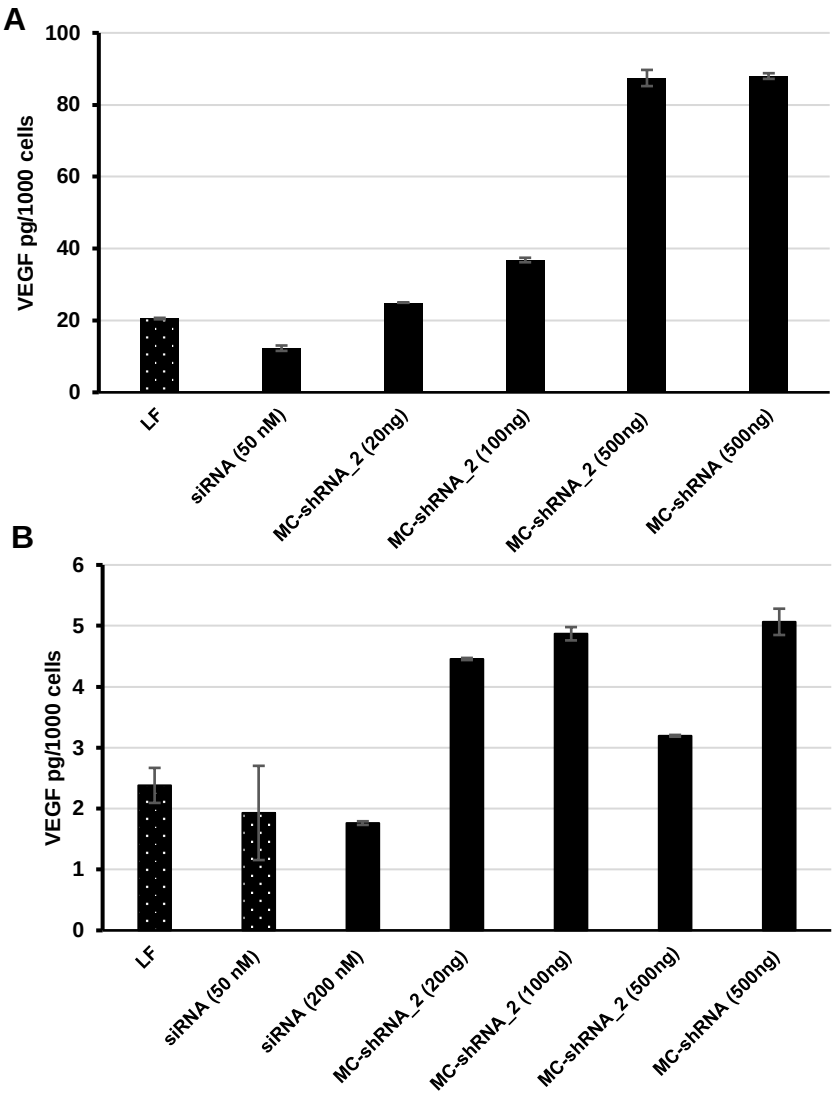

Figure 4.40 - Evaluation of transgene delivery 48 hours after transfection of **(A)** BM-MSC and **(B)** MCF-7 with the synthetic siRNA, MC-shRNA or MC-shRNA_2, by analysis the VEGF protein production by ELISA. Cells transfected with LF were used as control and values are presented as mean ± SD of sample duplicates (solid bar) or as mean values ± SEM from two samples of independent experiments (dotted).

Although the results are derived from a single experiment, leading to the need of performing further studies, similar tendencies in expression change were observed. Overall, the synthetic siRNA is able to silence VEGF expression leading to a decrease in protein production and consequent secretion. This result was expected, since this siRNA sequence was used in previous studies reporting a substantial decrease in VEGF protein levels.[91,92,116] Regarding the MC-derived shRNA, it was possible to conclude that it induces the expression of VEGF, leading to increased levels of protein production and secretion, eliminating the hypothesis that the shRNA could be silencing VEGF by translation repression instead of target cleavage/degradation.

4.12. Angiogenic capacity of the engineered BM-MSC and MCF-7 assessed by *in vitro* tube formation assay

Endothelial cell differentiation on basement membrane recapitulates many steps in angiogenesis and the basement membrane matrix, which contains many critical functional and structural components, is the key EC differentiation and formation of capillary-like tubes.[126] VEGF is an example of growth factor present in the EC basement membrane matrix that is important for growth and migration of ECs, potentiating EC re-organization and formation of tube-like structures that resemble blood vessels.[102,127]

Therefore, within the scope of this thesis, it was performed an assay that relies on the capacity of human umbilical vein endothelial cells (HUVEC) to form tube networks when cultured in Matrigel to evaluate the angiogenic potential of the transfected cells – *in vitro* tube formation assay. For that, conditioned medium (CM) from transfected cells collected after 48h in culture, was used to cultivate HUVECs. After 6h, tube formation capacity by HUVECs was quantified accounting the number of tubes and branch points. The tube formation assay was accomplished using CM from BM-MSCs and MCF-7 (*Figure 4.41* and *4.42*) transfected with the synthetic siRNA and MC-shRNA_2. CM from cells transfected only with Lipofectamine were used as controls and all samples were tested in duplicate.

Regarding the results obtained with BM-MSC (*Figure 4.41*), it is possible to observe that the CM retrieved from the culture of BM-MSC transfected with Lipofectamine induced the formation of more tubes (45±5.5) and connections (34±5.5) compared to the negative control (basal medium EBM-2) (28±1.5 and 21±1.0, respectively). Additionally, CM from cells transfected with the siRNA showed a decreased potential to induce tube formation, with HUVECs exhibiting the formation of 33±0.50 tubes and 24 branch points, suggesting a reduced angiogenic potential compared to control BM-MSC. These results were expected since the amount of VEGF in the CM determined by ELISA (*Supplementary Data 6*) was lower in the case of the cells transfected with the siRNA. As such, lower VEGF levels would minimize HUVEC tube formation capacity due to its pro-angiogenic features. On the other hand, the tube formation results obtained for the CM retrieved from cells transfected with MC-shRNA_2 were not the expected ones, since they also resulted in a decreased potential to induce tube formation and the levels of VEGF were superior or at least similar to ones for BM-MSC LF (*Supplementary Data 6*). However, it is important to consider that the CM is composed by a variety of different molecules and some of those might be repressing HUVEC's capacity to form tubes. In fact, this result could be associated to the secretion of toxic elements to the CM after transfection with the MC, despite this effect not being reported in previous studies[102] and further experiments are required in order to validate it. Through the analysis of the results obtained with MCF-7 CM (*Figure 4.42*), it is possible to verify that the number of tubes and connections by HUVECs are very similar to the ones obtained in the EBM-2 negative control. This result is supported by the levels of VEGF in the CM obtained ELISA (*Supplementary Data 6*), which showed that MCF-7 CMs have extremely reduced amounts of VEGF, even in the MCF-7 LF control, and therefore the differences between the tube formation conditions were not detectable and were similar to the negative control.

Overall, the results with CM from BM-MSC cultures indicating that the siRNA-mediated reduction of VEGF production from transfected cells potentiates a decrease in HUVEC tube formation capacity and therefore in the angiogenic potential of transfected cells. Additional experiments using concentrated CM or CM retrieved after more days in culture (*i.e.* in order to accumulate more VEGF) should be performed, to further evidence the differences between CM from cells transfected with the siRNA and control cells.

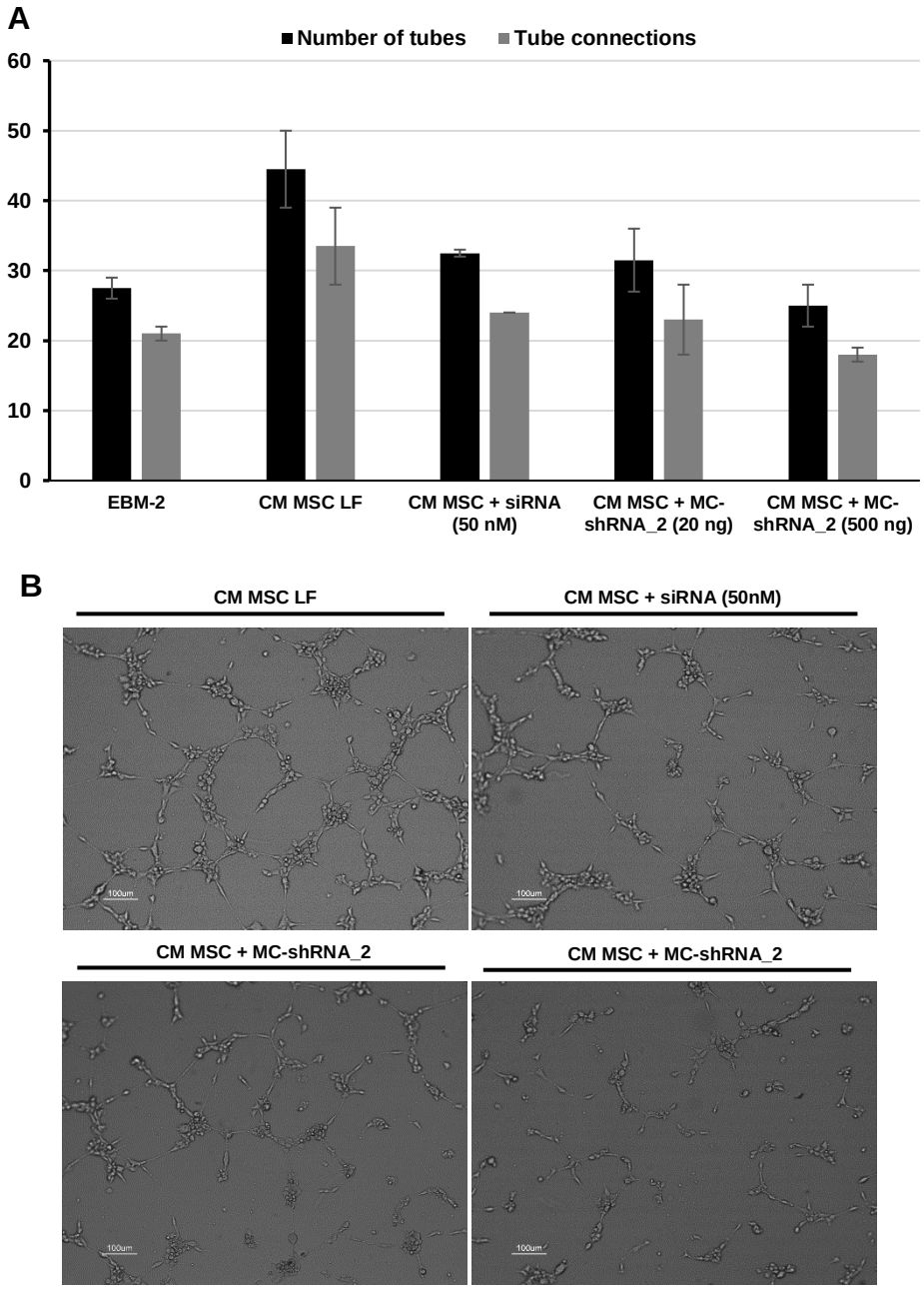

Figure 4.41- *In vitro* tube formation assay results obtained for BM-MSCs conditioned medium after transfection with the synthetic siRNA and MC-shRNA_2. **(A)** Number of tubes and tube connections for each condition observed per optical field after 6 h in culture. Values are presented as mean ± SD of sample duplicates. **(B)** Bright field images (100X) of HUVECs tube formation after 6h in culture with each condition of BM-MSC CM.

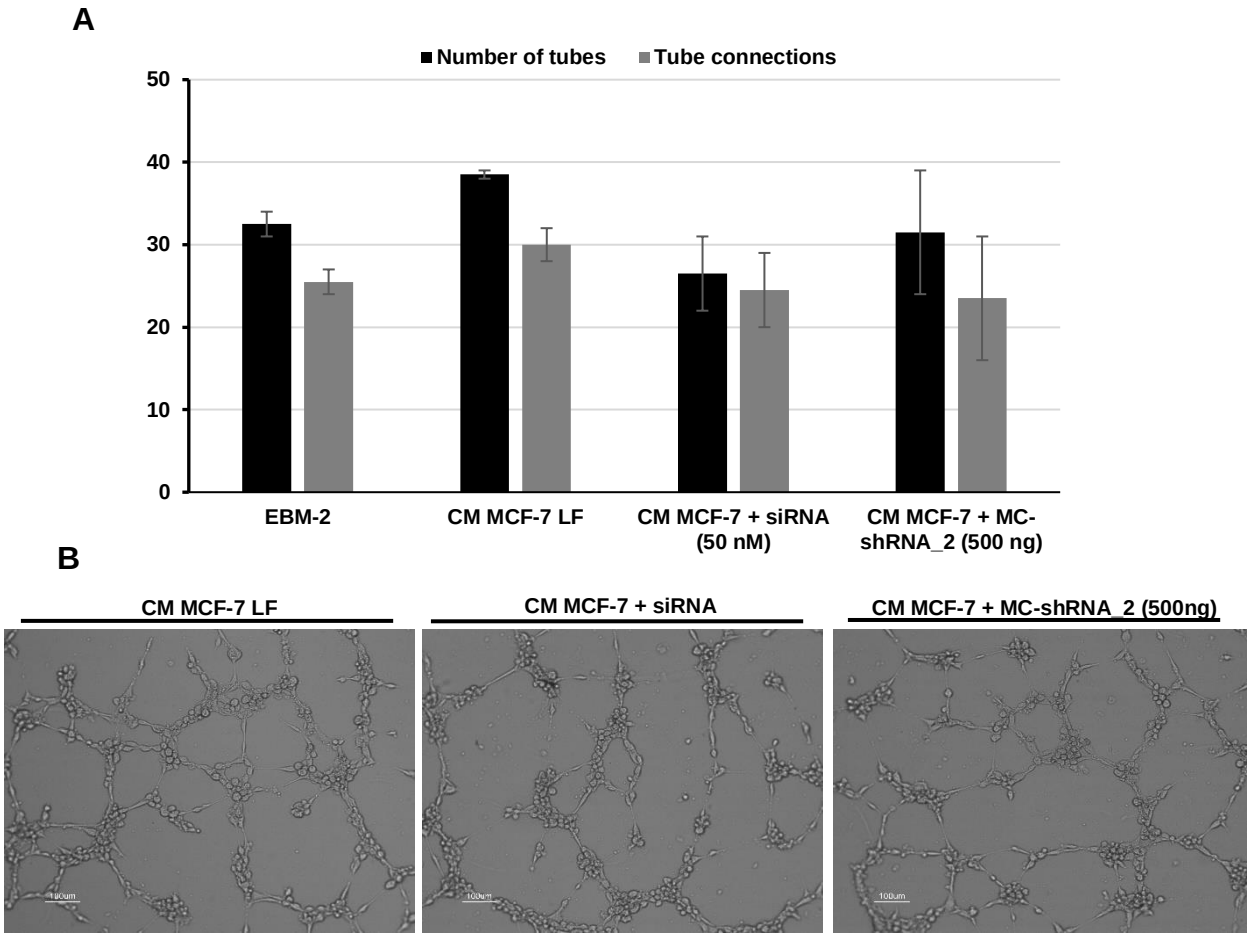

Figure 4.42 – *In vitro* tube formation assay results obtained for MCF-7 conditioned medium after transfection with the synthetic siRNA and MC-shRNA_2. **(A)** Number of tubes and tube connections for each condition observed per optical field after 6 h in culture. Values are presented as mean ± SD of sample duplicates. **(B)** Bright field images (100X) of HUVECs tube formation after 6h in culture with each condition of MCF-7 CM.

5. Conclusions and Future Studies

MSCs have an active role in supporting the maintenance of a dynamic and homeostatic tissue microenvironment by secretion of a broad range of biologically active molecules. Upon interaction with cancer cells, MSCs became active participants in tumour development namely by promoting angiogenesis through the secretion of pro-angiogenic molecules such as VEGF. Since tumour angiogenesis is one of the hallmarks of cancer progression, targeting this phenomenon by using a genetic engineering approach seems a promising strategy to slow down tumour growth.

In the present work, the primary goal was to develop a siRNA-based system capable of blocking VEGF expression and secretion in BM-MSCs and cancer cells, and consequently diminishing their pro-angiogenic potential. For that, a selected synthetic siRNA was used in the *in vitro* transfection MSCs and MCF-7 cells. Parallelly, minicircle vectors encoding a shRNA, targeting the same location of VEGF-mRNA, were also constructed, produced and purified for further transfection. Contrarily to the synthetic siRNA, which is degraded with gene silencing, the MC continues to deliver the transcribed shRNA to the transfected cells. In order to evaluate VEGF silencing, VEGF-mRNA and VEGF-protein levels were quantified by RT-qPCR and ELISA, respectively. Finally, tube formation assays were used to evaluate the effect of VEGF silencing on the angiogenic potential of the transfected cells.

Concerning siRNA transfection, it revealed to efficiently silence VEGF expression at the mRNA level, inducing a knockdown of approximately 50% and 40%, 48 hours post-transfection with a concentration of 50nM and Lipofectamine, in MSCs and MCF-7, respectively. The ELISA results indicate a decrease in VEGF production and secretion relatively to the control, being more pronounced in BM-MSC transfection, with a 40% decrease. Regarding the preliminary results of functional assays (tube formation assays), the siRNA-mediated reduction of VEGF production from transfected cells appears to potentiate a decrease in HUVEC tube formation capacity, and therefore, a decrease in their angiogenic potential.

Nevertheless, further studies should be performed in order to optimize siRNA transfection, and consequently silencing efficiency, namely by testing different LF/siRNA ratios, since a fixed amount of LF was used throughout the work. Additionally, although out of the aim of this master thesis, alternative delivery systems, that could facilitate the transition into *in vivo* studies should be explored. One possibility would be to test MSC-derived exosomes, since increasing evidence has revealed that the mechanism of interaction between stem cells and tumour cells involves the exchange of biological material through exosomes.[128]

Regarding the development of the shRNA-expression system, a minicircle vector was selected based on the high transfection efficiencies and lack of biosafety concerns reported. A first parental plasmid expressing a pre-miRNA-like shRNA, targeting the same region as the synthetic siRNA, was successfully constructed as designed. The production and purification methods previously developed at the iBB-BERG laboratory[100] were shown to successfully isolate the MC, although problems associated

with excess RNA leading to the chromatographic column overload and consequent incomplete MC isolation, should be addressed.

The transfection experiments with the shRNA-expressing MC, revealed that, contrarily to the expected, increased VEGF-mRNA levels were obtained, exhibiting ~3-fold and ~5-fold higher mRNA copies of VEGF than the control cells, 48h after transfection with 500 ng of MC, in BM-MSC and MCF-7 respectively. The opposite effects between the transfection of the synthetic siRNA and shRNA-expressing MC indicate that the transcribed shRNA does not result in the theoretical siRNA molecule (identical to the synthetic siRNA) after processing. Thus, a problem involving the correct shRNA processing into functional siRNA duplexes might be causing the observed discrepancies. Since poly-adenylation coupled with Pol II transcription (CMV promoter) abolishes its ability to express RNA with clear-cut ends, originating long, undefined shRNAs molecules possibly preventing Dicer recognition, and consequently the correct processing. As a result of this incorrect processing, the transcribed shRNA can be acting as transcriptional activator of VEGF, as a consequence of off-target effects, namely by silencing non-target genes that downregulate VEGF. In addition, an off-target effect by partial sequence complementarity with VEGF regulatory regions, might be inducing its expression, since miRNA/siRNA can also serve as activators by targeting gene regulatory sequences. Considering this hypothesis, a second MC vector mimicking the expressing unit of a commercial viral vector, with a different CMV promoter sequence and alternative termination signal, was developed as an attempt to obtain a more defined transcript. After transfection of BM-MSC and MCF-7, it was possible to verify that, although up-regulation seems to be attenuated, the effect of increased expression is conserved, exhibiting ~1.5-fold higher mRNA copies of VEGF than the control cells, 48h after BM-MSC and MCF-7 transfection with 500 ng of MC. Furthermore, the quantification of VEGF expression by ELISA indicate once more an increase in VEGF secretion in the conditions transfected with the two MCs relatively to the control. As such, the modifications performed in the MC promoter and termination signal could not be enough to originate a well-defined pre-miRNA-like shRNA capable of being processed by Dicer. In this regard, further experiments should focus on determining the final structure of the shRNA transcript, such as by microRNA-sequencing[129] or by Northern-blot using probes targeting the guide sequence the siRNA[130]. Additionally, a transfection experiment with the empty MC vector (i.e MC's expression cassette without the shRNA sequence) should be performed in order to verify if the vector *per se* is not the cause of the increase in VEGF expression. An alternative approach might be the development of a vector containing a Pol III promoter, such as U6 promoter, that will lead to a more defined and easier to process pre-miRNA-like shRNA, or by maintaining the Pol II promoter, developing a vector with the shRNA sequence adapted into a pri-miRNA-like structure that will be readily recognized and processed by Drosha-DGCR8 microprocessor, before Dicer processing.[60]

In conclusion, the present work provides insights regarding the implementation of an siRNA-based system that specifically targets VEGF expression with aim of diminishing the angiogenic potential of cells present in tumour microenvironment, and consequently slow down cancer progression.

6. References

1. Adair, T. H. & Montani, J.-P. *Angiogenesis*. *Angiogenesis* (Morgan & Claypool Life Sciences, 2010).

2. Salajegheh, A. Introduction to Angiogenesis in Normal Physiology, Disease and Malignancy. in *Angiogenesis in Health, Disease and Malignancy* 1–9 (Springer International Publishing, 2016).

3. Bronckaers, A. & Lambrichts, I. The role of mesenchymal stem/stromal cells in angiogenesis. in *The Biology and Therapeutic Application of Mesenchymal Cells* 347–365 (John Wiley & Sons, Inc., 2016).

4. Carmeliet, P. & Jain, R. K. Principles and mechanisms of vessel normalization for cancer and other angiogenic diseases. *Nat. Rev. Drug Discov.* **10,** 417–427 (2011).

5. Potente, M., Gerhardt, H. & Carmeliet, P. Basic and therapeutic aspects of angiogenesis. *Cell* **146,** 873–887 (2011).

6. Carmeliet, P. Angiogenesis in life, disease and medicine. *Nature* **438,** 932–936 (2005).

7. Yoo, S. Y. & Kwon, S. M. Angiogenesis and its therapeutic opportunities. *Mediators Inflamm.* **2013,** 1-11 (2013).

8. Sudhakar, A. The Matrix Reloaded: New Insights from Type IV Collagen Derived Endogenous Angiogenesis Inhibitors and their Mechanism of Action. *J. Bioequiv. Availab.* **1,** 52-62 (2009).

9. Ucuzian, A. A., Gassman, A. A., East, A. T. & Greisler, H. P. Molecular mediators of angiogenesis. *J. Burn Care Res.* **31,** 158–75 (2010).

10. Gunda, V. & Sudhakar, Y. Regulation of Angiogenesis in Choroidal Neovascularization of Age Related Macular Degeneration by Endogenous Angioinhibitors. in *Advances in Ophthalmology* (InTech, 2012).

11. Ferrara, N., Gerber, H.-P. & LeCouter, J. The biology of VEGF and its receptors. *Nat. Med.* **9,** 669–676 (2003).

12. Hoeben, A. Vascular Endothelial Growth Factor and Angiogenesis. *Pharmacol. Rev.* **56,** 549–580 (2004).

13. Shibuya, M. Vascular Endothelial Growth Factor (VEGF) and Its Receptor (VEGFR) Signaling in Angiogenesis: A Crucial Target for Anti- and Pro-Angiogenic Therapies. *Genes Cancer* **2,** 1097–105 (2011).

14. LaGory, E. L. & Giaccia, A. J. The ever-expanding role of HIF in tumour and stromal biology. *Nat. Cell Biol.* **18,** 356–65 (2016).

15. De Palma, M., Biziato, D. & Petrova, T. V. Microenvironmental regulation of tumour angiogenesis. *Nat. Rev. Cancer* **17,** 457–474 (2017).

16. Wang, Z. *et al.* Broad targeting of angiogenesis for cancer prevention and therapy. *Semin. Cancer Biol.* **35,** 224–243 (2015).

17. Albers, J. *et al.* Combined mutation of Vhl and Trp53 causes renal cysts and tumours in mice. *EMBO Mol. Med.* **5,** 949–64 (2013).

18. Rajabi, M. & Mousa, S. The Role of Angiogenesis in Cancer Treatment. *Biomedicines* **5,** 34 (2017).

19. Keating, G. M. Bevacizumab: A Review of Its Use in Advanced Cancer. *Drugs* **74,** 1891–1925 (2014).

20. Hudes, G. *et al.* Temsirolimus, Interferon Alfa, or Both for Advanced Renal-Cell Carcinoma. *N. Engl. J. Med.* **356,** 2271–2281 (2007).

21. Llovet, J. M. *et al.* Sorafenib in Advanced Hepatocellular Carcinoma. *N. Engl. J. Med.* **359,** 378–390 (2008).

22. Pittenger, M. F. *et al.* Multilineage potential of adult human mesenchymal stem cells. *Science* **284,** 143–7 (1999).

23. Crisan, M. *et al.* A perivascular origin for mesenchymal stem cells in multiple human organs. *Cell Stem Cell* **3,** 301–13 (2008).

24. Horwitz, E. M. *et al.* Clarification of the nomenclature for MSC: The International Society for Cellular Therapy position statement. *Cytotherapy* **7,** 393–395 (2005).

25. Sipp, D., Robey, P. G. & Turner, L. Clear up this stem-cell mess. *Nature* **561,** 455–457 (2018).

26. Dominici, M. *et al.* Minimal criteria for defining multipotent mesenchymal stromal cells. The International Society for Cellular Therapy position statement. *Cytotherapy* **8,** 315–317 (2006).

27. Friedenstein, A. J., Gorskaja, J. F. & Kulagina, N. N. Fibroblast precursors in normal and irradiated mouse hematopoietic organs. *Exp. Hematol.* **4,** 267–74 (1976).

28. Hass, R., Kasper, C., Böhm, S. & Jacobs, R. Different populations and sources of human mesenchymal stem cells (MSC): A comparison of adult and neonatal tissue-derived MSC. *Cell Commun. Signal.* **9,** 12 (2011).

29. Klingemann, H., Matzilevich, D. & Marchand, J. Mesenchymal Stem Cells - Sources and Clinical Applications. *Transfus. Med. Hemother.* **35,** 272–277 (2008).

30. Bronckaers, A. *et al.* Mesenchymal stem/stromal cells as a pharmacological and therapeutic approach to accelerate angiogenesis. *Pharmacol. Ther.* **143,** 181–196 (2014).

31. Spees, J. L., Lee, R. H. & Gregory, C. A. Mechanisms of mesenchymal stem/stromal cell function. *Stem Cell Res. Ther.* **7,** 125 (2016).

32. da Silva Meirelles, L., Fontes, A. M., Covas, D. T. & Caplan, A. I. Mechanisms involved in the therapeutic properties of mesenchymal stem cells. *Cytokine Growth Factor Rev.* **20,** 419–427 (2009).

33. Caplan, A. I. & Correa, D. The MSC: an injury drugstore. *Cell Stem Cell* **9,** 11–15 (2011).

34. Tse, W. T., Pendleton, J. D., Beyer, W. M., Egalka, M. C. & Guinan, E. C. Suppression of allogeneic T-cell proliferation by human marrow stromal cells: implications in transplantation. *Transplantation* **75,** 389–397 (2003).

35. Shabbir, A., Cox, A., Rodriguez-Menocal, L., Salgado, M. & Badiavas, E. Van. Mesenchymal Stem Cell Exosomes Induce Proliferation and Migration of Normal and Chronic Wound Fibroblasts, and Enhance Angiogenesis In Vitro. *Stem Cells Dev.* **24,** 1635-1647 (2015).

36. Liang, X., Zhang, L., Wang, S., Han, Q. & Zhao, R. C. Exosomes secreted by mesenchymal stem cells promote endothelial cell angiogenesis by transferring miR-125a. *J. Cell Sci.* **129,** 2182–2189 (2016).

37. Lazennec, G. & Richmond, A. Chemokines and chemokine receptors: new insights into cancer-related inflammation. *Trends Mol. Med.* **16,** 133–44 (2010).

38. Lazennec, G. & Lam, P. Y. Recent discoveries concerning the tumor - mesenchymal stem cell interactions. *Biochim. Biophys. Acta - Rev. Cancer* **1866,** 290–299 (2016).

39. Klopp, A. H. *et al.* Tumor Irradiation Increases the Recruitment of Circulating Mesenchymal Stem Cells into the Tumor Microenvironment. *Cancer Res.* **67,** 11687–11695 (2007).

40. Huang, W.-H. *et al.* Mesenchymal stem cells promote growth and angiogenesis of tumors in mice. *Oncogene* **32,** 4343–4354 (2012).

41. Spaeth, E. L. *et al.* Mesenchymal Stem Cell Transition to Tumor-Associated Fibroblasts Contributes to Fibrovascular Network Expansion and Tumor Progression. *PLoS One* **4,** e4992

(2009).

42. Zhang, T. *et al.* Bone marrow-derived mesenchymal stem cells promote growth and angiogenesis of breast and prostate tumors. *Stem Cell Research & Therapy* **4,** 1-15 (2013).

43. Beckermann, B. M. *et al.* VEGF expression by mesenchymal stem cells contributes to angiogenesis in pancreatic carcinoma. *Br. J. Cancer* **99,** 622–31 (2008).

44. Wang, H.-H. *et al.* Mesenchymal stem cells generate pericytes to promote tumor recurrence via vasculogenesis after stereotactic body radiation therapy. *Cancer Lett.* **375,** 349–359 (2016).

45. Liu, Y. *et al.* Effects of inflammatory factors on mesenchymal stem cells and their role in the promotion of tumor angiogenesis in colon cancer. *J. Biol. Chem.* **286,** 25007–15 (2011).

46. Zhang, X. *et al.* Human colorectal cancer-derived mesenchymal stem cells promote colorectal cancer progression through IL-6/ JAK2/STAT3 signaling. *Cell Death Dis.* **9,** (2018).

47. Muehlberg, F. L. *et al.* Tissue-resident stem cells promote breast cancer growth and metastasis. *Carcinogenesis* **30,** 589–597 (2009).

48. Zhu, W. *et al.* Exosomes derived from human bone marrow mesenchymal stem cells promote tumor growth in vivo. *Cancer Lett.* **315,** 28–37 (2012).

49. Shi, S. *et al.* Mesenchymal stem cell-derived exosomes facilitate nasopharyngeal carcinoma progression. *Am. J. Cancer Res.* **6,** 459–72 (2016).

50. Carthew, R. W. & Sontheimer, E. J. Origins and Mechanisms of miRNAs and siRNAs. *Cell* **136,** 642–655 (2009).

51. Lam, J. K. W., Chow, M. Y. T., Zhang, Y. & Leung, S. W. S. siRNA versus miRNA as therapeutics for gene silencing. *Mol. Ther. - Nucleic Acids* **4,** e252 (2015).

52. Wilson, R. C. & Doudna, J. A. Molecular Mechanisms of RNA Interference. *Annu. Rev. Biophys.* **42,** 217–239 (2013).

53. Lee, R. C., Feinbaum, R. L. & Ambros, V. The C. elegans heterochronic gene lin-4 encodes small RNAs with antisense complementarity to lin-14. *Cell* **75,** 843–54 (1993).

54. Elbashir, S. M. *et al.* Duplexes of 21-nucleotide RNAs mediate RNA interference in cultured mammalian cells. *Nature* **411,** 494–498 (2001).

55. Ling, H., Fabbri, M. & Calin, G. A. MicroRNAs and other non-coding RNAs as targets for anticancer drug development. *Nat. Rev. Drug Discov.* **12,** 847–865 (2013).

56. Han, J. *et al.* Molecular Basis for the Recognition of Primary microRNAs by the Drosha-DGCR8 Complex. *Cell* **125,** 887–901 (2009).

57. Lim, L. P. *et al.* Microarray analysis shows that some microRNAs downregulate large numbers of target mRNAs. *Nature* **433,** 769–773 (2005).

58. Song, E. *et al.* RNA interference targeting Fas protects mice from fulminant hepatitis. *Nat. Med.* **9,** 347–351 (2003).

59. Wittrup, A. & Lieberman, J. Knocking down disease: a progress report on siRNA therapeutics. *Nat. Rev. Genet.* **16,** 543–552 (2015).

60. Bofill-De Ros, X. & Gu, S. Guidelines for the optimal design of miRNA-based shRNAs. *Methods* **103,** 157–166 (2016).

61. Ozcan, G., Ozpolat, B., Coleman, R. L., Sood, A. K. & Lopez-Berestein, G. Preclinical and clinical development of siRNA-based therapeutics. *Adv. Drug Deliv. Rev.* **87,** 108–119 (2015).

62. Karagiannis, T. C. & El-Osta, A. RNA interference and potential therapeutic applications of short interfering RNAs. *Cancer Gene Ther.* **12,** 787–795 (2005).

63. Moore, C. B., Guthrie, E. H., Huang, M. T.-H. & Taxman, D. J. Short hairpin RNA (shRNA):

design, delivery, and assessment of gene knockdown. *Methods Mol. Biol.* **629,** 141–58 (2010).

64. Miyagishi, M. & Taira, K. U6 promoter–driven siRNAs with four uridine 3′ overhangs efficiently suppress targeted gene expression in mammalian cells. *Nat. Biotechnol.* **20,** 497–500 (2002).

65. Giering, J. C., Grimm, D., Storm, T. A. & Kay, M. A. Expression of shRNA From a Tissue-specific pol II Promoter Is an Effective and Safe RNAi Therapeutic. *Mol. Ther.* **16,** 1630–1636 (2008).

66. Brake, O. ter *et al.* Lentiviral Vector Design for Multiple shRNA Expression and Durable HIV-1 Inhibition. *Mol. Ther.* **16,** 557–564 (2008).

67. Brummelkamp, T. R., Bernards, R. & Agami, R. A system for stable expression of short interfering RNAs in mammalian cells. *Science (80-.).* **296,** 550–553 (2002).

68. Paddison, P. J. *et al.* A resource for large-scale RNA-interference-based screens in mammals. *Nature* **428,** 427–431 (2004).

69. Rubinson, D. A. *et al.* A lentivirus-based system to functionally silence genes in primary mammalian cells, stem cells and transgenic mice by RNA interference. *Nat. Genet.* **33,** 401–406 (2003).

70. Chu, L. *et al.* Oncolytic adenovirus-mediated shRNA against Apollon inhibits tumor cell growth and enhances antitumor effect of 5-fluorouracil. *Gene Ther.* **15,** 484–494 (2008).

71. Pinkenburg, O., Platz, J., Beisswenger, C., Vogelmeier, C. & Bals, R. Inhibition of NF-κB mediated inflammation by siRNA expressed by recombinant adeno-associated virus. *J. Virol. Methods* **120,** 119–122 (2004).

72. Hong, C.-S., Goins, W. F., Goss, J. R., Burton, E. A. & Glorioso, J. C. Herpes simplex virus RNAi and neprilysin gene transfer vectors reduce accumulation of Alzheimer's disease-related amyloid-β peptide in vivo. *Gene Ther.* **13,** 1068–1079 (2006).

73. Yin, H. *et al.* Non-viral vectors for gene-based therapy. *Nat. Rev. Genet.* **15,** 541–555 (2014).

74. Thomas, C. E., Ehrhardt, A. & Kay, M. A. Progress and problems with the use of viral vectors for gene therapy. *Nat. Rev. Genet.* **4,** 346–358 (2003).

75. Borja-Cacho, D. & Matthews, J. MicroRNA-210 as a Novel Therapy for Treatment of Ischemic Heart Disease. *Circulation* **6,** 2166–2171 (2008).

76. Huang, M., Nguyen, P., Jia, F. & Hu, S. Double Knockdown of Prolyyl Hydroxylase and Factor Inhibiting HIF with Non-Viral Minicircle Gene Therapy Enhances Stem Cell Mobilization and Angiogenesis After Myocardial Infarction. *Circulation* **124,** S46–S54 (2011).

77. Zhao, N., Fogg, J. M., Zechiedrich, L. & Zu, Y. Transfection of shRNA-encoding Minivector DNA of a few hundred base pairs to regulate gene expression in lymphoma cells. *Gene Ther.* **18,** 220–224 (2011).

78. Gaspar, V. *et al.* Minicircle DNA vectors for gene therapy: advances and applications. *Expert Opin. Biol. Ther.* **15,** 353–379 (2015).

79. Mayrhofer, P., Schleef, M. & Jechlinger, W. Use of Minicircle Plasmids for Gene Therapy. in *Methods in molecular biology (Clifton, N.J.)* **542,** 87–104 (2009).

80. Miguel Prazeres, D. F. & Monteiro, G. A. Plasmid Biopharmaceuticals. *Microbiol. Spectr.* **2,** (2014).

81. Hadj-Slimane, R., Lepelletier, Y., Lopez, N., Garbay, C. & Raynaud, F. Short interfering RNA (siRNA), a novel therapeutic tool acting on angiogenesis. *Biochimie* **89,** 1234–1244 (2007).

82. Mulkeen, A. *et al.* siRNA-mediated gene silencing in colorectal cancer: A novel anti-angiogenic targeted therapy. *J. Surg. Res.* **121,** 279–280 (2004).

83. Takei, Y., Kadomatsu, K., Yuzawa, Y., Matsuo, S. & Muramatsu, T. A Small Interfering RNA Targeting Vascular Endothelial Growth Factor as Cancer Therapeutics. *Cancer Res.* **64,** 3365–

3370 (2004).

84. Zhao, X. *et al.* Lentivirus-mediated shRNA interference targeting vascular endothelial growth factor inhibits angiogenesis and progression of human pancreatic carcinoma. *Oncol. Rep.* **29,** 1019–1026 (2013).

85. Schiffelers, R. M. *et al.* Cancer siRNA therapy by tumor selective delivery with ligand-targeted sterically stabilized nanoparticle. *Nucleic Acids Res.* **32,** e149–e149 (2004).

86. Yang, G., Cai, K. Q., Thompson-Lanza, J. A., Bast, R. C. & Liu, J. Inhibition of breast and ovarian tumor growth through multiple signaling pathways by using retrovirus-mediated small interfering RNA against Her-2/neu gene expression. *J. Biol. Chem.* **279,** 4339–45 (2004).

87. Dolinsek, T. *et al.* Multiple Delivery of siRNA against Endoglin into Murine Mammary Adenocarcinoma Prevents Angiogenesis and Delays Tumor Growth. *PLoS One* **8,** e58723 (2013).

88. Li, D.-C. *et al.* A study of the suppressive effect on human pancreatic adenocarcinoma cell proliferation and angiogenesis by stable plasmid-based siRNA silencing of c-Src gene expression. *Oncol. Rep.* **27,** 628–36 (2011).

89. Huang, C. *et al.* STAT3-targeting RNA interference inhibits pancreatic cancer angiogenesis in vitro and in vivo. *Int. J. Oncol.* **38,** 1637–1644 (2011).

90. Zhang, Y. *et al.* Short interfering RNA targeting Net1 reduces the angiogenesis and tumor growth of in vivo cervical squamous cell carcinoma through VEGF down-regulation. *Hum. Pathol.* **65,** 113–122 (2017).

91. Zuo, L., Fan, Y., Wang, F., Gu, Q. & Xu, X. A SiRNA targeting vascular endothelial growth factor-A inhibiting experimental corneal neovascularization. *Curr. Eye Res.* **35,** 375–384 (2010).

92. Feng, W. *et al.* siRNA-mediated knockdown of VEGF-A, VEGF-C and VEGFR-3 suppresses the growth and metastasis of mouse bladder carcinoma in vivo. *Exp. Ther. Med.* **1,** 899–904 (2010).

93. Eswarappa, S. M. *et al.* Programmed translational readthrough generates antiangiogenic VEGF-Ax. *Cell* **157,** 1605–1618 (2014).

94. Park, J. H., Hong, S. W., Yun, S., Lee, D. & Shin, C. Effect of siRNA with an Asymmetric RNA/dTdT Overhang on RNA Interference Activity. *Nucleic Acid Ther.* **24,** 364–371 (2014).

95. Moore, C. B., Guthrie, E. H., Huang, M. T. & Taxman, D. J. Short Hairpin RNA (shRNA): Design, Delivery, and Assessment of Gene Knockdown. *Methods Mol. Biol.* 1–15 (2013). doi:10.1007/978-1-60761-657-3

96. Brummelkamp, T. R. A System for Stable Expression of Short Interfering RNAs in Mammalian Cells. *Science (80-.).* **296,** 550–553 (2002).

97. Protocol for Annealing Oligonucleotides | Sigma-Aldrich. Available at: https://www.sigmaaldrich.com/technical-documents/protocols/biology/annealing-oligos.html. (Accessed: 13th January 2018)

98. Brito, L. *Minicircle production and delivery to human mesenchymal stem/stromal cells for angiogenesis stimulation*. Instituto Superior Técnico, Lisboa (2014).

99. Michaela Simcikova. Development of a process for the production and purification of minicircles for biopharmaceutical applications. (Instituto Superior Técnico, Universidade de Lisboa, 2013).

100. Silva-Santos, A. R., Alves, C. P. A., Prazeres, D. M. F. & Azevedo, A. M. A process for supercoiled plasmid DNA purification based on multimodal chromatography. *Sep. Purif. Technol.* **182,** 94–100 (2017).

101. Alves, C. P. A., Šimčíková, M., Brito, L., Monteiro, G. A. & Prazeres, D. M. F. Development of a nicking endonuclease-assisted method for the purification of minicircles. *J. Chromatogr. A* **1443,** 136–144 (2016).

102. Serra, J. *et al.* Engineering of human mesenchymal stem/stromal cells (MSC) with VEGF-encoding minicircles for angiogenic gene therapy. *Hum. Gene Ther.* hum.2018.154 (2018).

103. Boura, J. S., Santos, F., Gimble, J. M., Cardoso, C. M. P. & Madeira, C. Direct Head-To-Head Comparison of Cationic Liposome-Mediated Gene Delivery to Mesenchymal. **48,** 38–48 (2013).

104. Chen, Z. Y., He, C. Y., Meuse, L. & Kay, M. A. Silencing of episomal transgene expression by plasmid bacterial DNA elements in vivo. *Gene Ther.* **11,** 856–864 (2004).

105. Brees, C. & Fransen, M. A cost-effective approach to microporate mammalian cells with the Neon Transfection System. *Anal. Biochem.* **466,** 49–50 (2014).

106. Madeira, C. *et al.* Gene delivery to human bone marrow mesenchymal stem cells by microporation. *J. Biotechnol.* **151,** 130–136 (2011).

107. Madeira, C. *et al.* Nonviral Gene Delivery to Mesenchymal Stem Cells Using Cationic Liposomes for Gene and Cell Therapy. *J. Biomed. Biotechnol.* **2010,** 1–12 (2010).

108. Perrot-Applanat, M. & Di Benedetto, M. Autocrine functions of VEGF in breast tumor cells: adhesion, survival, migration and invasion. *Cell Adh. Migr.* **6,** 547–53 (2012).

109. Fisher Scientific, T. *Neon ® Transfection System for transfecting mammalian cells, including primary and stem cells, with high transfection efficiency (Catalog Number MPK5000)*. (2014).

110. Portnoy, V. & Huang, V. Small RNA and transcriptional upregulation. *… Rev. RNA* **2,** 748–760 (2011).

111. Li, L.-C. *et al.* Small dsRNAs induce transcriptional activation in human cells. *Proc. Natl. Acad. Sci. U. S. A.* **103,** 17337–42 (2006).

112. Ahlemeyer, B., Vogt, J. F., Michel, V., Hahn-Kohlberger, P. & Baumgart-Vogt, E. Microporation is an efficient method for siRNA-induced knockdown of PEX5 in HepG2 cells: evaluation of the transfection efficiency, the PEX5 mRNA and protein levels and induction of peroxisomal deficiency. *Histochem. Cell Biol.* **142,** 577–591 (2014).

113. La Vega, J. De, Braak, B. Ter, Azzoni, A. R., Monteiro, G. A. & Prazeres, D. M. F. Impact of plasmid quality on lipoplex-mediated transfection. *J. Pharm. Sci.* **102,** 3932–3941 (2013).

114. Kumar, R., Conklin, D. S. & Mittal, V. High-throughput selection of effective RNAi probes for gene silencing. *Genome Res.* **13,** 2333–40 (2003).

115. Ovcharenko, D., Jarvis, R., Hunicke-Smith, S., Kelnar, K. & Brown, D. High-throughput RNAi screening in vitro: from cell lines to primary cells. *RNA* **11,** 985–93 (2005).

116. Qazi, Y. *et al.* Nanoparticle-mediated delivery of shRNA.VEGF-A plasmids regresses corneal neovascularization. *Investig. Ophthalmol. Vis. Sci.* **53,** 2837–2844 (2012).

117. Xia, H., Mao, Q., Paulson, H. L. & Davidson, B. L. siRNA-mediated gene silencing in vitro and in vivo. *Nat. Biotechnol.* **20,** 1006–1010 (2002).

118. pSilencer adeno 1.0-CMV System: Shuttle Vector 1.0 CMV. *ThermoFisher Scientific* Available at: https://www.thermofisher.com/pt/en/home/life-science/dna-rna-purification-analysis/napamisc/vector-maps/psilencer-adeno-1.html#vector. (Accessed: 3rd October 2018)

119. Lin, L. *et al.* Adenovirus-mediated transfer of siRNA against Runx2/Cbfa1 inhibits the formation of heterotopic ossification in animal model. *Biochem. Biophys. Res. Commun.* **349,** 564–572 (2006).

120. Das, A., Xi, L. & Kukreja, R. C. Protein kinase G-dependent cardioprotective mechanism of phosphodiesterase-5 inhibition involves phosphorylation of ERK and GSK3β. *J. Biol. Chem.* **283,** 29572–29585 (2008).

121. Sun, L. L., Han, Y., Chen, J. H. & Yao, Y. Q. Down-regulation of HLA-G boosted natural killer cell-mediated cytolysis in JEG-3 cells cultured in vitro. *Fertil. Steril.* **90,** 2398–2405 (2008).

122. Heathman, T. R. J. *et al.* Characterization of human mesenchymal stem cells from multiple donors and the implications for large scale bioprocess development. *Biochem. Eng. J.* **108,** 14–23 (2016).

123. Grimm, D. *et al.* Fatality in mice due to oversaturation of cellular microRNA/short hairpin RNA pathways. *Nature* **441,** 537–541 (2006).

124. Van Gestel, M. A. *et al.* ShRNA-induced saturation of the microRNA pathway in the rat brain. *Gene Ther.* **21,** 205–211 (2014).

125. Guo, P. *et al.* Overexpression of vascular endothelial growth factor by MCF-7 breast cancer cells promotes estrogen-independent tumor growth in vivo. *Cancer Res.* **63,** 4684–91 (2003).

126. Liu, Y.-C. *et al.* RNAi-mediated gene silencing of vascular endothelial growth factor C suppresses growth and induces apoptosis in mouse breast cancer in vitro and in vivo. *Oncol. Lett.* **12,** 3896–3904 (2016).

127. Arnaoutova, I., George, J., Kleinman, H. K. & Benton, G. The endothelial cell tube formation assay on basement membrane turns 20: state of the science and the art. *Angiogenesis* **12,** 267–274 (2009).

128. Wu, J., Qu, Z., Fei, Z.-W., Wu, J.-H. & Jiang, C.-P. Role of stem cell-derived exosomes in cancer. *Oncol. Lett.* **13,** 2855–2866 (2017).

129. Tam, S., Tsao, M.-S. & McPherson, J. D. Optimization of miRNA-seq data preprocessing. *Brief. Bioinform.* **16,** 950–963 (2015).

130. Koscianska, E. *et al.* Northern blotting analysis of microRNAs, their precursors and RNA interference triggers. *BMC Mol. Biol.* **12,** 14 (2011).

7. Supplementary Information

Supplementary Data 1 – Human VEGF-A gene sequence. Sequence highlighted in yellow represents the synthetic siRNA target's region.

ATGAACTTTCTGCTGTCTTGGGTGCATTGGAGCCTTGCCTTGCTGCTCTACCTCCACCATGCCAAGTGGTCCCAGGCTGCA
CCCATGGCAGAAGGAGGAGGGCAGAATCATCACGAAGTGGTGAAGTTCATGGATGTCTATCAGCGCAGCTACTGCCATCC
AATCGAGACCCTGGTGGACATCTTCCAGGAGTACCCTGATGAGATCGAGTACATCTTCAAGCCATCCTGTGTGCCCCTGAT
GCGATGCGGGGGCTGCTGCAATGACGAGGGCCTGGAGTGTGTGCCCACTGAGGAGTCCAACATCACCATGCAGATTATG
CGGATCAAACCTCACCAAGGCCAGCACATAGGAGAGATGAGCTTCCTACAGCACAACAAATGTGAATGCAGACCAAAGAAA
GATAGAGCAAGACAAGAAAATCCCTGTGGGCCTTGCTCAGAGCGGAGAAAGCATTTGTTTGTACAAGATCCGCAGACGTGT
AAATGTTCCTGCAAAAACACAGACTCGCGTTGCAAGGCGAGGCAGCTTGAGTTAAACGAACGTACTTGCAGATGTGACAAG
CCGAGGCGG

Supplementary Data 2 – DNA sequencing results

A) Portion of the alignment between the DNA sequencing results and the reference sequence of pshRNA. Sequence highlighted in grey represents the CMV promoter, in orange the shRNA insert, and in red the BGH polyadenylation signal.

```
  65 aattaatacgactcactatagggagacccaagctggctagcgtttaaacttaagcttggtaccagatctctgcaggatatcctcgagatgtgaatgcaga 164
     ||||||||||||||||||||||||||||||||||||||||||||||||||||||||||||||||||||||||||||||||||||||||||||||||||||
1401 AATTAATACGACTCACTATAGGGAGACCCAAGCTGGCTAGCGTTTAAACTTAAGCTTGGTACCAGATCTCTGCAGGATATCCTCGAGATGTGAATGCAGA 1500
          *         *         *         *         *         *         *         *         *         *

          *         *         *         *         *         *         *         *         *         *
 165 ccaaagttcaagagactttggtctgcattcacatttttttggatcctctagagggcccgtttaaacccgctgatcagcctcgactgtgccttctagttgc 264
     ||||||||||||||||||||||||||||||||||||||||||||||||||||||||||||||||||||||||||||||||||||||||||||||||||||
1501 CCAAAGTTCAAGAGACTTTGGTCTGCATTCACATTTTTTTGGATCCTCTAGAGGGCCCGTTTAAACCCGCTGATCAGCCTCGACTGTGCCTTCTAGTTGC 1600
          *         *         *         *         *         *         *         *         *         *

          *         *         *         *         *         *         *         *         *         *
 265 cagccatctgttgtttgcccctcccccgtgccttccttgaccctggaaggtgccactcccactgtcctttcctaataaaatgaggaaattgcatcgcatt 364
     ||||||||||||||||||||||||||||||||||||||||||||||||||||||||||||||||||||||||||||||||||||||||||||||||||||
1601 CAGCCATCTGTTGTTTGCCCCTCCCCCGTGCCTTCCTTGACCCTGGAAGGTGCCACTCCCACTGTCCTTTCCTAATAAAATGAGGAAATTGCATCGCATT 1700
          *         *         *         *         *         *         *         *         *         *
```

B) Portion of the alignment between the DNA sequencing results and the reference sequence of pshRNA. Sequence highlighted in grey represents the CMV promoter, in orange the CMV+shRNA+polyA insert, and in green the MRS.

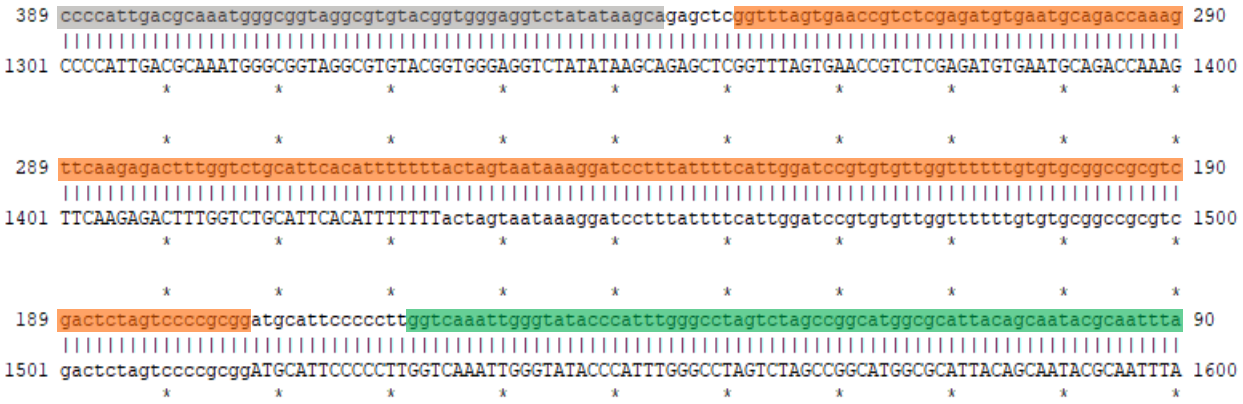

Supplementary Data 3 – Comparison between the expression unit of pshRNA and pshRNA_2. Sequence highlighted in grey represents the CMV promoter, in orange the shRNA insert, in red the BGH polyadenylation signal and in blue the synthetic polyA signal.

- pshRNA

TAGTTATTAATAGTAATCAATTACGGGGTCATTAGTTCATAGCCCATATATGGAGTTCCGCGTTACATAACTTACGGTAAATG
GCCCGCCTGGCTGACCGCCCAACGACCCCCGCCCATTGACGTCAATAATGACGTATGTTCCCATAGTAACGCCAATAGGG
ACTTTCCATTGACGTCAATGGGTGGAGTATTTACGGTAAACTGCCCACTTGGCAGTACATCAAGTGTATCATATGCCAAGTA
CGCCCCCTATTGACGTCAATGACGGTAAATGGCCCGCCTGGCATTATGCCCAGTACATGACCTTATGGGACTTTCCTACTT
GGCAGTACATCTACGTATTAGTCATCGCTATTACCATGGTGATGCGGTTTTGGCAGTACATCAATGGGCGTGGATAGCGGT
TTGACTCACGGGGATTTCCAAGTCTCCACCCCATTGACGTCAATGGGAGTTTGTTTTGGCACCAAAATCAACGGGACTTTCC
AAAATGTCGTAACAACTCCGCCCCATTGACGCAAATGGGCGGTAGGCGTGTACGGTGGGAGGTCTATATAAGCAGAGCTC
TCTGGCTAACTAGAGAACCCACTGCTTACTGGCTTATCGAAATTAATACGACTCACTATAGGGAGACCCAAGCTGGCTAGC
GTTTAAACTTAAGCTTGGTACCAGATCTCTGCAGGATATCCTCGAGATGTGAATGCAGACCAAAGTTCAAGAGACTTTGGTC
TGCATTCACATTTTTTTGGATCCTCTAGAGGGCCCGTTTAAACCCGCTGATCAGCCTCGACTGTGCCTTCTAGTTGCCAGCC
ATCTGTTGTTTGCCCCTCCCCCGTGCCTTCCTTGACCCTGGAAGGTGCCACTCCCACTGTCCTTTCCTAATAAAATGAGGAA
ATTGCATCGCATTGTCTGAGTAGGTGTCATTCTATTCTGGGGGGTGGGGTGGGGCAGGACAGCAAGGGGGAGGATTGGGA
AGACAATAGCAGGCATGCTGGGGATGCGGTGGGCTCTATGG

- pshRNA_2

TAGTTATTAATAGTAATCAATTACGGGGTCATTAGTTCATAGCCCATATATGGAGTTCCGCGTTACATAACTTACGGTAAATG
GCCCGCCTGGCTGACCGCCCAACGACCCCCGCCCATTGACGTCAATAATGACGTATGTTCCCATAGTAACGCCAATAGGG
ACTTTCCATTGACGTCAATGGGTGGAGTATTTACGGTAAACTGCCCACTTGGCAGTACATCAAGTGTATCATATGCCAAGTA
CGCCCCCTATTGACGTCAATGACGGTAAATGGCCCGCCTGGCATTATGCCCAGTACATGACCTTATGGGACTTTCCTACTT
GGCAGTACATCTACGTATTAGTCATCGCTATTACCATGGTGATGCGGTTTTGGCAGTACATCAATGGGCGTGGATAGCGGT
TTGACTCACGGGGATTTCCAAGTCTCCACCCCATTGACGTCAATGGGAGTTTGTTTTGGCACCAAAATCAACGGGACTTTCC
AAAATGTCGTAACAACTCCGCCCCATTGACGCAAATGGGCGGTAGGCGTGTACGGTGGGAGGTCTATATAAGCAGAGCTC
GGTTTAGTGAACCGTCTCGAGATGTGAATGCAGACCAAAGTTCAAGAGACTTTGGTCTGCATTCACATTTTTTTACTAGTAAT
AAAGGATCCTTTATTTTCATTGGATCCGTGTGTTGGTTTTTTGTGTGCGGCCGCGTCGACTCTAGTCCCCGCGG

Supplementary Data 4 – Calibration curve of VEGF concentrations. OD_{450nm} values represent the mean of standard sample duplicates, after subtracting the average zero standard absorbance.

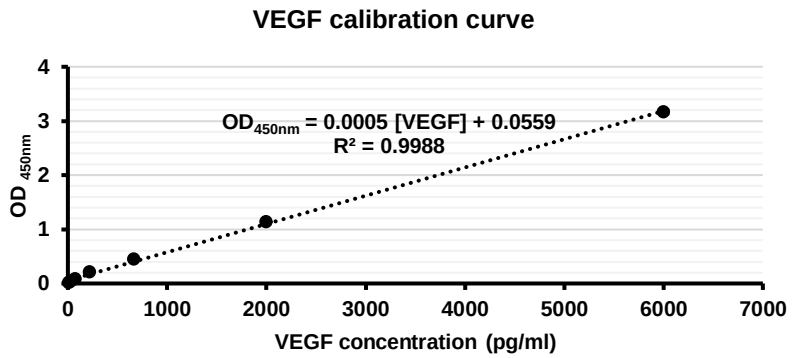

Supplementary Data 5 – Data for determination of VEGF protein production in pg/1000 cells.

		OD_{450nm}	VEGF (pg/ml)	Cell number	Supernatant volume (mL)	VEGF (pg/1000 cells)	Mean	SD
BM-MSC	LF	0.673 0.664	1.23E+3 1.22E+3	1.21E+5 1.21E+5	2.0 2.0	20.5 20.2	**20.3**	0.1
	LF	0.975 0.967	1.84E+3 1.82E+3	8.83E+4 8.83E+4	1.0 1.0	20.8 20.6	**20.7**	0.1
	siRNA (50 nM)	0.261 0.237	4.09E+2 3.62E+2	6.28E+4 6.28E+4	2.0 2.0	13.0 11.5	**12.3**	0.8
	MC-shRNA_2 (20ng)	0.977 0.978	1.84E+3 1.84E+3	7.39E+4 7.39E+4	1.0 1.0	24.9 24.9	**24.9**	0.01
	MC-shRNA_2 (100ng)	0.880 0.909	1.65E+3 1.71E+3	4.56E+4 4.56E+4	1.0 1.0	36.2 37.4	**36.8**	0.6
	MC-shRNA_2 (500ng)	0.542 0.517	9.72E+2 9.23E+2	2.17E+4 2.17E+4	2.0 2.0	89.7 85.2	**87.5**	2.3
	MC-shRNA (500ng)	0.637 0.648	1.16E+3 1.18E+3	2.67E+4 2.67E+4	2.0 2.0	87.2 88.8	**88.0**	0.8
MCF-7	LF	0.478 0.476	8.44E+2 8.41E+2	8.05E+5 8.05E+5	2.0 2.0	2.10 2.09	**2.09**	0.0
	LF	1.52 1.46	2.93E+3 2.80E+3	2.15E+6 2.15E+6	2.0 2.0	2.72 2.61	**2.67**	0.06
	siRNA (50 nM)	0.184 0.185	2.55E+2 2.59E+2	4.45E+5 4.45E+5	2.0 2.0	1.15 1.16	**1.16**	0.01
	siRNA (50 nM)	0.910 0.886	1.71E+3 1.66E+3	1.25E+6 1.25E+6	2.0 2.0	2.74 2.66	**2.70**	0.04
	siRNA (200 nM)	0.979 0.948	1.85E+3 1.78E+3	2.06E+6 2.06E+6	2.0 2.0	1.79 1.73	**1.76**	0.03
	MC-shRNA_2 (20ng)	1.65 1.64	3.19E+3 3.17E+3	1.43E+6 1.43E+6	2.0 2.0	4.47 4.44	**4.46**	0.02
	MC-shRNA_2 (100ng)	1.80 1.87	3.48E+3 3.64E+3	1.46E+6 1.46E+6	2.0 2.0	4.76 4.98	**4.87**	0.1
	MC-shRNA_2 (500ng)	0.370 0.373	6.28E+2 6.34E+2	3.95E+5 3.95E+5	2.0 2.0	3.18 3.21	**3.19**	0.01
	MC-shRNA (500ng)	0.395 0.426	679 739	2.80E+5 2.80E+5	2.0 2.0	4.85 5.28	**5.07**	0.2

Supplementary Data 6 – Evaluation of VEGF content present in the conditioned media (CM) of cultured BM-MSC (black bars) and MCF-7 (grey bars) 72 hours after transfection with the synthetic siRNA, MC-shRNA or MC-shRNA_2, by ELISA